Comparison of Magnetic Resonance Imaging and Computed Tomography for the detection of specific brain and cervical spine abnormalities in small animals

Thesis submitted in fulfillment of the requirements for the degree of Doctor in Veterinary Sciences (PhD), Faculty of Veterinary Medicine, Ghent University

2016

Kaatje Kromhout

Promotors

Dr. I. Gielen

Prof. Dr. L. Van Ham

Dr. S. Bhatti

Department of Veterinary Medical Imaging and Small Animal Orthopaedics

Department of Medicine and Clinical Biology of Small Animals

Faculty of Veterinary Medicine

Ghent University

Comparison of Magnetic Resonance Imaging and Computed Tomography for the detection of specific brain and cervical spine abnormalities in small animals.

Kaatje Kromhout

Department of Veterinary Medical Imaging and Small Animal Orthopaedics

Department of Medicine and Clinical Biology of Small Animals

Faculty of Veterinary Medicine

Ghent University

Cover art designed by 

"Nothing is impossible, the word itself says 'I'm possible'!"
Audrey Hepburn

LIST OF ABBREVIATIONS

AOO	atlanto-occipital overlapping
CH	cerebellar herniation
CHL	cerebellar herniation length
CSF	cerebrospinal fluid
CKCS	Cavalier King Charles Spaniels
CM	Chiari-like malformation
CT	computed tomography
CTM	computed tomography myelography
DWI	diffusion weighted imaging
FLAIR	fluid attenuated inversion recovery
GME	granulomatous meningoencephalitis
GRE	gradient echo
HU	Hounsfield units
HF	high-field
LF	low-field
MPR	multiplanar reconstruction
MRI	magnetic resonance imaging

MUO	meningoencephalitis of unknown origin
PWI	perfusion weighted imaging
SM	syringomyelia
SNR	signal to noise ratio
STIR	short tau inversion recovery
SW	syrinx width
T1WSE	T1-weighted spin echo sequence
T2WSE	T2-weighted spin echo sequence
WL	window level
WW	window width

Preface

Magnetic resonance imaging (MRI) and computed tomography (CT) are diagnostic imaging procedures that are more and more used in veterinary medicine. They are worldwide available in veterinary universities and large referral institutes. Nowadays smaller clinics and first opinion practices are acquiring these modalities. Especially CT machines are more readily available because the equipment and maintenance are less expensive and operation is more user-friendly than MRI. Both cross-sectional methods enable precise, non-invasive visualization of neuroanatomic structures and they play both an important role in imaging neurological diseases of the brain and spinal cord. Each modality has its specific advantages and disadvantages in detecting selected lesions. MRI is generally considered as the modality of choice for imaging of the brain and spinal cord. Veterinarians are often faced with a choice between MRI or CT for the optimal diagnostic workup of their patients. This selection must be based on indications as well as knowledge of the modalities strengths and weaknesses. In veterinary medicine there is a lack of studies comparing MRI and CT in detecting intracranial and spinal cord lesions.

Chapter 1

General introduction

1) Cross-sectional imaging techniques

1.1. Magnetic Resonance Imaging (MRI)

Basic principles

Magnetic resonance imaging uses the magnetic properties of protons to produce images. The proton that is the most present in the body of animals and humans is hydrogen.[1] Most pathological processes result in changes of the normal tissues and cause therefore changes in the hydrogen composition of the tissues. When the patient is positioned in an external strong magnetic field (the MRI scanner) the hydrogen protons align with the direction of the field. A radio frequency pulse is then transmitted with a coil which causes a misalignment of certain protons. When the pulse is turned off the misaligned protons align again with the magnetic field during a process called relaxation. During this process, radio frequency energy is submitted that is captured by a receiver coil. Differences in relaxation times (T1 and T2 relaxation[2]) of tissues create different signal intensities and tissue contrast. The images created are gray scale images in which the degree of relative darkness or lightness is referred to as intensity. Dark areas are called hypointense and light areas are called hyperintense. Because the variations in T1 and T2 values are much greater than variations in tissue density, MRI provides better soft tissue contrast than conventional radiographs or CT.[3] Due to a variation of radio frequency pulses and magnetic fields, different sequences are created. The most frequently used are the T1-weighted (T1WSE) and T2-weighted (T2WSE) spin-echo sequences (Fig. 1).

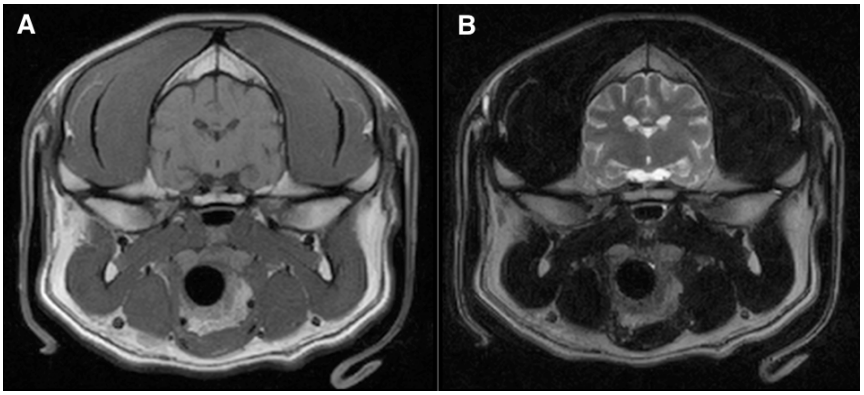

Fig. 1: Transverse (A) T1WSE and (B) T2WSE image of the normal brain of a dog.

On T1WSE images, contrast between tissues depends on differences in T1 relaxation. Fluids have a long T1 relaxation time and are hypointense, whereas fat has a short T1 relaxation time and is hyperintense. The T1WSE images have excellent resolution, which allows identification of anatomic structures. On T2WSE images, contrast between tissues depends on differences in T2 relaxation times. Fluids appear strongly hyperintense and the intensity of fat is variable on these images. T2WSE images are used to identify pathology. Abnormal fluid collections and tissues with abnormal increased fluid content (e.g. oedema, inflammation, neoplasia,..) will appear hyperintense[4]. The tissue characteristics on T1WSE and T2WSE images are displayed in table 1.

Table 1. Tissue characteristics on MRI images

Tissue/Material	T1WSE	T2WSE
air	black	black
fat	very bright	bright
fluid	dark	bright
mineralisations/bone	black	black
muscle	dark	more dark

Gadolinium based contrast[4] can be intravenously injected to highlight lesions and the vascularization of tissues. Images can be acquired in three different planes (transverse, dorsal and sagittal). No ionizing radiation is used during the examination. Disadvantages are the long anaesthesia time (for example, a normal brain protocol will take between 45 and 60 minutes using a low-field machine) and the presence of artefacts on the images in patient with metallic implants such as surgical screws, a skin staple and foreign bodies,… due to the magnetic field.[5] One main advantage of MRI is the ability to use different sequences in the imaging process to facilitate the diagnosis of lesions. For example the STIR (short tau inversion recovery) sequence is used to null the signal from fat. This sequence offers good conspicuity of fluids and tissues with increased water content including many pathologies which appear hyperintense on a STIR sequence without the distraction of body fat.[6] Fluid attenuated inversion recovery (FLAIR) can be obtained as a T2W sequence. It suppresses the signal from fluid with low or no protein content such as cerebrospinal fluid (CSF), so that it appears hypointense rather than hyperintense on the images.

This sequence allows improved identification of pathologies, such as tissue edema, and aids in identifying those lesions anatomically adjacent to areas such as a ventricle.[7] Ultrafast heavily T2-weighted sequences such as HASTE (half Fourier-acquisition single-shot turbo spin-echo) are used to evaluate the subarachnoid space for localizing vertebral canal lesions or spinal cord swelling comparable with a myelogram.[8] T2*-weighted gradient echo recalled sequences are valuable for their increased ability to detect the paramagnetic blood degradation products associated with haemorrhage.[9] Recent articles describe which sequences should be used for optimal imaging of the brain and the spinal cord.[10,11]

Low-field MRI versus high-field MRI

Most MRI scanners used in veterinary medicine are low-field (LF) with a permanent magnet (field strength approximately 0.2-0.4 Tesla). There are LF scanners for human use and dedicated veterinary scanners who use adapted software and coils optimized for veterinary patients.[12] LF scanners are open systems (Fig 2.).

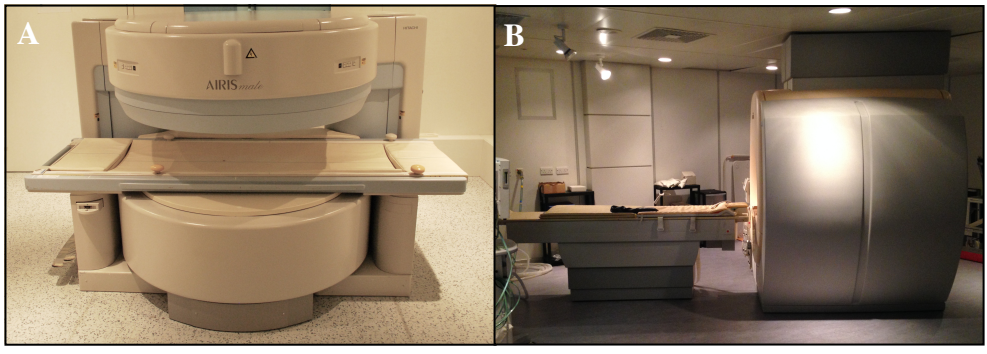

Fig. 2: The external appearance of a (A) low-field MR scanner and (B) high-field MR scanner (photograph, The Royal Veterinary College, University of London).

The magnetic field is created between two horizontal discs. This is advantageous to scan larger patients and allows easy access to the dog or cat. High-field (HF) scanners are increasingly used in universities. They have a field strength above 1 Tesla. The magnetic field is created by a large cylindrical gantry composed of electromagnets supercooled with liquid helium. These are long enclosed tubular systems, which is a limitation for large animals and creates challenges for monitoring the patients.LF scanners compared to HF are relative low in purchase price and maintenance costs. A limitation of LF MR is the reduced signal to noise ratio (SNR). SNR determines the appearance of the MR image. This ratio is measured by calculating the difference in signal intensity between the area of interest (the patient) and the background.[13] SNR increases almost lineary with the field strength.[14] Increased SNR is associated with improved resolution, detail and information present within each pixel/voxel[15], smaller voxel size and thinner slice thickness.[12] LF MR is therefore generally associated with longer scan times and decreased resolution leading to less sharp, but still diagnostic images.[12] Also LF MR have a smaller field of view then HF MR, this may necessitate frequent patient repositioning when examining larger animals, thus making it more time consuming. Older LF MR cannot provide thin slices with sufficient SNR within a reasonable time. Nowadays all LF systems allow high-resolution T1W three-dimensional (3D) gradient echo imaging. Data is acquired as a volume (slab), which can then be divided into thin slices for high spatial resolution and multiplanar reformatting. These sequences allow acquisition of isotropic (= equal intensity in all directions) 1mm slices. Small and/or subtle contrast uptake can be detected because of the high resolution.[12] This can allow identification of small cranial nerves.[16] They have and added advantage of providing a dataset for 2D and 3D reconstructions without needing to acquire additional imaging planes. Imaging artefacts[17] affect both LF and HF magnets but some may be pronounced more in one than the other. For example, motion artefacts (Fig. 3) occur independently of the field strength, but require fast scanning to overcome them. HF MR is therefore less vulnerable to motions artefacts than LF. Partial volume artefact can be

seen when tissues of different signal become part of the same voxel.[17] This appears more frequently in LF MR imaging due to the often larger slice thickness.

Susceptibility artefact (Fig. 4) occurs when there is local alteration of the magnetic field, e.g. because of the presence of a microchip, resulting in spatial misregistration and image distortion. These artefacts are less marked in LF MR. [18]

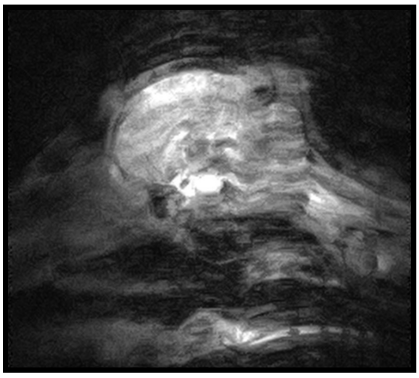

Fig. 3: Motion artefact in a LF MR system.

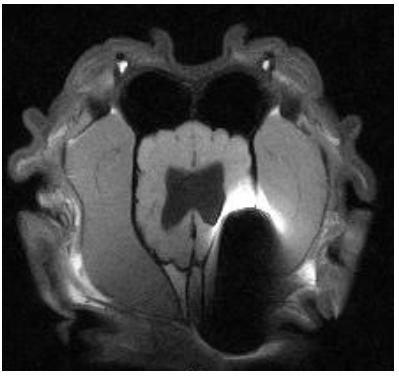

Fig. 4: Suspectibility artefact in a LF MR system.

HF MRI scanners are more suited for advanced techniques, such as MR angiography because of the possibility to use thinner slices and shorter acquisition time for each sequence. In addition, the visibility of e.g. intracranial vessels is higher in HF MR imaging.[19] Also molecular imaging and MR spectroscopy require high field strengths of at least 1 Tesla.[20] Table 2 gives a summary of the main differences between LF an HF MR.

Table 2. Summary of the main differences between LF and HF MR

Low-field MR	High-field MR
widespread available	less available
open system	closed system
0.2-0.4 Tesla	> 1 Tesla
less expensive (purchase + maintenance)	expensive
long imaging times (aneasthesia)	shorter imaging times
low SNR	high SNR
less contrast resolution	excellent contrast resolution

1.2. Computed Tomography

Basic principles

CT is a tomographic diagnostic technique that is based on the same x-ray principles as conventional radiography. CT scanners (Fig. 5) are composed of a gantry, that houses an x-ray tube and detectors. X-rays are produced by the x-ray tube that rotates 360 degrees around the animal. When passing through the patient, the x-rays are attenuated. The amount of attenuation depends on the density of the penetrated tissue. Opposite the x-ray tube, detectors absorb the remaining x-rays and convert them into a digital signal. As the animal passes through the gantry, on a sliding table, information regarding a cross section or slice is obtained.

Fig. 5: Four-slice helical CT device.

The contrast in CT images is the result of differences in attenuation between body tissues. The higher the density of the tissue (e.g. bone), the higher the attenuation of the x-rays, the brighter the tissue on the CT images (hyperattenuated or hyperdense). The lower the density of the tissue (e.g. fluid), the lower the attenuation of the x-rays, the darker the tissues on the CT images (hypoattenuated or hypodense).

The attenuation values are specified in Hounsfield units (HU) or CT numbers and represent different shades of grey. Water has an HU = 0 and air has an HU = -1000. The HU's of other tissues are displayed as a value relative to the attenuation of water (Fig. 6).

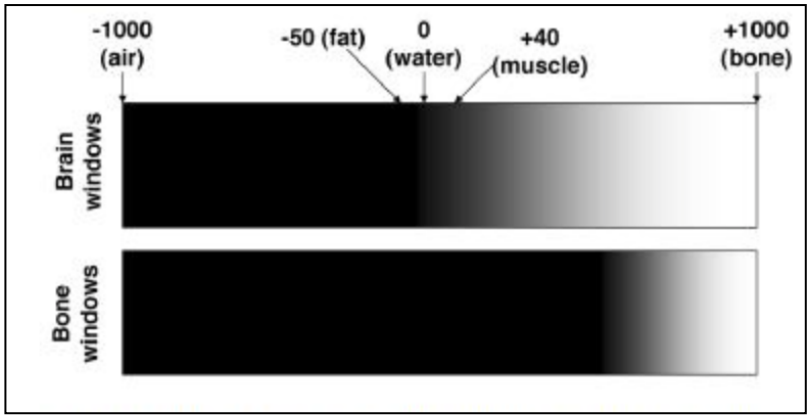

Fig. 6: CT Hounsfield scale.

The computer is able to define thousands of different shades of grey, but the human eye is only able to perceive around 20.[21] Therefore it is essential to adjust the images after acquisition by selecting a center (window level = WL) and range (window width = WW) of CT numbers in which the tissue of interest is highlighted. Doing so we create images for example where bone (bone window) or brain tissues (brain window) are enhanced (Fig. 7 & 8).

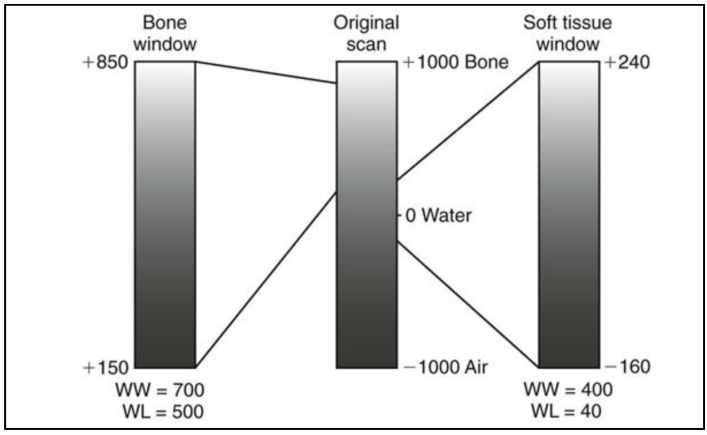

Fig. 7: WW and WL of e.g. a bone and soft tissue window.

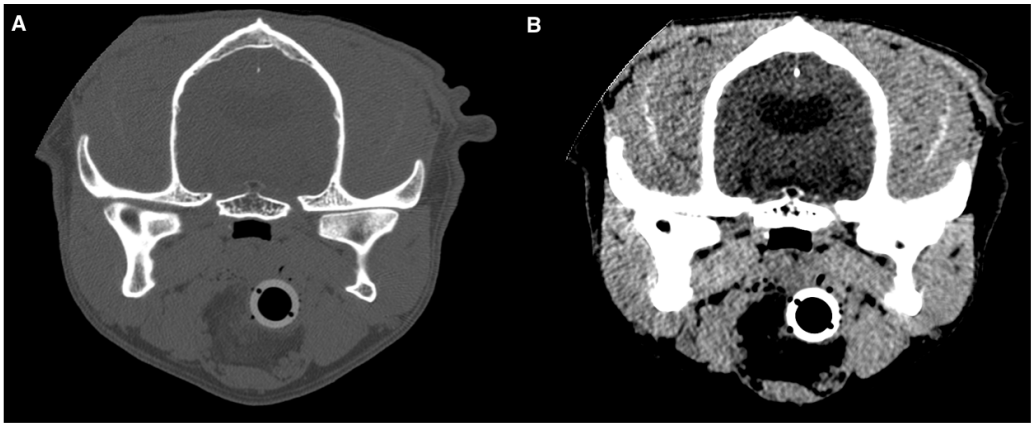

Fig. 8: The effect of WW and WL on CT image interpretation. CT image of the brain in A) bone window WW= 1500 WL= 500 and B) brain window WW= 150 WL= 35.

CT is superior to other cross-sectional techniques for the detection of calcification and to evaluate the structure of bones. Iodinated contrast media can be used to increase the contrast between normal tissue and pathologies and to visualise the vessels. Iodinated contrast[22] has more adverse effects than gadolinium based contrast[23] used with MRI and can cause vomiting, anxiety and hypotension in veterinary patients. With CT, images are standardly acquired in transverse planes.

With special software, reconstructions such as multiplanar reconstructions (MPR) and volume rendering can be provided (Fig. 9 & 10).

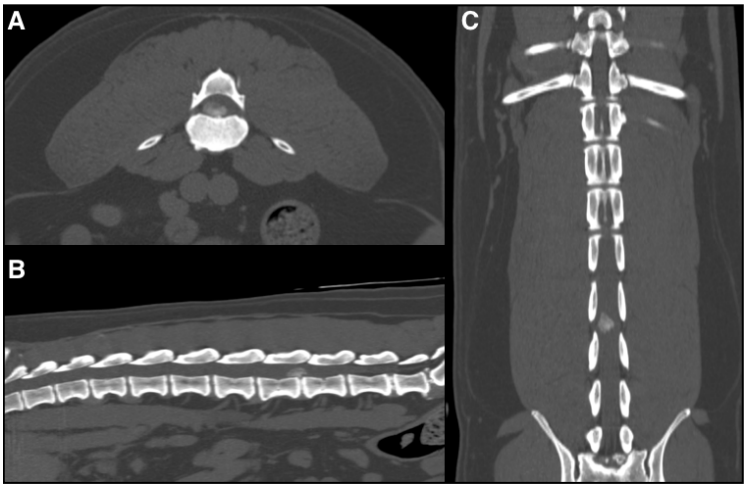

Fig. 9: Multiplanar reconstruction (MPR) of a Hansen Type I disc extrusion at the level of the intervertebral lumbar space 4-5. A) Transverse image B) sagittal and C) dorsal view.

Fig. 10: Volume rendering image of a dog with multiple skull fractures.

There are two types of CT scanners: *single-slice* and *multislice* scanners. In single-slice scanners only one row of detectors is present and during each rotation a single slice of anatomy is imaged. In multislice scanners several rows of detectors are present and during rotation multiple slices of anatomy are acquired. Most modern CT scanners used in veterinary medicine are multislice scanners. They can acquire thin slices (< 0.5mm) which give more detail to the images and reduce artefacts such as partial volume averaging (see supra). The acquisition time is faster with these machines. This decreases motion artefacts and makes it possible to acquire multiphase studies (e.g. arterial, venous and portal studies). Some artefacts such as beam hardening, which appear as dark bands or streaks adjacent to highly attenuating structures, can influence the diagnostic value of CT. This is especially the case in evaluation of the caudal fossa in animals due to the presence of dens temporal bones (Fig. 11).

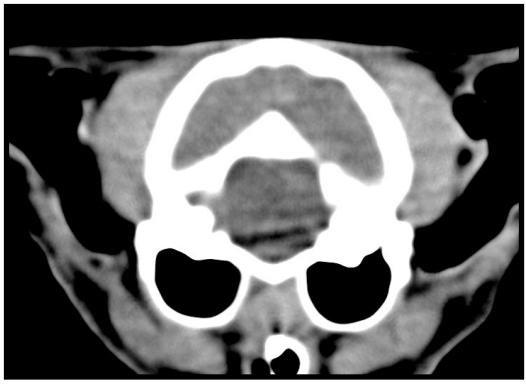

Fig. 11: Beam hardening artefact at the level of the caudal fossa.

CT may be combined with myelography to allow visualization of the subarachnoid space, improve accuracy in differentiating intramedullary from extradural causes of spinal cord swelling, and determine the location of herniated disk material.

CT myelography can be achieved by injecting iodinated contrast medium in the subarachnoid space, at 25% of the regular myelographic dose.[24] This allows excellent delineation of the spinal cord. However this technique is invasive and is reported to cause adverse effects such as seizures or neurological deterioration.[25] As an example, CT myelography has shown its effectiveness in veterinary patients in the diagnosis of brachial plexus avulsion[26] and spinal arachnoid diverticula.[27]

Table 3. Summary of the main differences between MRI and CT

MRI	CT
magnetic field	X-rays (ionizing radiation)
not widely available	widespread available
expensive	less expensive
long imaging times (aneasthesia)	short imaging times
thick slices (usually minimal 2mm)	thinner slices (up to 0.5mm)
different planes	transverse plane (+ reconstructions)
not suitable for patients with metallic implants	suitable for patients with implants
gadolinium based contrast	iodinated contrast (more adverse effects)
excellent soft-tissue contrast	excellent resolution of bony detail

1.3. References

1. Westbrook C., Kaut Roth C, Talbot J. MRI in practice. Oxford (UK): Blackwell Publishing Ltd; 2005.
2. Tidwell A.S. Principles of computed tomography and magnetic resonance imaging. In: Thrall DE, editor. Textbook of veterinary diagnostic radiology. 5th edition. St. Louis (MO): Saunders Elsevier; 2007. p. 50–77.
3. Edelman R.R., Warach S. Magnetic resonance imaging: first of two parts. *N Engl J Med* 1993; 328:708–716.Kuriashkin IV, Losonsky JM. Contrast enhancement in magnetic resonance imaging using intravenous paramagnetic contrast media: a review. *Vet Radiol Ultrasound* 2000; 41: 4–7.
4. Hecht S., Adams W.H., Narak J. et al. Magnetic resonance imaging susceptibility artifacts due to metallic foreign bodies. *Vet Radiol Ultrasound* 2011; 52: 409-414.
5. Benigni L., Lamb C.R. Comparison of fluid-attenuated inversion recovery and T2-weighted magnetic resonance images in dogs and cats with suspected brain disease. *Vet Radiol Ultrasound* 2005; 46: 287-292.
6. Eminaga S., Cherubini G.B., Villiers E. et al. STIR muscle hyperintensity in the cervical muscles associated with inflammatory spinal cord disease of unknown origin. *J Small Anim Pract* 2013; 54: 137-42.
7. Mankin J.M., Hecht S., Thomas W.B. Agreement between T2 and haste sequences in the evaluation of thoracolumbar intervertebral disc disease in dogs.*Vet Radiol Ultrasound* 2012; 53: 162-166.
8. Hammond L.J., Hecht S. Susceptibility artifacts on T2*-weighted magnetic resonance imaging of the canine and the feline spine. *Vet Radiol Ultrasound* 2015; 56: 398-406.
9. Dennis R. Optimal magnetic resonance imaging of the spine. *Vet Radiol Ultrasound* 2011; 52 Suppl. 1: S72-S80.
10. Robertson I. Optimal magnetic resonance imaging of the brain. *Vet Radiol Ultrasound* 2011; 52 Suppl. 1: S15-22.

11. Gavin P.R. Basic Physics. In: Gavin P.R., Bagley R. eds. Practical small animal MRI. 1st ed. Iowa, Wiley-Blackwell, 2009; 4-7.
12. Magee T., Shapiro M., Williams D. Comparison of High-Field-Strength Versus Low-Field-Strength MRI of the shoulder. *Am J Roentgenol* 2003; 181: 1211-1215.
13. Werpy NM. Magnetic resonance imaging of the equine patient: a comparison of high and low field systems. In: Dyson S, Orsini JA. *Clinical Techniques in Equine Practice*. Philadelphia, PA: Elsevier Saunders, 2007, pp. 37–46.
14. Gonçalves R., Malalana F., McConnell J.F. et al. Anatomical study of cranial nerve emergency and skull foramina in the horse using magnetic resonance imaging and computed tomography. *Vet Radiol Ultrasound* 2015; 56: 391–397.
15. Bellon E.M., Haacke E.M., Coleman P.E., et al. MR artifacts: a review. *Am J Roentgenol* 1986; 147: 1271– 1281.
16. Farahani K., Sinha U., Sinha S. et al. Effect of field strength on susceptibility artifacts in magnetic resonance imaging. *Comput Med Imaging Graph* 1990; 14: 409–413.
17. Rodriguez D., Rylander H., Vigen K.K. et al. Influence of field strength on intracranial vessel conspicuity in canine magnetic resonance angiography. *Vet Radiol Ultrasound* 2009; 50: 477–482.
18. Westbrook C., Kaut C., Talbot J. MRI in practice, 3rd ed. Oxford: Blackwell Publishing Ltd, 2005.
19. Tidwell AS, Jones JC: Advanced imaging concepts: a pictorial glossary of CT and MRI technology. *Clin Tech Small Anim Pract* 1999; 14: 65–111.
20. Vance A., Nelson M., Hofmeister E.H. Adverse reactions following administration of an ionic iodinated contrast media in anesthetized dogs. *J Am Anim Hosp Assoc* 2012; 48: 172-175.
21. Girard N.M., Leece E.A. Suspected anaphylactoid reaction following intravenous administration of a gadolinium-based contrast agent in three dogs undergoing magnetic resonance imaging. *Vet Anaesth Analg* 2010; 37: 352-6.

22. Sharp N.J.H., Cofone M., Robertson I. et al. Computed tomography in the evaluation of caudal cervical spondylomyelopthy of the doberman pinsher. *Vet Radiol Ultrasound* 1995; 36: 100–108.
23. Barone G, Ziemer L.S, Shofer F.S, et al. Risk factors associated with development of seizures after use of iohexol for myelography in dogs: 182 cases J Am Vet Med Assoc 1998; 220: 1499–1502.
24. Forterre F., Gutmannsbauer B., Schmall W. et al. CT myelography for diagnosis of brachial plexus avulsion in small animals. Tierarztl Praxis K H 1988; 26: 322–329.
25. Mauler D.A., De Decker S., De Risio L. et al. Signalment, clinical presentation, and diagnostic findings in 122 dogs with spinal arachnoid diverticula. J Vet Int Med 2014; 28: 175-81.

2. Review of roles and choices of MRI versus CT in brain and spinal diseases in small animals

2.1. Introduction

Magnetic resonance imaging (MRI) and computed tomography (CT) are diagnostic imaging techniques that are widespread available for veterinary patients. Veterinarians are often faced with the choice of which modality to use in the diagnostic workup of a patient. This chapter offers a review of the applications of both techniques in a variety of diseases of the brain and the spinal cord.

2.2. Indications in brain and spinal diseases

Congenital and developmental anomalies

Ventricular size in dogs or cats with hydrocephalus can be accurately assessed on CT[1] and MRI.[2] Dilation of the lateral ventricles, or ventriculomegaly, is however not necessarily associated with development of clinical signs and ventriculomegaly is commonly seen in clinically normal brachycephalic breeds.[3] Although this complicates interpretation of imaging studies, a recent study has identified several MRI variables, which could aid in differentiating clinically relevant from irrelevant ventricular dilation. These variables include elevation of the corpus callosum, dorsoventral flattening of the interthalamic adhesion and periventricular oedema.[4] It is currently however unclear if these variables can also be evaluated by CT imaging. The extent of cortical atrophy, and the presence of focal lesions that can be observed in hydrocephalus can be seen on both techniques.[5] MRI is however more sensitive than CT in imaging small focal lesions, especially those in the

caudal fossa.[2] This region (brainstem and cerebellum) between the temporal bone is sensitive to beam hardening artifacts on CT images which appear as dark bands or streaks which can obscure lesions[6]. Both imaging methods are useful for evaluation of patients with ventriculoperitoneal shunts after surgical placement.[7] Both CT and MRI can be used for follow-up assessments of changes in post-operative ventricular size or ventriculoperitoneal shunt position.[8] MRI characteristics of a ventriculoperitoneal shunt associated infection have also been described.[9] *Cystic lesions* such as intracranial intra-arachnoid diverticula can be visualised with CT and MRI[10] whereas spinal arachnoid diverticula can be best appreciated with CT myelography and MRI.[11]

Given the superior imaging characteristics for bone, *vertebral malformations and atlanto-axial instability* are best visualised on CT.[12,13] Thoracic vertebral malformations, such as hemivertebra, are however commonly seen in clinically normal screw-tailed brachycephalic dogs and it has been estimated that up to 78% of clinically normal French Bulldogs have thoracic hemivertebra and associated vertebral kyphosis.[14] It is therefore important to consider other causes for spinal dysfunction in French Bulldogs with radiological apparent vertebral malformations. MRI offers the advantage of directly detecting spinal cord compression or intraparenchymal lesions in these patients (Fig. 1A & B).

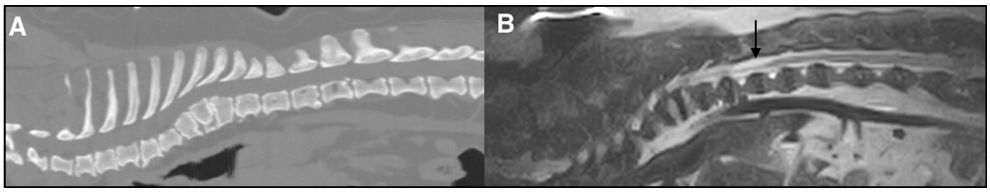

Fig. 1A : A) Precontrast sagittal MPR CT (bone window) and B) T2WSE sagittal MRI image of the thoracolumbar spine. A) Several vertebral malformations and a mild kyphosis are visible at the level of T5-T10 B) a dorsal arachnoid diverticulum is visible at the level of T10-T11 (arrow).

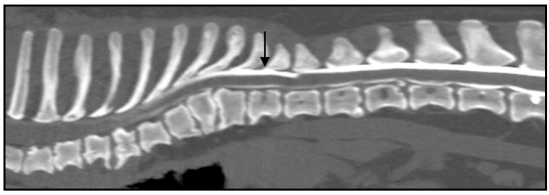

Fig. 1B : A) Sagittal MPR CT myelogram (bone window) confirmed the presence of a dorsal arachnoid diverticulum (arrow).

In contrast, atlanto-axial instability is typically not seen as an incidental radiological finding. As stated above, CT is useful to assess bony changes and proves very useful for assessment of dogs with suspected atlanto-axial instability. Atlanto-axial subluxation is often associated with abnormalities of the dens, such as hypoplasia, aplasia or dorsal angulation. CT is especially useful to evaluate the size and shape of the dens, detect craniodorsal displacement of the axis, incomplete ossification, pre-operative planning and evaluate postoperative surgical implant positioning.[15] MRI provides the opportunity to visualize secondary spinal cord compression. The ligamentous structures of the atlantoaxial articulation have recently been described on MRI in cadaveric studies but these structures are not well visualised in small patients.[16] In multifactorial disorders, which are associated with both bony and soft tissue abnormalities CT an MRI can be used in a complementary matter, for example in *Chiari-like malformation*.[17] Anatomical abnormalities such as occipital hypoplasia and assessment of cranial over-riding of the atlas are visible on CT.[18] MRI is considered the imaging modality of choice to detect Chiari-like malformation and syringomyelia.[19,20] Generally MRI is considered the modality of choice in dogs with suspected *cervical spondylomyelopathy (CSM)*.[21-23]

The main advantages of MRI over CT is the ability to directly visualise the spinal cord and asses the intramedullary spinal cord changes[24] which are associated with the presence of clinical signs. Although anatomical features of CSM on MR images are similar to those in CT, CT(-myelography) is suggested to be the most reliable imaging modality to assess articular process abnormalities, intervertebral foraminal stenosis, narrowing of intervertebral disc spaces and spondylosis deformans compared to low-field MRI.[25] This is also reflected in a recent study comparing non contrast CT and high-field MRI.[26]

Vascular disease

In *haemorrhagic infarcts*, acute and subacute bleedings can be readily visualized on CT because of the hyperdense characteristics of haemorrhage compared to normal brain parenchyma. The density gradually decreases to become isodense over days and weeks.[27] Nowadays, MRI is as sensitive as CT for the detection of hyperacute intracranial haemorrhages[28] and superior for detecting subtle microbleeds and haemorrhagic transformations.[29,30] The appearance of a bleeding on MRI is dependent on the time and the form of haemoglobine, which has variable magnetic properties.[31]

Gradient echo MR sequences are highly sensitive for the detection of blood products and chronic haemorrhage, which may not be visible on CT.[27] For the detection of *ischemic infarcts* MRI is superior to CT (Fig. 2) due to its excellent soft tissue contrast and its ability to detect subtle lesions.[32]

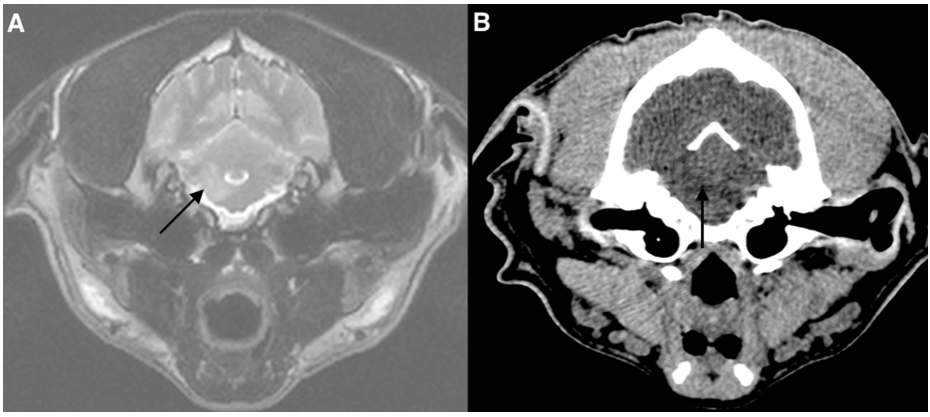

Fig. 2: A)T2WSE MRI and B) precontrast CT image at the level of the rostral part of the cerebellum. A) A hyperintense ischemic infarct (arrow) is visible right at the rostral part of the cerebellum. B) The lesion is not visible due to the presence of beam hardening (streaks) (arrow).

These types of cerebrovascular accidents tend to have distinguishing characteristics on conventional MRI and have been well described in recent years.[33] Functional MRI sequences, such as diffusion-weighted imaging (DWI) and perfusion-weighted imaging (PWI) can be used to identify hyperacute lesions and to localise specific regions of perfusion deficits.[32-35] One study described the potential use of these functional MRI sequences in differentiating neoplastic, inflammatory, haemorrhagic, and ischemic brain diseases.[36] CT has no advantages in identifying ischemic infarcts compared to MRI and is only valuable to exclude other lesions such as intracerebral haemorrhages (i.e. haemorrhagic infarcts). *Intracranial aneurysms and cerebrovascular malformations* can be evaluated on both CT an MR images.[34,37] Although a definitive diagnosis can only be made by histopathological examination of the spinal cord, a presumptive ante-mortem diagnosis of *fibrocartilaginous embolism*, the most common cause of ischaemic myelopathy in small animals is based on a combination of characteristic clinical findings and specific MRI abnormalities[38,39] (Fig. 3).

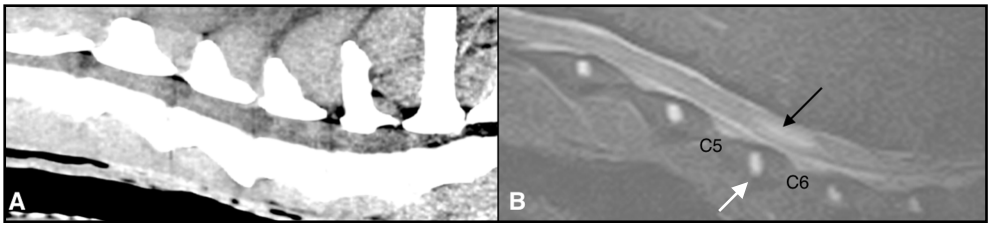

Fig. 3: A) Postcontrast sagittal MPR CT (bone window) and B) sagittal STIR images of the cervical region of a dog: A) No lesions are visible. B) A hyperintense signal is visible in the spinal cord (black arrow). The intervertebral disc at the level of C5-C6 is less hydrated (white arrow) compared to the cranial adjacent disc. A presumptive diagnosis of a fibrocartilaginous embolism is made.

CT findings of animals with ischaemic myelopathy have not yet been described and this imaging modality is most likely not useful for obtaining a presumptive diagnosis of this disorder.

Intracranial and spinal neoplasia

In general, MRI is superior to CT for detecting neoplastic lesions because of the superior soft tissue contrast. MRI is more accurate in defining the extent and the morphology of the tumor. CT is excellent for visualization of osseous lesions, which are commonly observed in spinal neoplasia. Veterinary studies have revealed that CT imaging is less accurate than MRI for detection of a suspected intracranial lesion.[40] Although MRI will allow easy detection of brain lesions, it is not always possible to differentiate between a neoplastic lesion, inflammatory lesions, or a vascular lesion[41], nor will MRI always allow to determine the exact tumor type.[42,43] After a presumptive diagnosis of neoplasia is made, a differential diagnosis can be made dependent on different characteristics including: anatomic location, distribution, CT density or MR signal characteristics, intensity and pattern of contrast enhancement, tumor margin definition, secondary mass effects and the extent of associated

oedema.[44-47] Obtaining a final diagnosis requires histopathological examination of neoplastic tissue, which can be collected during surgery or imaging guided biopsy procedures. Imaging guided biopsies were classically obtained by CT-guided stereotactic biopsy techniques.[48-50]

More recently, MRI-compatible stereotactic[51] and MRI-guided free hand[52] biopsy techniques have been developed. When a tumor of the pituitary gland is suspected CT and MRI provide comparable information.[53,54] Dynamic contrast CT and MRI are frequently used to diagnose pituitary microtumors.[55,56] For the differentiation of the distribution (intradural-extramedullary, intramedullary) of spinal cord tumors myelography is more useful then CT and MRI.[44,57]

Inflammatory disease

Inflammatory brain and spinal disease can manifest as multifocal, focal or diffuse lesions. Some diseases have signal attenuation similar to surrounding tissue and little or no contrast uptake and therefore can be missed on CT (Fig. 4).

Hence MRI is in these cases the modality of choice. MRI sequences such as FLAIR suppress the hyperintense signal associated with free fluid, such as CSF. This sequence can therefore aid in differentiation of hyperintense pathological lesions (such as brain oedema) and adjacent CSF, which have similar imaging characteristics on more conventional T2WSE.[58] When compared to T2WSE, FLAIR has also a higher sensitivity for detecting subtle abnormalities and for lesions with multifocal localisations.[59]

Meningoencephalitis of unknown origin (MUO) is the most common inflammatory disorder of the central nervous system in dogs and includes more specific disorders, such as granulomatous meningoencephalitis (GME), necrotizing meningoencephalitis (NME), and necrotizing leucoencephalitis (NLE).[60]

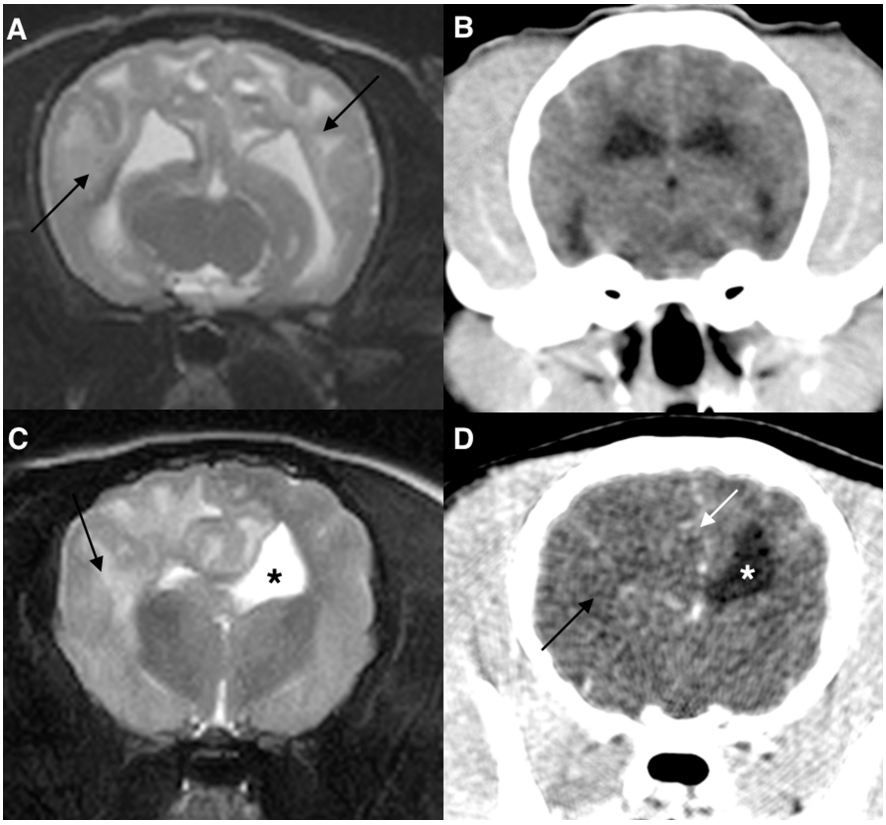

Fig. 4: A & C) Transverse T2WSE and B & D) postcontrast CT (brain window) images of 2 pug dogs with a suspected meningoencephalitis of unknown origin. Dog 1: A) Diffuse hyperintensities (arrows) are visible bilateral in the subcortical white matter of the occipital and temporal lobes. B) No lesions are visible. Dog 2: C) Asymmetric hyperintensities (arrow) are visible in the cortical gray and subcortical white matter of the parietal and temporal lobes. An asymmetric lateral ventricle is present. (asterisk). D) Hypodense aspect at the right side of the parietal and temporal lobes (black arrow). A midline shift is present (white arrow). An asymmetric lateral ventricle is visible (asterisk).

Although several studies have reported the MRI characteristics of GME, NME or NLE[59,61-63], it is currently unknown how well these more specific disorders can be differentiated by MRI. Furthermore, a previous study[64] determined that approximately 25% of brain MR images of dogs with inflammatory CSF revealed no abnormalities, emphasizing that a normal brain MR image does not rule out the presence of inflammatory disease. In agreement with the situation of intracranial neoplasia, definitive diagnosis of this group of diseases requires histopathology.[52,65]

Only a few reports have described the CT and MR imaging abnormalities of non-infectious inflammatory spinal disease. Reported abnormalities were considered non-specific.[59,64,66] Although CSF analysis can support the diagnosis of inflammatory spinal disease, 10% of affected cases may have normal CSF findings.[65,67]

Recently, the addition of a STIR sequence to the MRI protocol has been suggested to improve the detection of inflammatory spinal cord disease.[68] STIR suppresses the signal from fat on T2W-like sequences[69] and offers good conspicuity of fluids and tissues with increases water content, including pathologies. In case of suspected inflammatory spinal cord disease STIR muscle hyperintensities were detected and had a positive correlation with inflammatory CSF changes (sensitivity 78%, specificity 92%).[68] Conventional radiographic examination is traditionally used to diagnose discospondylitis.[70] Collapse of the intervertebral disc is seen initially, followed by bone lysis centered at the vertebral endplates, sclerosis and spondylosis. The main limitations of radiography are the delay (up to 2 weeks) between the onset of clinical signs and detection of radiographic findings. CT is more sensitive than radiography for identifying early endplate osteolysis.[71] MRI is more sensitive than CT for detecting soft tissue inflammation of the intervertebral disc and bone marrow changes in affected vertebrae, which precede osteolysis.

MRI is preferred over CT in early cases where clinical signs are present but no radiographic abnormalities are present[72] (Fig. 5 & 6).

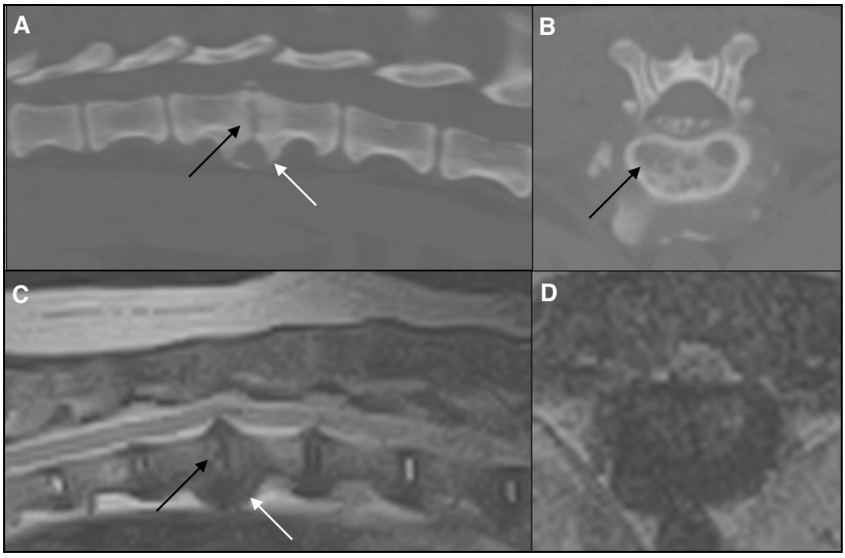

Fig. 5 : A) Precontrast sagittal MPR and B) transverse CT (bone window) images of a dog: A) Irregular sclerotic endplates (black arrow) and spondylosis (white arrow) is visible at the level of T12-T13. B) Lytic lesions are visible at the caudal endplate of T12. C) T2WSE sagittal and D) transverse MRI image of the same region of the dog: C) Sclerotic hypointense endplates (black arrow) and spondylosis (white arrow) is visible at the level of T12-T13. D) No signs of inflammation are present at the level of the intervertebral space T12-T13 or surrounding tissues. Images are indicative for an old or non-active discospondylitis.

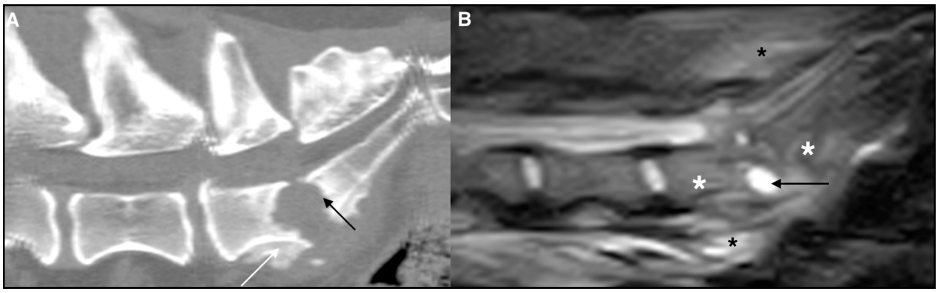

Fig. 6: A) Precontrast sagittal MPR CT (bone window) and B) sagittal STIR images of the lumbosacral region of a dog: A) Lytic endplates (black arrow) and spondylosis (white arrow) is visible at the level of L7-S1. B) A hyperintense signal consistent with inflammation is visible in the paravertebral soft tissues (black asterisk) and vertebral bodies (white asterisk). Hyperintense and abnormal shape of disc is present (black arrow). Images are indicative for an active discospondylitis.

Intervertebral disc disease and degenerative disorders

Intervertebral disc disease (IVDD) is the most common spinal disease of dogs (Fig. 7 & 8). Several studies have compared the accuracy of conventional myelography, non enhanced CT, contrast-enhanced CT and MRI for the detection of disc extrusions. Conventional CT has been reported to be 89-100% accurate to localize the lesion.[73-75] Computed tomography has a similar sensitivity for the detection of the site of disc herniation compared to myelography (81% versus 84%). CT had an increased sensitivity for the detection in large dogs and chronic cases, while myelography was found to be more useful in small dogs (<5kg).[76] Overall the sensitivity of MRI is greater than CT for detection of disc herniation (98.5 versus 88.6%).[75]

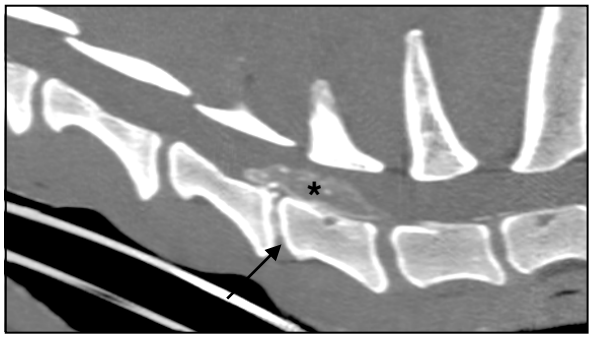

Fig. 7: Precontrast sagittal MPR CT image (bone window) of a dog with a disc extrusion at the level of C5-C6. A narrowed intervertebral space is visible (black arrow). Mineralized disc material is present (asterisk).

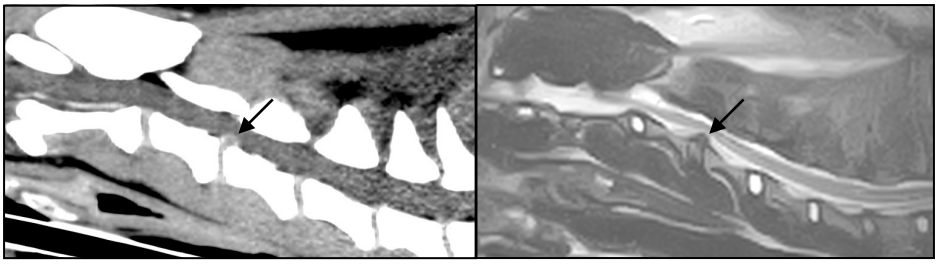

Fig. 8: A) Precontrast sagittal MPR CT (soft tissue window) and B) sagittal T2WSE images of a dog with a disc protrusion (arrow) at the level of C3-C4.

More specifically, MRI is more accurate to detect the site of intervertebral disc herniation associated spinal cord compression and to differentiate between extrusions and protrusions.[75] CT may be less accurate for the detection of protrusions.[74,75] In cases of hydrated nucleus pulposus extrusion (HNPE) only MR imaging features are available.[77] Acute non compressive nucleus pulposus extrusions (ANNPE) have the same clinical characteristics as FCE and can be presumptivly distinguished due to specific MRI characteristics.[78,79] No CT characteristics of ANNPE have been reported.

Degenerative lumbosacral stenosis (DLSS) (Fig. 9) is a relative common disorder that has a high prevalence in large dogs, especially German Shepard dogs.[80] DLSS is a multifactorial disorder in which cauda equina compression is predominantly caused by disc protrusion. Hypertrophy of the surrounding bony and soft tissue structures can contribute to progressive stenosis of the lumbosacral vertebral canal.[81] CT and MRI are both considered standard diagnostic tools for DLSS. CT findings are comparable to conventional radiography but provide extra information because of the possibility of reconstructing transverse images in different planes as well as demonstrating the loss of epidural fat.[82] This gives the ability to identify e.g. entrapped thickened nerve roots and to give more detail of the L7-S1 intervertebral foramina.[83] MR findings in dogs with DLSS are the same as for CT[84] but MRI provides more detailed information on IVD degeneration, dural sac, and/or nerve root displacement as well as loss of epidural fat. CT is more sensitive for soft-tissue calcifications, cortical bone spurs, and degenerative changes in the facet joints.[85] Although there seems to be a high degree of agreement between findings on CT and MR for DLSS the correlation of these features with surgical findings is only moderate.[84,86] In other degenerative diseases e.g. diffuse idiopathic skeletal hyperostosis (DISH) and spondylosis deformans (SD) both modalities can be used.[87] A recent study revealed that MRI allows differentiation between the two by providing information about the signal intensity of new bone.[88]

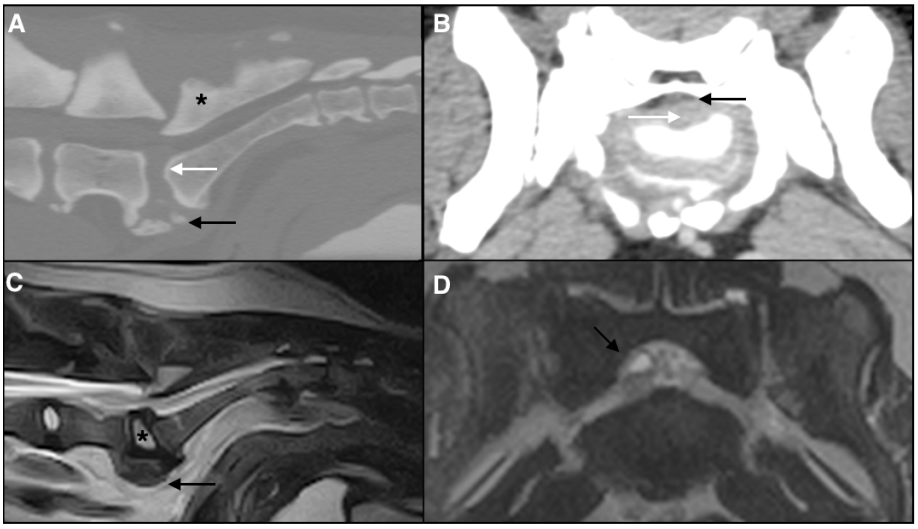

Fig. 9 : A) Precontrast sagittal MPR (bone window) and B) postcontrast transverse CT (soft tissue window) images of the lumbosacral region of a dog: A) A lumbosacral step (white arrow) and spondylosis (black arrow) is visible at the level of L7-S1. Ventral displacement of the roof of the sacrum (asterisk) B) Loss of epidural fat (white arrow) and disc protrusion is visible. C) T2WSE sagittal and D) transverse MRI image of the same region of the dog: C) A degenerative disc (black arrow) and spondylosis (black arrow) is visible at the level of L7-S1. D) A dorsal Tarlov cyst is present (black arrow).

Metabolic/ toxic/ degenerative brain disease

In these diseases e.g. lysomal storage disease, mitochondrial encephalopathy, hepatic encephalopathy, thiamine deficiency,… MRI is the modality of choice (Fig. 10). MRI characteristics are well described and include bilateral symmetric lesions and abnormal findings of the corpus callosum.[89] In degenerative disease such as age-related degeneration, CT and MR features are described and include enlargement of the ventricular system and prominence of the brain cortical margins and sulci due to expansion of subarachnoid space volume.[90] MRI findings have been reported that can be used to differentiate between age related cerebrocortical atrophy and cognitive dysfunction syndrome. [91]

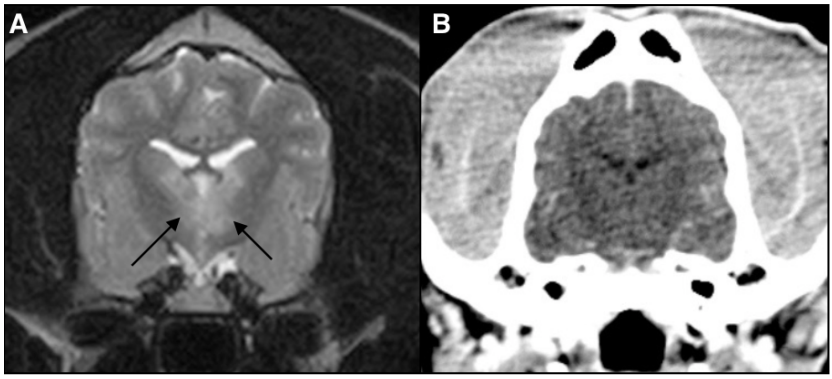

Fig. 10 : A) T2WSE transverse MRI and B) postcontrast transverse CT (brain window) image at the level of the thalamus of a dog. A) Bilateral hyperintense symmetric lesions (arrows) are visible at the thalamus. B) No lesions are visible. The images are suggestive for a metabolic disease (osmotic myelinolysis).

Craniospinal trauma

In human medicine, CT is the modality of choice for evaluating traumatic brain injury (TBI). Scan times are relatively short which provide the opportunity to perform these studies without general anesthesia in unstable patients. Use of the more recent multislice CT units reduce scanning time and allow for quick selective rescanning of slices affected by motion artefact[92]. CT is very sensitive for acute haemorrhages, cerebral oedema and skull fractures (Fig. 11). CT is the imaging modality of choice especially in the first 6 hours after brain injury to evaluate haemorrhages[29,93]. Magnetic resonance imaging is preferred when clinical signs are not explained by CT findings or in patients with subacute to chronic brain trauma[94,95]. The ability of MRI to detect hematomas improves over time as the haemoglobin composition of blood changes (see above). To our knowledge there are no reports investigating the value of CT in TBI in dogs and cats. A recent study[96] revealed that 66% of dogs imaged with MRI within 14 days of TBI had abnormal findings, which were associated with prognosis.

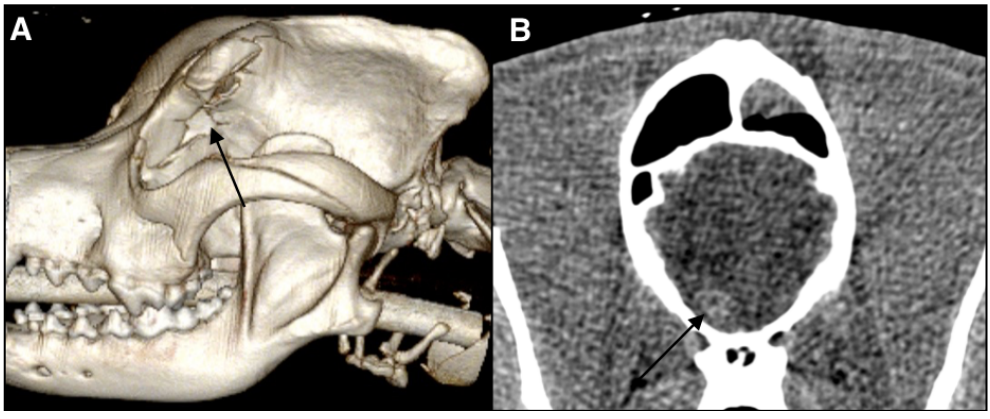

Fig. 11: A) Volume rendering and B) precontrast transverse CT image of a dog with an acute brain trauma. A) Multiple fractures (arrow) are visible at the level of the frontal bone. B) An intraparenchymal hemorrhage (arrow) is visible ventrally in the frontal lobe.

CT is an ideal modality for evaluating the extent of vertebral fractures and to observe for bone fragments resulting from vertebral fracture into the vertebral canal.[97,98]

Compared to CT, survey radiographs have a sensitivity of 72% for the detection of fractures and 77,5% for the detection of subluxation.[99] MRI is considered a superior diagnostic modality for imaging soft-tissue structures (e.g. spinal cord, nerve roots, and intervertebral discs) and is the imaging modality of choice for evaluating parenchymal injuries[100] (Fig.12). MRI is less sensitive and specific for detecting and characterizing vertebral fractures or subluxations. GRE sequences can be used to better delineate bone (signal void) from surrounding soft tissues, and thin collimation and reformatted images can aid fracture diagnosis.[101] CT can be used in vertebral stabilization surgeries to define optimal safe implant position/corridors in dogs and cats.[102,103]

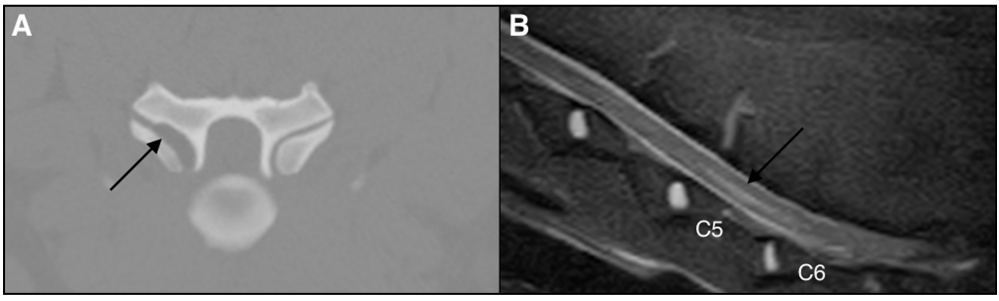

Fig. 12 : A) Precontrast transverse CT (bone window) and B) STIR transverse MRI image of the cervical spine of a dog. A) A widened right articular facet joint (arrow) is present at the level of C5-C6. B) A hyperintense intramedullary lesion is visible. A subluxation is present at the level of C5-C6 with a presumed intramedullary hemorrhage or oedema.

Cranial nerves, brachial and lumbosacral plexus

CT and MRI imaging of normal cranial nerves have been described.[104,105] However, not all individual cranial nerves can be identified using conventional MRI sequences used in veterinary medicine. Image slices are thick relative to the diameter of the nerves, and subtle abnormalities of nerves might therefore be missed.[104] Sensitivity and specificity can be increased, in detecting e.g. facial nerve abnormalities, by using specific sequences such as volumetric interpolated breath-hold examination sequences.[106] Brachial plexus avulsions with the presence of a dural tear can be diagnosed by CT myelography.[107] Conventional MR imaging is a standard procedure used in humans to detect nerve root avulsions although it is less reliable than CT myelography.[108] In veterinary medicine conventional MRI findings and MRI with intrathecal contrast is described in one dog.[109] For the detection of primary or secondary nerve sheath tumors both modalities can be used.[110,111] STIR MR sequences are valuable because of the ability to suppress signal from fat, making the hyperintense neoplastic nerve lesions more noticeable.[112] Masses as small as 1.0 cm can be identified on contrast- enhanced CT scans with a single slice machine[110] (Fig. 13).

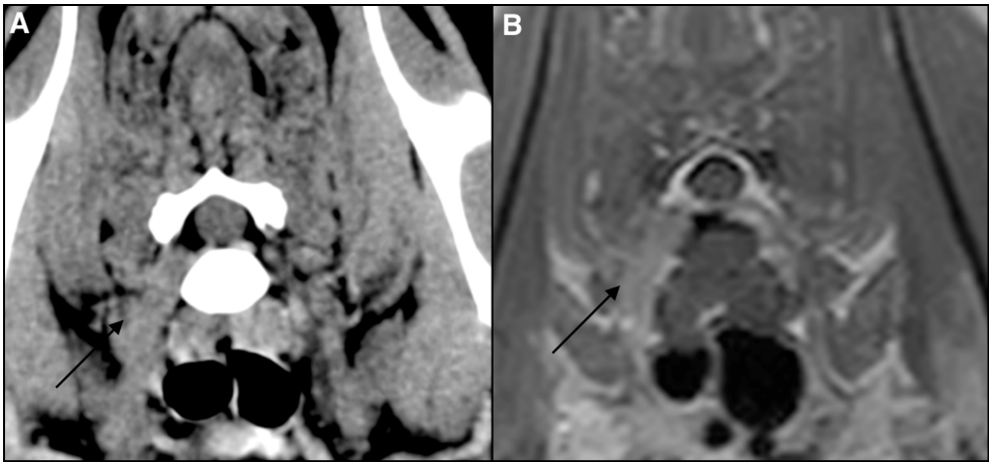

Fig. 13: Postcontrast transverse A) CT and B) T1WSE image at the level of C7-T1. A & B) An enlarged right spinal nerve is visible. Images are suggestive for a peripheral nerve sheath tumor.

Table 1. Indications for CT and MRI in brain and spinal disease

Indication	CT	MRI
Congenital and developmental anomalies	x - assessment of bony changes/abnormalities e.g. vertebral malformations, articular process abnormalities,… - multifactorial disease e.g. cervical spondylomyelopathy	xxx
Vascular disease	(x) acute haemorrhage	xxx
Intracranial and spinal neoplasia	x - detection of calcifications, lytic lesions, hyperostosis,.. - lesions caudal fossa can be missed	xx
Inflammatory disease	to exclude other lesions	xxx
IVD and degenerative disorders	x - mineralized disc material - multifactorial disease e.g. degenerative lumbosacral stenosis	xx
Metabolic/toxic/degenerative brain disease	to exclude other lesions	xxx
Craniospinal trauma	xx(x) - unstable patient - vertebral & skull fractures, luxations,… - acute haemorrhage (< 6 hours)	xx
Cranial nerves, brachial and lumbosacral plexus	x - CT myelography (dural tear)	xx

Role of MRI and CT in the diagnostic work-up of epileptic veterinary patients

MRI is the diagnostic imaging modality of choice for evaluation of the brain in animals with seizures. MRI is indicated when a structural epilepsy is suspected or to support the diagnosis of idiopathic epilepsy.[113] Recently a standardized veterinary epilepsy-specific MRI protocol was developed which will facilitate more detailed examination of areas susceptible to generating and perpetuating seizures.[114] MRI plays an additional role in the detection of postictal damage of the brain. Severe seizure activity can cause reversible MR signal changes in certain areas of the brain. In dogs, these changes have been identified unilaterally or bilaterally, predominantly in the piriform and temporal lobes, but also in the olfactory bulb and frontal lobe on MRI. These changes most probably represent cytotoxic and vasogenic oedema induced by seizures.[115] In human medicine, guidelines for neuroimaging studies suggest that a CT can be the diagnostic imaging of choice in patients with epilepsy if an MRI is not available. CT can be used in emergency situations, the perioperative period and can be useful to assess electrode placement.[116]

2.3. Conclusion

Overall MRI is the modality of choice in patients with suspected lesions of the brain or the spinal cord (table 1). CT can be used when MRI is not available or in cases where the patient is unstable and a quick assessment is necessary such as in hyperacute traumatic events. In some diseases both techniques can be used in a complementary matter. This is especially true for multifactorial disorders e.g. CSM, DLSS,.. which are associated with both bony and soft tissue abnormalities.

2.4. References

1. Schroder H., Meyer-Lindenberg A., Nolte I. Comparative examination of the lateral cerebral ventricles of different dog breeds using quantitative computer tomography. *Berl Munch Tierarztl* 2006; 119: 506-511.

2. Adamiak Z., Jaskolska M., Pomianowski A. Low field Magnetic Resonance Imaging of canine hydrocephalus. *Pak Vet J* 2012; 32: 128–130.

3. Ryan R.T., Glass E.N., Seiler G. et al. Magnetic resonance imaging findings associated with lateral cerebral ventriculomegaly in English Bulldogs. *Vet Rad Ultrasound* 2013; 55: 292-299.

4. Laubner S., Ondreka N., Failing K. et al. Magnetic resonance imaging signs of high intraventricular pressure - comparison of findings in dogs with clinically relevant internal hydrocephalus and asymptomatic dogs with ventriculomegaly. *BMC Vet Res* 2015, 11: 181.

5. Thomas W.B. Diskospondylitis and other vertebral infections *Vet Clin N Am-Small* 2009; 30: 169-182.

6. Porat-Mosenco Y., Schwarz T., Kass P.H. Thick-section reformatting of thinly collimated computed tomography for reduction of skull-base-related artifacts in dogs and horses. *Vet Radiol Ultrasound* 2004; 45: 131-135.

7. Pomianowski A., Adamiak Z. Magnetic Resonance Imaging as a useful tool for the selection of pharmacological and surgical treatment options for canine hydrocephalus. *B Vet I Pulawy* 2012; 56: 389–391.

8. Shihab N., Davies E., Kenny P.J. et al. Treatment of hydrocephalus with ventriculoperitoneal shunting in twelve dogs.*Vet Surg* 2011; 40: 477-84.

9. Platt S.R., McConnell J.F. & Matiasek Imaging diagnosis—Ventriculo-peritoneal shunt associated infection in a dog. *Vet Rad Ultrasound* 2012; 53: 80-83.

10. Vernau K.M., Kortz G.D., Koblik P.D. et al. Magnetic resonance imaging and computed tomography characteristics of intracranial intra-arachnoid cysts in 6 dogs. *Vet Radiol Ultrasound* 1997; 38: 171-176.

11. Mauler D.A., De Decker S., De Risio L. et al. Signalment, clinical presentation, and diagnostic findings in 122 dogs with spinal arachnoid diverticula. *J Vet Int Med* 2014; 28: 175-81.

14. Moissonnier P., Blot S., Devauchelle P. et al. Stereotactic CT-guided brain biopsy in the dog. *J Small Anim Pract* 2002; 43: 115-23.

15. Vizcaino Reces N., Stahl C., Stoffel M. et al. CT scan based determination of optimal bone corridor for atlantoaxial ventral screw fixation in miniature breed dogs. *Vet Surg* 2013; 42: 819-824.

16. Middelton G., Hillmann D.J., Trichel J. et al. Magnetic resonance imaging of the ligamentous structures of the occipitoatlantoaxial region in the dog. *Vet Radiol Ultrasound* 2012; 53: 545–551.

17. Marino D.J., Loughin C.A., Dewey C.W. et al. Morphometric features of the craniocervical junction region in dogs with suspected Chiari-like malformation determined by combined use of magnetic resonance imaging and computed tomography. *Am J Vet Res* 2012; 73: 105-11.

18. Cerda-Gonzales S., Olby N.J., McCullough S. at al. Morphology of the caudal fossa in Cavalier King Charles Spaniels. *Vet Radiol Ultrasound* 2009; 50: 37–46.

19. Rusbridge C., Greitz D., Iskandar B.J. Syringomyelia: Current Concepts in Pathogenesis, Diagnosis, and Treatment. *J Vet Intern Med* 2006; 20: 469-479.

20. Couturier J., Rault D., Cauzinille L. Chiari-like malformation and syringomyelia in normal Cavalier King Charles spaniels: a multiple diagnositic imaging approach. *J Small Anim Practice* 2008; 49: 438-443.

21. Lipsitz D., Levitski R.E., Chauvet A.E. et al. Magnetic resonance imaging features of cervical stenotic myelopathy in 21 dogs. *Vet Radiol Ultrasound* 2001; 42: 20–27.

22. Da Costa R.C., Parent J., Dobson H. et al. Comparison of magnetic resonance imaging and myelography in 18 Doberman Pinscher dogs with cervical spondylomyelopathy. *Vet Radiol Ultrasound* 2006; 47: 523–531.

23. De Decker S., Gielen I.M., Duchateau, L. et al. Low-field magnetic resonance imaging findings of the caudal portion of the cervical region in clinically normal Doberman Pinschers and Foxhounds. *Am J Vet Res* 2010; 71: 428–434.

24. Gutierrez-Quintana R., Penderis J. MRI features of cervical articular process degenerative joint disease in Great Dane dogs with cervical spondylomyelopathy. *Vet Radiol Ultrasound* 2012; 53: 304-311.

25. De Decker S., Gielen I.M., Duchateau, L. Intraobserver, interobserver and intermethod agreement of myelography, computed tomography–myelography, and low field magnetic resonance imaging in dogs with disc associated wobbler syndrome. *J Am Vet Med Assoc* 2011; 238: 1601-1608.

26. Martin-Vaquero P.M., Da Costa R.C., Drost W.M.T. Comparison of noncontrast computed tomography and high-field magnetic resonance imaging in the evaluation of great danes with cervical spondylomyelpathy. *Vet Radiol Ultrasound* 2014; 55: 496-505.

27. Hoggard N., Wilkinson I.D., Paley M.N. et al. Imaging of haemorrhagic stroke. *Clin Radiol* 2002; 57: 957–968.

28. Schellinger P.D., Jansen O., Fiebach J.B. et al. A standardized MRI stroke protocol: comparison with CT in hyperacute intracerebral hemorrhage. *Stroke* 1999; 30: 765–768.

29. Tidwell C.S., Chalela J.A., SAaver J.L. Comparison of MRI and CT for detection of acute intracerebral hemorrhage. *J Am Med Assoc* 2004; 292: 1823-1830.

30. Fulkerson C.V., Young, B.J., Jackson N.D. et al. MRI characteristics of cerebral microbleeds in four dogs. *Vet Radiol Ultrasound* 2012; 53: 389-393.

31. Parizel P.M., Makkat S., Van Miert E. Intracranial hemorrhage: principles of CT and MRI interpretation. *Eur Radiol* 2001; 11: 1770-1783.

32. Heiland S. Diffusion- and perfusion-weighted MR imaging in acute stroke: principles, methods, and applications. *Imaging Decisions MRI* 2003; 7: 4–12.

33. Garosi L., McConnell J.F., Platt S.R. et al. Clinical and topographic magnetic resonance characteristics of suspected brain infarction in 40 dogs. *J Vet Int Med* 2006; 20: 311–321.

34. Tidwell A.S., Robertson I.D. Magnetic resonance imaging of normal and abnormal brain perfusion. *Vet Radiol & Ultrasound* 2011; 52 supplement 1: 62–71.

35. Hartmann A., Soffler C., Failing K. et al. Diffusion-weighted magnetic resonance imaging of the normal canine brain. *Vet Radiol Ultrasound* 2014; 55: 592-598.

36. Sutherland-Smith J., King R., Faissler, D. et al. Magnetic resonance imaging apparent diffusion coefficients for histologically confirmed intracranial lesions in dogs. *Vet Radiol Ultrasound* 2011; 52: 142–148.

37. Tidwell A.S., Ross L.A., Kleine L.J. Computed tomography and magnetic resonance imaging of cavernous sinus enlargement in a dog with unilateral exophtalmos. *Vet Radiol Ultrasound* 1997; 38: 363-370.

38. Grunenfelder F.L., Weishaupt D., Green R. et al. Magnetic resonance imaging findings in spinal cord infarction in three small breed dogs. *Vet Radiol Ultrasound* 2005; 46: 91–96.

39. De Risio L., Adams V., Dennis R. Magnetic resonance imaging findings and clinical associations in 52 dogs with suspected ischemic myelopathy. *J Vet Int Med* 2007; 21: 1290–1298.

40. Snyder J.M., Shofer F.S., Van Winkle T.J. et al. Canine intracranial primary neoplasia: 173 Cases (1986–2003). *J Vet Int Med* 2006; 20: 669–675.

41. Young B.D., Fosgate G.T., Holmes S.P. et al. Evaluation of standard magnetic resonance characteristics used to differentiate neoplastic, inflammatory, and vascular brain lesions in dogs. *Vet Radiol Ultrasound* 2014; 55: 399-406.

42. Young B.D., Levine J.M., Porter B.F. et al. Magnetic resonance imaging features of intracranial astrocytomas and oligodendrogliomas in dogs. *Vet Radiol Ultrasound* 2011; 52: 132-141.

43. Rodena S., PumarolaM., Gaiteri L. et al. Magnetic resonance imaging findings in 40 dogs with histologically confirmed intracranial tumours. *Vet J* 2011; 187: 85-91.

44. Kippenes H., Gavin P.R., Bagley R.S. Magnetic resonance imaging features of tumors of the spine and spinal cord in dogs. *Vet Radiol Ultrasound* 1999; 40: 627–633.

45. Fuchs C., Meyer-Lindenberg A., Wohlsein P. et al. Computertomographic characteristics of primary brain tumors in dogs and cats. *Berl Munch Tierarztl* 2003; 116: 436-42.

46. Wisner E.R., Dickinson P.J., Higgins R.J. Magnetic resonance imaging features of canine intracranial neoplasia. *Vet Radiol Ultrasound* 2011; 52: S52-61.

47. Bentley R.T. Magnetic resonance imaging diagnosis of brain tumors in dogs. *Vet J* 2015; 205: 204-16.

48. Koblik P.D., Lecouteur, R.A., Higgings R.J et al. CT-guided brain biopsy using a modified Pelorus Mark III stereotactic system: experience with 50 dogs. *Vet Radiol Ultrasound* 1999; 40: 434-440.

49. Moissonnier P., Blot S., Devauchelle P. et al. Stereotactic CT-guided brain biopsy in the dog. *J Small Anim Practice* 2002; 43: 115-23.

50. Vignoli M., Ohlreth S., Rossi F. Computed tomography-guided fine-needle aspiration and tissue-core biopsy of bone lesions in small animals. *Vet Radiol Ultrasound* 2004; 45: 125-130.

51. Chen A.V., Wininger F.A., Frey S. et al. Description and validation of a magnetic resonance imaging-guided stereotactic brain biopsy device in the dog. *Vet Radiol Ultrasound* 2012; 53: 150-156.

52. Flegel T., Oevermann A., Oechtering G. et al. Diagnostic yield and adverse effects of MRI-guided free-hand brain biopsies through a mini-burr hole in dogs with encephalitis. *J Vet Int Med* 2012; 26: 969–976.

53. Auriemma E., Barthez P.Y., Van Der Vlugt-Meijer R.h. et al. Computed tomography and low−field magnetic resonance imaging of the pituitary gland in dogs with pituitary−dependent hyperadrenocorticism: 11 cases (2001–2003). *J Am Vet Med Assoc* 2009; 235: 409–414.

54. Pollard R.E., Reilly C.M., Uerling M.R. Cross-sectional imaging characteristics of pituitary adenomas, invasive adenomas and adenocarcinomas in dogs: 33 cases (1988–2006). *J Vet Int Med* 2010; 24: 160–165.

55. Van Der Vlugt-Meijer R.H., Meij, B.P., Van Den Ingh T.S.et al. Dynamic computed tomography of the pituitary gland in dogs with pituitary-dependent hyperadrenocorticism. *J Vet Int Med* 2003; 17: 773–780.

56. Taoda T., Hara Y., Masuda H. et al. Magnetic resonance imaging assessment of pituitary posterior lobe displacement in dogs with pituitary-dependent hyperadrenocorticism. *J Vet Med Sci* 2011; 73: 725–731.

57. Drost W.T., Love N.E., Berry C.R. Comparison of radiography, myelography and computed tomography in the evaluation of canine vertebral and spinal cord tumors in sixteen dog. *Vet Radiol Ultrasound* 1996; 37: 28-33.

58. Benigni L., Lamb C.R. Comparison of fluid-attenuated inversion recovery and T2-weighted magnetic resonance images in dogs and cats with suspected brain disease. *Vet Radiol Ultrasound* 2005; 46: 287-292.

59. Cherubini G.B., Platt S.R., Anderson T.J. et al. Characteristics of magnetic resonance images of granulomatous meningoencephalomyelitis in 11 dogs. *Vet Rec* 2006; 159:110–115.

60. Talarico L.R., Schatzberg S.J. Idiopathic granulomatous and necrotising inflammatory disorders of the canine central nervous system: a review and future perspectives. *J Small Anim Pract* 2010; 51: 138–149.

61. Von Praun F., Matiasek K., Grevel V. Magnetic resonance imaging and pathologic findings associated with necrotizing encephalitis in two Yorkshire terriers. *Vet Radiol Ultrasound* 2006; 47: 260–264.

62. Adamo P.F., Adams W.M., & Steinbergh H. Granulomatous meningoencephalomyelitis in dogs. *Compendium* 2007; 27: 678-690.

63. Young B.D., Levine J.M., Fosgate G.T. et al. Magnetic resonance imaging characteristics of necrotizing meningoencephalitis in Pug dogs. *J Vet Int Med* 2009; 23: 527–535.

64. Lamb C.R., Croson P.J., Cappello R. Magnetic resonance imaging findings in 25 dogs with inflammatory cerebrospinal fluid. *Vet Radiol Ultrasound* 2005; 46: 17–22.

65. Tipold, A. Diagnosis of inflammatory and infectious diseases of the central nervous system in dogs: a retrospective study. *J Vet Int Med* 1995; 9: 304–314.

66. Levine G. J., Cook J.R., Kerwin S.C. et al. Relationships between cerebrospinal fluid characteristics, injury severity, and functional outcome in dogs with and without intervertebral disk herniation. *Vet Clin Path* 2014; 43: 437- 446.

67. Cizinauskas S., Jaggy A., Tipold A. Long-term treatment of dogs with steroid-responsive meningitis-arteritis: clinical, laboratory and therapeutic results. *J Small Anim Pract* 2000; 41: 295-301

68. Eminaga S., Cherubini G.B., Villiers E. et al. STIR muscle hyperintensity in the cervical muscles associated with inflammatory spinal cord disease of unknown origin. *J Small Anim Pract* 2013; 54: 137-42.

69. Mulkern R.V. (2009) Fast imaging principles. In: Magnetic Resonance Imaging of the Brain and Spine. Ed. S. W. Atlas. 4th edn. Wolters Kluver/Lippincott Williams & Wilkins,. pp. 94-150.

70. Thomas, W.B. Hydrocaphalus in dogs and cats. *Vet Clin N Am Small Anim Pract* 2010; 40: 143-159.

71. Gonzalo-Orden J.M., Altonoga J.R., Orden M.A. Magnetic resonance, computed tomographic and radiologic findings in a dog with discospondylitis. *Vet Radiol Ultrasound* 2000; 41: 142-144.

72. Carrera L., Sullivan M., McConnell F. et al. Magnetic resonance imaging features of discospondylitis in dogs. *Vet Radiol Ultrasound* 2011; 52: 125-131.

73. Shimizi J., Yamada K., Mochida K. et al. Comparison of the diagnosis of intervertebral disc herniations in dogs by CT before and after contrast enhancement of the subarachnoid space. *Vet Rec* 2009; 165: 200-202.

74. Bibevski J.D., Daye R.M., Henrickson T.D. A prospective evaluation of CT in acutely paraparetic chondrodystrophic dogs. *J Am Anim Hosp Assoc* 2013; 49: 363-369.

75. Cooper J.J., Young B.B., Griffin J.F. at al. Comparison between non contrast computed tomography and magnetic resonance imaging for detection and characterization of thoracolumbar myelopathy caused by intervertebral disk herniation in dogs. *Vet Radiol Ultrasound* 2014; 55: 182-189.

76. Israel S.K., LevineJ.M., Kerwin S.C. et al. The relative sensitivity of computed tomography and myelography for identification of thoracolumbar intervertebral disk herniations in dogs. *Vet Radiol Ultrasound* 2009; 50: 246-252.

77. Manunta M.L., Evangelisti M.A., Bergknut N.et al. Hydrated nucleus pulposus herniation in seven dogs. *Vet J* 2015; 203: 342-344.

78. De Risio L., Adams V., Dennia R. et al. Association of clinical and magnetic resonance imaging findings with outcome in dogs with presumptive acute noncompressive nucleus pulposus extrusion: 42 cases (2000–2007). *J Am Vet Med Assoc* 2009; 234: 495–504.

79. Fenn J., Dress R., Volk H.A. et al. Inter- and intraobserver agreement for diagnosing presumptive ishemic myelopathy and acute noncompressive nucleus pulposus extrusion in dogs using magnetic resonance imaging. *Vet Radiol & Ultrasound*, Epub 2015 Aug 25

80. Suwangkon N., Meij B.P., Voorhout G. et al. Review and retrospective analysis of degenerative lumbosacral stenosis in 156 dogs treated by dorsal laminectomy. *Vet Comp Ortho Trauma* 2008; 21: 285–293.

81. De Decker S., Wawrzenski, L.A. & Volk H.A. Clinical signs and outcome of dogs treated medically for degenerative lumbosacral stenosis: 98 cases (2004–2012). *J Am Vet Med Assoc* 2014; 245: 408-413.

82. Ramirez O. 3rd, Thrall D.E. A review of imaging techniques for canine cauda equina syndrome. *Vet Radiol Ultrasound* 1998; 39: 283–296.

83. Wood B.C., Lanz O.I., Jones J.C. et al. Endoscopic-assisted lumbosacral foraminotomy in the dog. *Vet Surg* 2004; 33: 221–231.

84. Suwankong N., Voorhout G., Hazewinkel H.A. et al. Agreement between computed tomography, magnetic resonance imaging, and surgical findings in dogs with degenerative lumbosacral stenosis. *J Am Vet Med Assoc* 2006; 229: 1924-1929.

85. Sande R.D. Radiography, myelography, computed tomography, and magnetic resonance imaging of the spine. *Vet Clin N Am-Small* 2011; 22: 811–831.

86. Jones J.C., Inzana K.D. Subclinical CT abnormalities in the lumbosacral spine of older large breed dogs. *Vet Radiol Ultrasound* 2000; 41: 19–26.

87. Kranenburg H.C., Voorhout G., Grinwis G.C. Diffuse idiopathic skeletal hyperostosis (DISH) and spondylosis deformans in purebred dogs: a retrospective radiographic study. *Vet J* 2011; 190: 84-90.

88. Togni A., Hanenburg H.J., Morgan J.P. et al. Radiographic and MRI characteristics of lumbar disseminated idiopathic spinal hyperostosis and spondylosis deformans in dogs. *J Small Anim Pract* 2014; 55: 343-349.

89. Hasegawa D., Tamura S., Nakamoto Y. et al. Magnetic resonance findings of the corpus callosum in canine and feline lysosomal storage diseases. *Vet J* 2010; 186: 166-171.

90. Pugliese M., Carrasco J.L., Gomez- Anson B. et al. Magnetic resonance imaging of cerebral involutional changes in dogs as markers of aging: an innovative tool adapted from a human visual rating scale. *Vet J* 2013; 186: 166-171.

91. Hasegawa D., Tamura S., Nakamoto, Y. et al. Magnetic resonance findings of the corpus callosum in canine and feline lysosomal storage diseases. *Vet J* 2005; 186: 166-171.

92. Jones T.R., Kaplan R.T., Lane B. et al. Single- versus multi-detector row CT of the brain: quality assessment. *Radiol* 2001; 219; 750–755.

93. Enzmann D., Britt R., Lyons B. et al. Natural history of experimental intracerebral hemorrhage: sonography, computed tomography and neuropathology. *Am J Neurorad* 1981; 2: 517–526.

94. Le T.H., Gean A.D. Neuroimaging of traumatic brain injury. *Mt Sinai J Med* 2009; 76: 145-162.

95. TBI working group. Clinical practice guideline for management of concussion/mild traumatic brain injury. *J Rehabil Res Dev* 2009; 46: 1–68.

96. Beltran E., Platt S.R., McConnell J.F. et al. Prognostic value of early magnetic resonance imaging in dogs after traumatic brain injury: 50 cases. *J Vet Int Med* 2014; 28: 1256-1262.

97. Vitale C. & Coates J. Acute spinal cord injury. *Standards of Care: Emergency and critical care medicine* 2007; 9: 1–11.

98. Da Costa R.C., Samii V.F. Advanced imaging of the spine in small animals. *Vet Clin N Am-Small* 2010; 40: 765–790.

99. Kinns J., Mai W., Seiler G. et al. Radiographic sensitivity and negative predictive value for acute canine spinal trauma. *Vet Radiol Ultrasound* 2006; 47: 563-570.

100. Levine G., Levine, J., Budke C. et al. Description and repeatability of a newly developed spinal cord injury scale for dogs. *Prevent Vet Med* 2009; 89: 121–127.

101. Johnson P., Beltran E., Dennis R. et al. Magnetic resonance imaging characteristics of suspected vertebral instability associated with fracture or subluxation in eleven dogs. *Vet Radiol & Ultrasound* 2012; 53, 552–559.

102. Hettlich B.F., Fosgate G.T., Levine J.M. et al. (2010) Accuracy of conventional radiography and computed tomography in predicting implant position in relation to the vertebral canal in dogs. *Vet Surg* 2010; 39: 680-687.

103. Vallefuoco R., Bedu, A.S., Manaserro M. et al. Computed tomographic study of the optimal safe implantation corridors in feline thoracolumbar vertebrae. *Vet Comp Orthop Traumato* 2013; 26: 372-378.

104. Couturier L., Degueurce C., Ruel Y. et al. Anatomical study of cranial nerve emergence and skull foramina in the dog using magnetic resonance imaging and computed tomography. *Vet Radiol Ultrasound* 2005; 47: 375–383.

105. Gomes E., Degueurce C., Ruel Y. et al. Anatomic study of cranial nerve emergence and associated skull foramina in cats using CT and MRI. *Vet Radiol Ultrasound* 2009; 50: 398–403.

106. Smith P.M., Goncalves R., Mc Connell J.F. Sensitivity and specificity of MRI for detecting facial nerve abnormalities in dogs with facial neuropathy. *Vet Rec* 2012; 171: 349.

107. Forterre F., Gutmannsbauer B., Schmall W. et al. CT myelography for diagnosis of brachial plexus avulsion in small animals. *Tierarztl Praxis K H* 1988; 26: 322–329.

108. Carvalho G.A., Nikkhah G., Matthies C. et al. Diagnosis of root avulsions in traumatic brachial plexus injuries: value of computerized tomography myelography and magnetic resonance imaging. *J Neurosurg* 1997; 86: 69–76.

109. Munoz A., Mateo I., Lorenzo V. et al. Imaging diagnosis: traumatic dural tear diagnosed using intrathecal gadopentate dimeglumine. *Vet Radiol Ultrasound* 2009; 50: 502–505.

110. Rudich S.R., Feeney D.A., Anderson K.L. et al. Computed tomography of masses of the brachial plexus and contributing nerve roots in dogs. *Vet Radiol Ultrasound* 2004; 45: 46–50.

111. Kraft S., Ehrhart E.J., Gall D. et al. Magnetic resonance imaging characteristics of peripheral nerve sheath tumors of the canine brachial plexus in 18 dogs. *Vet Radiol Ultrasound* 2007; 48: 1–7.

112. Van Es H.W. MRI of the brachial plexus. *Eur Radiol* 2001; 11: 325– 336.

113. De Risio L. Chapter 10. In: De Risio L, Platt S, editors. Canine and feline epilepsy. Diagnosis and Management. 2014. p. 304–307.

114. Rusbridge C, Long S, Jovanovik J, et al. International Veterinary Epilepsy Task Force recommendations for a veterinary epilepsy-specific MRI protocol. *BMC Veterinary Research*. 2015;11: 194.

115. Mellema L.M., Koblik P.D., Kortz G.D. et al. Reversible magnetic resonance imaging abnormalities in dogs following seizures. *Vet Radiol Ultrasound* 1999; 40: 588–595.
116. Kuzniecky RI. Neuroimaging of Epilepsy: Therapeutic Implications. *NeuroRx*. 2005; 2: 384-393.

Scientific aims

CT and MRI are both cross-sectional imaging techniques used to visualize lesions of the brain, spinal cord and vertebral structures. In general MRI is considered the modality of choice because of its better contrast resolution and therefore better evaluation of soft tissue lesions. CT has its advantages due to the ability to better evaluate the bony structures. In human medicine comparative studies between both modalities in neurological diseases have been published. At present, veterinary medicine lacks these kinds of studies.

Because CT is more and more available in veterinary clinics and practices, the general aim of this of this work was to determine whether CT can be used as an alternative to MRI.

The aim of the first part of this research project was to see if there is an agreement between low-field MRI and CT in detecting suspected intracranial lesions in dogs and cats.

The aim of the second part was to determine if there was an agreement between low-field MRI and multislice CT in detecting specific brain and cervical spine abnormalities:

- detection of cerebellar (foramen magnum) herniation in Cavalier King Charles Spaniels,
- detection of cervical syringomyelia in dogs.

Chapter 3

Agreement between low-field MRI and CT for the detection of suspected intracranial lesions in dogs and cats

Adapted from: I.Gielen*, K. Kromhout*, P. Gavin, L. Van Ham, I. Polis, H. van Bree. Agreement between low-field MRI and CT for the detection of suspected intracranial lesions in dogs and cats. *Journal of the American Veterinary Medical Association* 2013; 243:367-375.

* *contributed equally to the study*

Summary

The objective of this study was to determine if there is agreement between CT and MRI for enabling detection of intracranial lesions in cats and dogs.

The CT and MR images of 51 dogs and 7 cats with suspected intracranial lesions were evaluated during a 2-year-period. Radiologists evaluated the images without awareness of subject identity. Agreement between methods was assessed for the ability to detect solitary or multiple lesions, selected lesions characteristics (via the Cohen κ statistic), and lesion dimensions (via Bland-Altman plots).

CT and MRI had substantial agreement for detection of lesions and whether the lesions were solitary or multiple. The presence of mass effect and contrast agent enhancement, which were considered principal diagnostic imaging signs, had almost perfect agreement, with a lower degree of agreement attained for identifying enhancement patterns and aspects of lesion margins. Agreement was substantial to almost perfect for lesion visualization in most anatomic brain regions, but poor for identifying lesion dimensions.

Degrees of agreement between CT and MRI for the detection and characterization of intracranial lesions ranged from poor to almost perfect, depending on the variable assessed. More investigation is needed into the relative analytic sensitivity and possible complementarities of CT and MRI in the detection of suspected intracranial lesions in dogs and cats.

Introduction

Computed tomography and MRI are both used in the detection of various intracranial lesions in humans and other animals. Each method has specific advantages and disadvantages in lesion characterization, but the method used is not chosen solely on the basis of a patient's neurological history, general condition, and suspected lesion type. Indeed, equipment availability and economic considerations also factor into that choice. Relative to MRI evaluations, CT examinations are faster and therefore require a shorter duration of anesthesia, the examinations are less costly, and CT scanners are more readily available in veterinary practices than MRI equipment.

Magnetic resonance imaging is considered superior to CT for visualizing pathologic changes in the brain because its analytic sensitivity for identifying soft tissue alterations is greater.[1] It is also the modality of choice for imaging lesions in specific anatomic locations such as the cerebellopontine angle. Lesions in certain anatomical locations such as the brainstem and cerebellum commonly fail to be identified when CT is used because of beam-hardening artifacts associated with the technique.[2,3] On the other hand, CT is more sensitive than MRI for visualizing bony changes such as osteolysis and hyperostosis.[4]

In humans, comparative studies[5-10] have shown that CT and MRI can be used in a complementary manner in the diagnosis of intracranial lesions. In veterinary medicine, CT and MRI have been extensively used for the detection of brain lesions.[3,11-19] In a study[20] in which CT, MRI, and myelography were evaluated for their usefulness in the diagnosis of vertebral disc herniation in dogs, MRI was deemed the superior imaging modality. However, to our knowledge, CT and MRI have not yet been compared for their usefulness in detecting intracranial lesions. The purpose of the study reported here was to prospectively evaluate the degree of agreement between CT and MRI for identification and characterization of lesions in cats and dogs with suspected intracranial pathologic change.

Materials and methods

Animals—Between January 2008 and March 2010, for a predetermined period of 2 weeks every 2 months, all cats and dogs with suspected intracranial disease that were evaluated through the Department of Veterinary Medical Imaging and Small Animal Orthopaedics of the Faculty of Veterinary Medicine, Ghent University were included in the study. Intermittent 2-week study periods at 2 month intervals were chosen for reasons of feasibility because continuous inclusion and examination of all cats and dogs evaluated would have interfered with daily patient care. The use of predefined periods at fixed intervals was an attempt to minimize selection bias.

After medical histories were obtained and a complete clinical evaluation including neurologic examination was performed, dogs and cats with a suspected intracranial lesion underwent MRI of the brain as part of the diagnostic work-up. Those patients evaluated during the predetermined 2-week inclusion periods also subsequently underwent CT of the brain on the same day. Owner consent was obtained prior to the examinations.

MRI protocol—Dogs and cats were anesthetized and positioned in dorsal recumbency, with their heads placed in a head or wrist coil for humans. Protocols included T2-weighted precontrast spin echo imaging in transverse and sagittal planes (repetition time, 3,500 to 6,100 milliseconds; echo time, 120 milliseconds), T1-weighted precontrast transverse and sagittal and postcontrast transverse spin echo imaging (repetition time, 400 to 800 milliseconds; echo time, 17 milliseconds), and transverse FLAIR imaging (repetition time, 1,000 to 1,150 milliseconds; echo time, 100 milliseconds). Four-millimeter-thick contiguous slices were chosen (image matrix, 512 X 512). Postcontrast images were obtained immediately after IV injection of 0.3 mL of contrast medium[b] (469.01 mg of gadopentetate dimeglumine/mL)/kg (0.14 mL/lb). Mean examination time was 90 minutes/subject.

CT protocol—Dogs and cats were anesthetized and positioned in dorsal recumbency. Computed tomographic transverse images in 4-mm-thick slices were obtained by use of a standard algorithm with a third-generation helical single-slice CT scanner[c] (image matrix, 512 X 512) before and immediately after IV administration of 2 mL of contrast medium[d] (62.24 g of iopromid)/kg (0.9 mL/lb). Mean examination time was 20 minutes/subject.

Image analysis—Images were reviewed with a DICOM (ie, Digital Imaging and Communications in Medicine) viewer.[e] Scans with patient information removed were evaluated by 2 experienced radiologists (IG and PG). The images were provided as CD-ROM's each containing a separate randomized sequence of studies of a particular diagnostic procedure (CT or MRI). All CT images were reviewed in a brain window (window width, 80 HU to 150 HU; window level, 40 HU to 75 HU). Adjustments of the window width and level were made by the radiologists to allow better visualization. The following parameters were evaluated: presence (vs absence) of an intracranial lesion, lesion pattern (solitary or multiple), lesion localization (lobe or region), aspect of margins (well or ill defined), pre- and postcontrast size of the lesion's mass effect, and presence (vs absence) and pattern of enhancement (homogeneous, heterogeneous, or ring enhancement).

Statistical analysis—Agreement between CT and MRI in allowing detection of intracranial lesions and their characteristics was calculated through calculation of the Cohen κ, with the degree of agreement defined as suggested elsewhere[21] (0.81 to 1.00, almost perfect agreement; 0.61 to 0.80, substantial agreement; 0.41 to 0.60, moderate agreement; 0.21 to 0.40, fair agreement; 0.20 to 0.0, slight agreement; and ≤ 0, no agreement). For κ values, confidence intervals and *P* values (reflecting the probability that the estimated κ was due to chance) are reported. Lesion dimensions as measured via CT and MRI were compared by means of Bland-Altman analysis.[22] Results are reported as bias and *P* values as well as limits of agreement.[f]

Results

Animals—Seven cats (4 males and 3 females; median age, 107 months [range, 66 to 168 months]) and 51 dogs (38 males and 13 females; median age, 77 months [range, 2 to 170 months]) were included in the study. Dog breeds included Labrador Retriever (n=6), German Shepherd Dog (5), Maltese (4), American Staffordshire Terrier (4), Staffordshire Bull Terrier (3), mixed breed (3), and 2 each of English Bulldog, Pug, French Bulldog, Boxer, and Border Collie as well as 1 each of various other breeds. Cat breeds were European Shorthair (n=6) and Persian (1). Clinical signs detected or reported by owners at the initial evaluation varied, the most common of which were seizures, paresis or paralysis, behavioral change, head tilt, apathy, drowsiness, strabismus, nystagmus, and ataxia.

Imaging—One or more intracranial lesions were detected in 38 of 58 cats and dogs either by CT, MRI, or both. In 30 of these 38 patients, the lesions were seen through both modalities (Fig. 1). Seven lesions detected by MRI were not detected by CT, and 1 lesion detected on CT was not visible on MRI images ($\kappa = 0.72$), reflecting substantial agreement (Table 1). Three of 7 patients with lesions that were detectable on MRI but not seen on CT were judged to have infarctions (2-month-old female Maltese evaluated for intention tremor and right vestibular strabismus, 2.5-year-old male Staffordshire Bull Terrier evaluated for circling to the right, signs of apathy, head pressing, and decrease in proprioception, and 7-year-old male Staffordshire Bull Terrier evaluated for seizures), 2 to have oedema (9-year-old mixed-breed dog with seizures and 2-year-old male Pug with seizures, signs of apathy, and tetraparesis), and 2 to have diffuse inflammatory lesions (6-year-old male Welsh Springer Spaniel with signs of apathy and 7-month-old male German Shepherd Dog with seizures). The 1 patient with a lesion that was detectable via CT but not via MRI was a 4-year-old male Maltese evaluated for seizures; the lesion seen on CT images was a contrast agent–enhanced multifocal lesion of suspected inflammatory origin (Fig. 2).

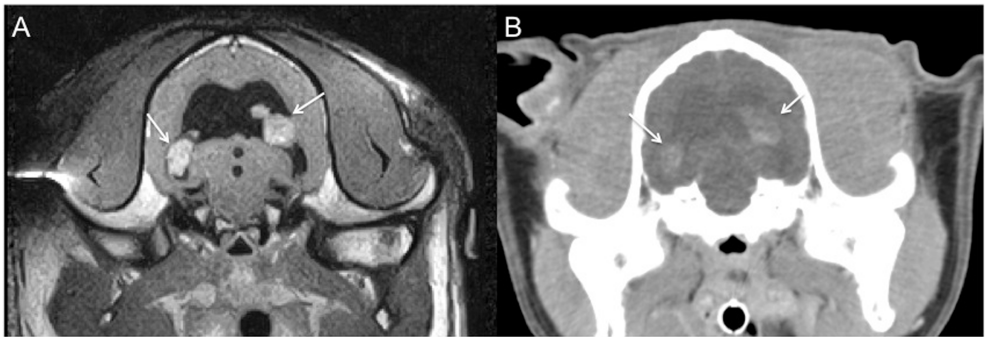

Fig. 1: Postcontrast transverse T1-weighted MRI (A) and postcontrast CT (B) images of the head of a dog with suspected intracranial lesions, as obtained at the level of the temporal lobe. Multiple homogeneously enhanced lesions are visible in both lateral ventricles (arrows) in both images.

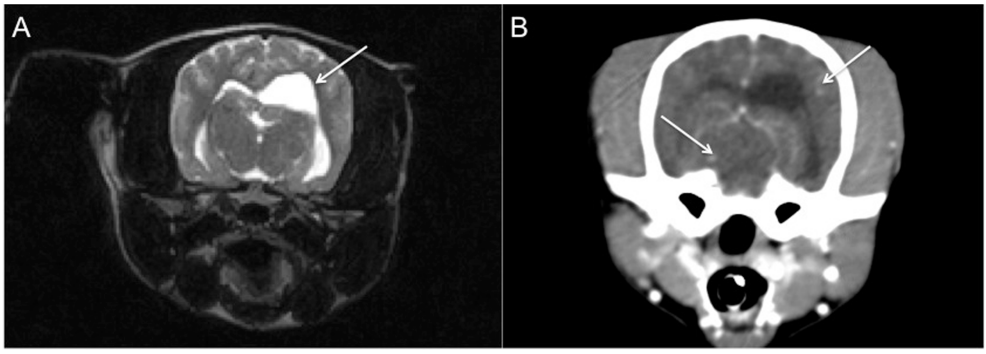

Fig. 2: Transverse T2-weighted MRI (A) and postcontrast CT (B) images of the head of a dog with suspected intracranial lesions. A) No lesion is visible in the parietal and temporal lobes; however, the lateral ventricles are asymmetric, with the left ventricle larger than the right (arrow). B) Multiple small hyperdense lesions (arrows) are visible in the telencephalon and diencephalon.

Images for the 30 patients with intracranial lesions visible via both MRI and CT were compared with respect to general lesion characteristics (Table 1). A mass effect was seen in 27 of these patients with each modality ($\kappa = 1$), reflecting perfect agreement between MRI and CT. Four of 30 patients had multiple lesions and 24 had solitary lesions visible through both imaging modalities ($\kappa = 0.76$), reflecting substantial agreement. However, only 16 lesions were interpreted as well defined and 5 as ill defined through both CT and MRI ($\kappa = 0.37$), reflecting fair agreement only.

Table 1: Number of cats and dogs (n = 58) with suspected intracranial disease in which space-occupying lesions were detected via CT and MRI and degree of agreement between imaging modalities for lesion detection and general imaging characteristics of detected lesions (30).

Characteristic	CT	MRI	CT and MRI	κ	95% CI	*P* value
Space-occupying lesion	31	37	30	0.72	0.54–0.9	< 0.001
Mass effect	27	27	27	1	1–1	< 0.001
Solitary (vs multiple) lesion	26	24	24	0.76	0.45–1.07	< 0.001
Well- (vs ill-) defined lesion	16	25	16	0.37	0.1–0.64	0.009

CI = Confidence interval.

Degrees of agreement were assessed as follows: almost perfect, $0.8 < \kappa \leq 1$; substantial, $0.6 < \kappa \leq 0.8$; moderate, $0.4 < \kappa \leq 0.6$; fair, $0.2 < \kappa \leq 0.4$; slight, $0.2 < \kappa < 0$, and no ≤ 0.

Images obtained by CT and MRI were compared with respect to the described anatomic localization of the intracranial lesions, revealing almost perfect agreement between the modalities for lesions located in the cerebrum ($\kappa = 0.86$) and the occipital lobe ($\kappa = 1$) and substantial agreement for lesions in the frontal lobe ($\kappa = 0.79$), parietal lobe ($\kappa = 0.79$), and cerebellum ($\kappa = 0.67$), and the intraventricular region ($\kappa = 0.67$; Table 2). The degree of agreement was moderate for lesions in the temporal lobe ($\kappa = 0.53$), fair for lesions in the brainstem ($\kappa = 0.38$) (Fig. 3), and slight for lesions in the piriform region ($\kappa = 0$) (Fig. 4).

Table 2: Number of cats and dogs (n = 30) with suspected intracranial disease in which space-occupying lesions* were detected in various anatomic regions via both CT and MRI and agreement between the imaging modalities for these findings.

Region	CT	MRI	CT and MRI	κ	95% CI	*P* value
Cerebrum	18	18	17	0.86	0.68–1.05	< 0.001
Lobe						
Frontal	10	13	10	0.79	0.57–1.01	< 0.001
Parietal	6	6	5	0.79	0.52–1.07	< 0.001
Temporal	8	10	6	0.53	0.2–0.85	0.004
Pyriform	0	7	0	0	-1–1	N/A
Occipital	4	4	4	1	1–1	< 0.001
Cerebellum	7	4	4	0.67	0.34–1.0	< 0.001
Brainstem	5	7	3	0.38	-0.02–0.78	0.03
Pituitary fossa	1	1	1	1	1–1	< 0.001
Intraventricular	4	7	4	0.67	0.34–1.0	< 0.001

*In some subjects, lesions were visible in > 1 anatomic region.

N/A = not applicable

See Table 1 for remainder of key.

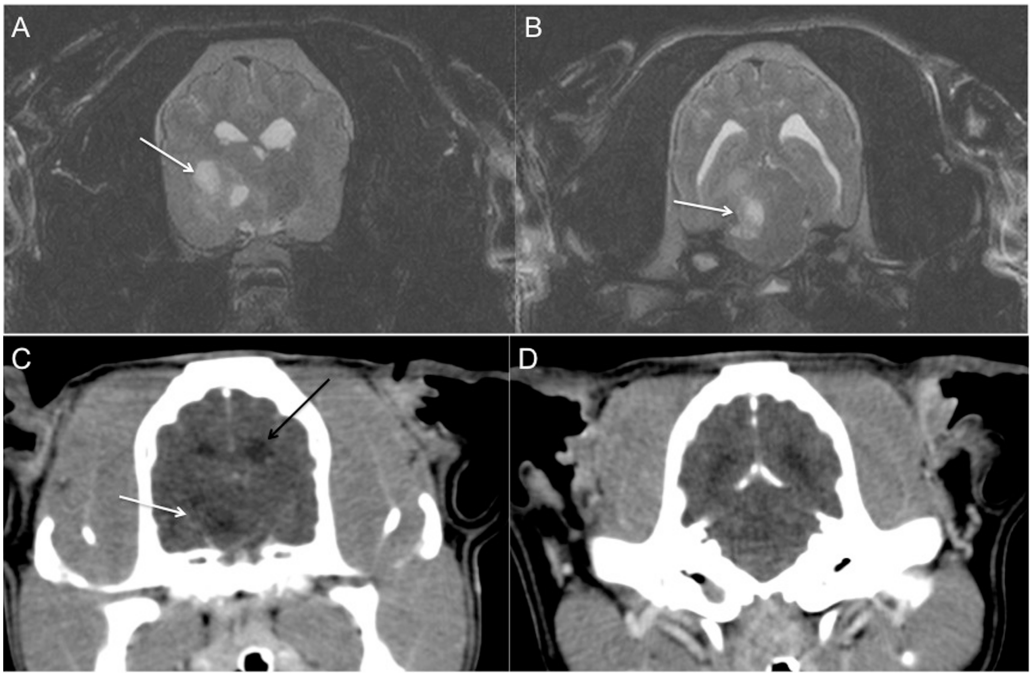

Fig. 3: Transverse T2-weighted MRI (A and B) and postcontrast CT (C and D) images of the head of a dog with suspected intracranial lesions. A) A hyperintense, diffuse, ill-defined intra-axial lesion is visible in the right thalamus (diencephalon; arrow). B) A hyperintense, diffuse, ill-defined intra-axial lesion is visible in the brainstem (mesencephalon; arrow). C) A hypodense intra-axial lesion (white arrow) is visible in the right thalamus. Asymmetry of the lateral ventricles is documented, the left ventricle being larger in size (black arrow). D) No lesion is visible at the level of the brainstem.

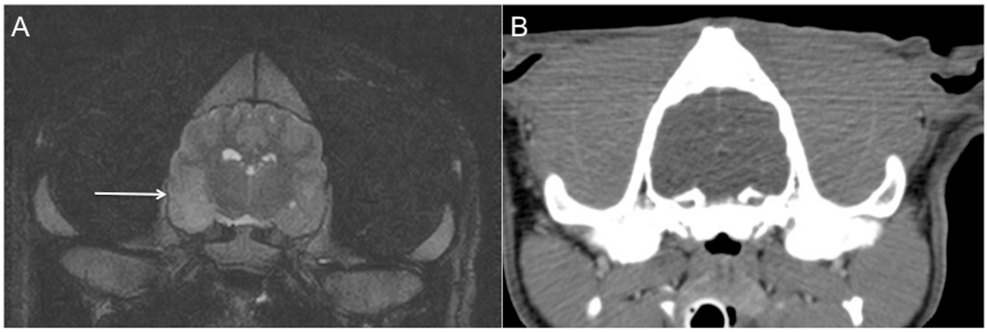

Fig. 4: Precontrast transverse T2-weighted MRI (A) and CT (B) images of the head of a dog with suspected intracranial lesions, as obtained at the level of the piriform lobe. A) A diffuse intra-axial hyperintensity (arrow) is visible in the right piriform lobe. B) No lesion is visible.

Analysis of the images obtained after contrast medium administration showed the presence of enhancement via CT or MRI in 19 patients (Table 3). Within this group, contrast agent enhancement was seen on both imaging modalities in 17 patients ($\kappa = 0.86$), reflecting almost perfect agreement. However, agreement between CT and MRI was less for the pattern of contrast agent enhancement: homogeneous, $\kappa = 0.49$; heterogeneous, $\kappa = 0.17$; ring, $\kappa = 1$; and patchy, $\kappa = 0$.

Table 3—Number of cats and dogs (n = 30) with suspected intracranial disease in which space-occupying lesions* were detected via both CT and MRI by presence and pattern of contrast agent enhancement and agreement between the imaging modalities for these findings.

Characteristic	CT	MRI	CT and MRI	κ	95% CI	*P* value
Enhancement (vs no enhancement)	17	19	17	0.86	0.68 to 1.05	< 0.001
Homogeneous appearance	8	8	5	0.49	0.14 to 0.84	0.007
Heterogeneous appearance	5	7	2	0.17	0.22 to 0.57	0.33
Ring-shaped appearance	3	3	3	1	1 to 1	< 0.001
Patchy appearance	1	0	0	0	−1 to 1	N/A

See Table 1 and 2 for key.

Finally, the CT and MRI image records were compared with respect to the dimensions of the detected lesions (Table 4; Fig. 5). The width and height of lesions recorded on precontrast CT images were compared with those on precontrast T1 and T2 MRI images; the lesion dimensions obtained on postcontrast CT images were compared with those on postcontrast T1 images. Patients with a variable number of lesions on CT and MRI and patients with lesions that could not be measured because of diffuse characteristics on either of set of images were excluded from this analysis. Bland-Altman plots showed that the bias was significantly different from zero for comparisons of lesion width ($P = 0.03$) and length ($P = 0.02$) on precontrast CT and precontrast T1 MRI images but not for the other comparisons. The limits of agreement for all measurements revealed that the range of the differences in dimensions between CT and MRI images was close to or > 2 cm.

Table 4—Comparisons of mean ± SD widths and heights (cm) of intracranial lesions in images obtained via CT and MRI for the dogs and cats in Tables 2 and 3.

Characteristic	Number evaluated	Technique	Value	Technique	Value
Width	17	Precontrast CT	1.64 ± 0.91	Precontrast T1-weighted MRI	1.29 ± 0.53
	18	Precontrast CT	1.59 ± 0.91	T2-weighted MRI	1.45 ± 0.74
	20	Postcontrast CT	1.61 ± 0.90	Postcontrast T1-weighted MRI	1.42 ± 0.62
	10	Postcontrast + oedema CT	1.72 ± 0.62	Postcontrast T1-weighted MRI	1.35 ± 0.44
Height	17	Precontrast CT	1.95 ± 1.00	Precontrast T1-weighted MRI	1.58 ± 0.68
	18	Precontrast CT	1.93 ± 0.97	T2-weighted MRI	1.93 ± 1.10
	20	Postcontrast CT	1.96 ± 1.02	Postcontrast T1-weighted MRI	1.68 ± 0.72
	10	Postcontrast + oedema CT	2.11 ± 0.74	Postcontrast T1-weighted MRI	1.53 ± 0.46

Excluded from analysis were cats and dogs with a variable number of lesions visible via CT and MRI and lesions that could not be measured because of diffuse characteristics on images obtained through either imaging modality.

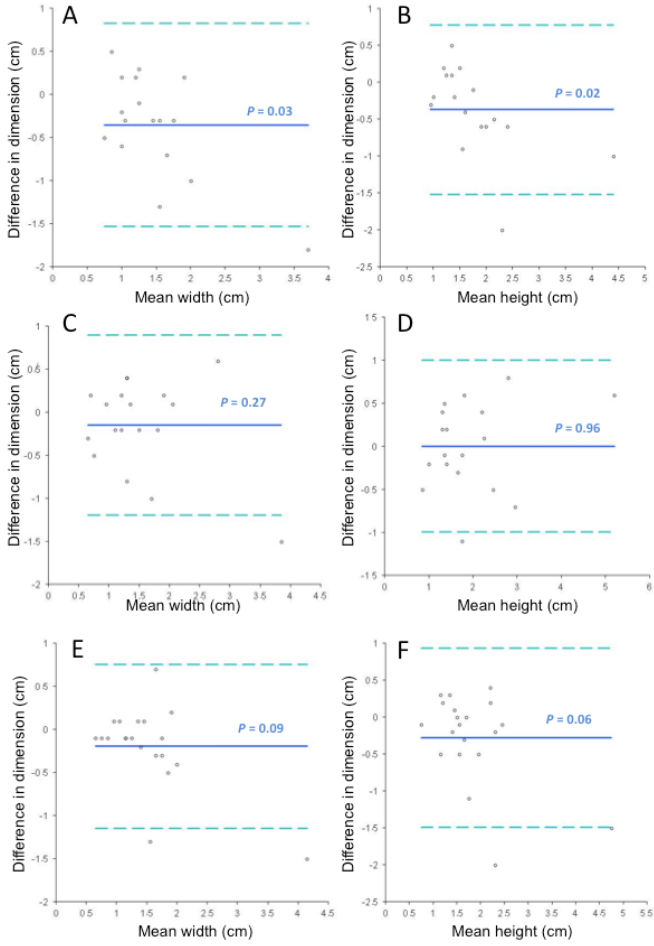

Fig. 5: Bland-Altman plots showing the agreement between CT and MRI for measurement of the width (A, C, and E) and height (B, D, and F) of intracranial lesions in dogs and cats. Analyses were performed for lesions measured on precontrast CT versus T1 images (panels A and B; n = 17), precontrast CT versus T2 images (panels C and D; 18), and postcontrast CT versus T1 images (panels E and F; 20). Solid lines represent bias (with values of *P* indicated), and dashed lines represent the limits of agreement.

Discussion

The present study was conducted to identify for the first time the degree of agreement between CT and low-field MRI in allowing visualization of intracranial lesions and their principal characteristics. The results indicated that agreement between the 2 imaging modalities was substantial for identifying the presence of a lesion and whether solitary or multiple lesions were involved. The modalities were in almost perfect agreement for detecting the presence of a mass effect and contrast enhancement. With the exception of the temporal and piriform lobes and the brainstem, substantial to almost perfect agreement was also achieved for the location of the detected lesion. Lower degrees of agreement were achieved for description of the lesion margins and for pattern of contrast agent enhancement, whereas poor agreement was observed for measurement of lesion dimensions via both pre- and postcontrast CT and MRI techniques.

Similar to in human radiology, the radiologic characteristics of an intracranial lesion in veterinary species provide important information on the possible nature of the lesion[3,11] and may be used to direct the diagnostic process. Lesion anatomic location, pattern, aspect of the margins, mass effect, and contrast agent uptake, however, may be differently interpreted when CT is used instead of MRI or vice versa. Although the definitive diagnosis of any intracranial lesion is obtained by histopathologic examination, the specific aim of our study was to evaluate the agreement between CT and MRI for visualization of intracranial lesions, irrespective of the eventual diagnosis.

Whereas substantial agreement was found between the 2 modalities CT and MRI for the initial visualization of intracranial lesions, 7 lesions, which were detected via MRI as suspected infarctions, oedema, or diffuse inflammatory lesions, were undetectable via CT. Conversely, a suspected inflammatory lesion was detected via CT but not via MRI.

These discrepancies may be clinically relevant and suggest that MRI is more useful or reliable for detecting lesions than CT. Although a definitive diagnosis was not obtained so the accuracy of lesion detection with either modality could not be assessed, the apparent higher detection rate of MRI relative to CT may be attributed to the technical characteristics of MRI. First, MRI is more sensitive than CT for detection of increasing amounts of water.[23] Second, MRI provides excellent soft tissue contrast.[1] Third, MRI produces images that are formed by using different sequences; FLAIR, for example, nullifies the signal of CSF, allowing an interpreter to differentiate CSF from oedema. For these reasons, MRI has been regarded as superior to CT for detection of ischemic stroke.[24–26] Similarly, oedema, which can develop in neoplastic or inflammatory and infectious diseases, can be more clearly identified via MRI. Oedema appears as hyperintense on T2- and FLAIR-weighted MRI sequences and hypointense on T1-weighted MRI sequences, whereas on CT images, it appears as a hypodense region within the healthy brain parenchyma.[3] Lastly, the higher sensitivity of MRI versus CT for detection of subtle lesions[27] may explain why 2 diffuse inflammatory lesions were not identified via CT in the present study. The inflammatory nature of these 2 lesions was confirmed after cerebral fluid analysis. On CT images, diffuse lesions result in signal attenuation that is similar to surrounding tissue and little or no enhancement following contrast agent infusion.[2]

The ability of MRI to yield images with better contrast resolution than CT[28] may explain the finding that 2 lesions identified as solitary via CT appeared as multiple via MRI. Whether an intracranial lesion is identified as solitary or multiple can influence the differential diagnostic process. Most intracranial tumors appear as solitary lesions and most inflammatory and infectious diseases as multifocal lesions, although the reverse situations may occur.[17,29,30] In particular, the 2 patients with discordant CT and MRI findings were suspected to have neoplastic disease. Despite this discordance, however, agreement between CT and MRI was substantial with respect to identification of the lesion pattern.

Interestingly, the single lesion that was detected via CT but not via MRI was a contrast agent enhanced multifocal lesion, and cerebral fluid analysis supported the diagnosis of encephalitis in the affected patient. The reason this lesion was undetectable via pre- and postcontrast MRI images is unclear, but the interval between contrast agent injection and image acquisition may have been too short.

Once a lesion is detected, further radiologic characterization aids in the differential diagnosis process. Results of the present study indicated various degrees of agreement for lesion characteristics. The presence of a mass effect is important because it indicates that healthy brain structures are being displaced, with potential functional consequences. In this respect, CT and MRI showed perfect agreement. As for contrast agent enhancement, 17 of 19 lesions for which enhancement was identified via MRI also had evidence of enhancement via CT, whereas all contrast agent–enhanced lesions identified via CT were similarly identified via MRI. Because of the presence of fenestrated capillaries, contrast agent enhancement is considered physiologic in the meninges, choroid plexus, and pituitary gland. However, in any other area of the brain, such enhancement is considered pathological and results from excess vascularization or disruption of the blood-brain barrier. This basic principle of contrast agent uptake by tissue is the same for iodinated and Gd-DTPA contrast media and might explain the almost perfect agreement between CT and MRI for detecting the presence of contrast agent enhancement.

However, the pattern of enhancement differed to a greater extent between the 2 imaging modalities. Reportedly, most lesions produce a typical enhancement intensity and pattern on CT and MRI.[3,13,15,17–19] Perfect agreement was found for ring enhancement, which was identified in 3 patients. In contrast, CT and MRI had only moderate to slight agreement for other types of enhancement. The disagreement in enhancement parameters may have resulted from the difference between CT and MRI in the kinetics of the visualization of contrast agent enhancement. Whereas CT contrast media absorb x-ray photons and are

directly visualized when the media accumulate in tissue, MRI contrast media function indirectly by altering the local magnetic environment.[31,32] In this respect, the timing of image acquisition is critical to visualize enhancement. Whereas MRI images are typically obtained 10 to 12 minutes after contrast medium injection,[31,32] CT images may already show evidence of enhancement during the IV medium infusion process.[33] On the other hand, gadolinium produces an amplification effect because a large number of water protons are relaxed by a single gadolinium atom. As a consequence, with respect to the magnitude of contrast agent response, MRI is more sensitive to the effect of gadolinium than CT is to the effect of iodine.[34] Reportedly, various technical elements may play a role in the analytic sensitivity of post-gadolinium MRI scans for visualizing intracranial inflammatory lesions in dogs, including the type and dose of contrast medium, timing of image acquisition, and use of magnetization transfer.[35]

Only fair agreement between imaging modalities was found for interpretation of the aspect of the margin lesion. Of 25 lesions identified as well-defined lesions via MRI, only 16 were identified as well-defined on CT. Of 14 lesions identified as ill-defined via CT, only 5 were identified as ill-defined via MRI. These findings suggest that MRI is better for characterizing lesion margins as well-defined than is CT, possibly because of the inherent ability of MRI technology to provide greater soft tissue detail.[1]

The Bland-Altman plot analyses of lesion dimensions indicated that CT and MRI findings did not agree well. The bias for width and length on precontrast CT and precontrast T1-weighted images was significantly different from zero, indicating that one of the methods consistently led to determination of larger or smaller lesion dimensions than the other method. For the other comparisons (ie, the precontrast CT vs T2 images and postcontrast CT vs postcontrast T1-weighted images), the bias did not differ significantly from zero.

More importantly, however, for all comparisons, the limits of agreement suggested that the 95% range of the differences between CT and MRI was close to or > 2 cm. Clinically, when an intracranial lesion is present, this would be a relevant difference, and the limits of agreement thereby indicated that overall results of CT and MRI do not agree well for determination of lesion dimensions. For most comparisons, the lesion dimensions were on average larger on CT images than on MRI images. Although actual lesion dimensions were not verified on the basis of histologic assessment, the observed difference in lesion dimensions may have been attributable to the technical properties of the imaging techniques. As mentioned previously, MRI provides greater soft tissue detail,[1] which may allow for an improved delineation of lesions relative to CT. A poor ability to detect lesion margins on CT images may thus lead to overestimation of the lesion size. In addition, CT artifacts such as partial volume averaging and blooming artifacts may also cause blurring and misinterpretation of lesion margins.[36] Contrast agent is routinely used to improve delineation of lesions and their margins.[37] However, our findings suggested that use of contrast agent did not lead to improved agreement between CT and MRI images. The presence of perilesional oedema may have clinical implications; however, the comparison of intrinsic lesion dimension including perilesional oedema via postcontrast CT and T1-weighted MRI showed equally poor agreement (data not shown).

Substantial to almost-perfect agreement between CT and MRI was found for lesion localization, except for lesions located in the temporal and piriform lobes and the brainstem. Magnetic resonance imaging characteristically provides multiplanar images in sagittal, dorsal, and transverse planes and is suggested to be the optimal imaging modality for visualization of the anatomic characteristics and location of lesions.[38] For example, sagittal MRI scans provide a clear view of the delineation of intracranial structures with a rostrocaudal orientation, such as the corpus callosum, brainstem, and cerebellar vermis.[39]

Likewise, multiplanar MRI scans of the head provide a clear view of the ventricular system.[38] In contrast, CT imaging software allows for the reconstruction of 3-D images from 2-D CT images, thereby also creating multiplanar views. Although such reconstructed views may not yield images with the same resolution as the primary obtained image, they facilitate the detection of lesions and their location. However, localization of brain lesions through use of CT may be hindered by beam-hardening artifacts, whereby high-density structures, such as the thick petrous temporal bone, prevent the CT scanner from detecting x-rays.[2] That beam hardening may obscure the ability to visualize structures in the piriform, parietal, brainstem, and cerebellar regions. The balance between these MRI- and CT-specific factors may explain the disagreement between CT and MRI in lesion localization.

The present study had some limitations. First, it was a descriptive study of the agreement between 2 imaging modalities, and because it did not take the final diagnosis into account, no conclusions could be made as to the accuracy of either technique. Second, although the Cohen κ and Bland-Altman analyses were appropriate techniques for this type of study, the interpretation of the degree of agreement was based on guidelines rather than on clinical relevance. Third, a limited number of study subjects (particular cats) were used. In selected analyses (lesion anatomic location and enhancement pattern), sample sizes were low, and κ values should be interpreted with caution. However, for most variables assessed, confidence intervals were acceptable, and for all but 1 variable, the *P* value for κ was significant. Last, we performed 4-mm collimation CT scans, the resolution of which may be considered inferior to the thinner collimation used in other clinical protocols. This CT collimation was chosen to correspond to the 4-mm collimation provided by low-field MRI. We recognized that the use of thinner collimation would have allowed for superior in-plane resolution as well as direct comparison of sagittal plane–reformatted CT images with sagittal MR images.

Given the aforementioned limitations, we draw the following conclusions regarding the clinical relevance of the study findings. In view of the clinical importance of intracranial disease, the degree of disagreement between CT and MRI for detection of intracranial lesions (whether solitary or multiple) should be regarded as clinically relevant, even though κ values indicated substantial agreement. Once a lesion is detected on CT, MRI may be considered concordant for the most diagnostically important imaging characteristics (i.e. mass effect and contrast agent enhancement). The lesion dimensions may direct treatment, and the poor agreement between CT and MRI may thus be clinically relevant. Poorer agreement was also found for lesion margins and pattern of contrast agent enhancement. Lastly, although substantial agreement between modalities was achieved for the localization of lesions to specific anatomic brain for most regions, the degree of agreement was highly variable, and this could influence diagnosis.

References

1. Berquist TH, Ehman RL, King BF, et al. Value of MR imaging in differentiating benign from malignant soft-tissue masses: study of 95 lesions. *AJR Am J Roentgenol* 1990; 155: 1251–1255.
2. LeCouteur RA. Current concepts in the diagnosis and treatment of brain tumours in dogs and cats. *J Small Anim Pract* 1999;40:411–416.
3. Kraft SL, Gavin PR. Intracranial neoplasia. *Clin Tech Small Anim Pract* 1999; 14: 112–123.
4. Tokgoz N, Oner YA, Kaymaz M, et al. Primary intraosseous meningioma: CT and MRI appearance. *AJNR Am J Neuroradiol* 2005; 26: 2053–2056.
5. Brant-Zawadzki M, Badami JP, Mills CM, et al. Primary intracranial tumor imaging: a comparison of magnetic resonance and CT. *Radiology* 1984; 150: 435–440.
6. Bradley WG, Waluch V, Yadley RA, et al. Comparison of CT and MR in 400 patients with suspected disease of the brain and cervical spinal cord. *Radiology* 1984; 152: 695–702.
7. Carter RMS, Pretorius PM. The use of CT and MRI in the characterization of intracranial mass lesions. *Imaging* 2007; 19: 173–184.
8. Chang KH, Han MC, Kim CW. Magnetic resonance imaging in neurological diseases —comparison with computed tomography. *J Korean Med Sci* 1987; 2: 53–63.
9. Go JL, Zee CS. Unique CT imaging advantages. Hemorrhage and calcification. *Neuroimaging Clin N Am* 1998; 8: 541–558.
10. Haughton VM, Rimm AA, Sobocinski KA, et al. A blinded clinical comparison of MR imaging and CT in neuroradiology. *Radiology* 1986; 160: 751–755.
11. Troxel MT, Vite CH, Massicotte C, et al. Magnetic resonance imaging features of feline intracranial neoplasia: retrospective analysis of 46 cats. *J Vet Intern Med* 2004; 18: 176–189.

12. Gandini G, Gentilini F, Cimatti L, et al. Evaluation of the clinical signs and computed tomographic findings in 27 dogs with intracranial space-occupying lesions (1999–2000). *Vet Res Commun* 2003; 27: 399–401.
13. Kraft SL, Gavin PR, DeHaan C, et al. Retrospective review of 50 canine intracranial tumors evaluated by magnetic resonance imaging. *J Vet Intern Med* 1997; 11: 218–225.
14. Sturges BK, Dickinson PJ, Bollen A, et al. Magnetic resonance imaging and histological classification of intracranial meningiomas in 112 dogs. *J Vet Intern Med* 2008; 22: 586–595.
15. Thomas WB. Nonneoplastic disorders of the brain. *Clin Tech Small Anim Pract* 1999; 14: 125–147.
16. Tidwell AS, Jones JC. Advanced imaging concepts: a pictorial glossary of CT and MRI technology. *Clin Tech Small Anim Pract* 1999; 14: 65–111.
17. Schwartz M, Lamb CR, Brodbelt DC, et al. Canine intracranial neoplasia: clinical risk factors for development of epileptic seizures. *J Small Anim Pract* 2011; 52: 632–637.
18. Freeman AC, Platt SR, Kent M, et al. What is the evidence? Diagnosis of an intracranial lesion as a meningioma on the basis of MRI characteristics. *J Am Vet Med Assoc* 2011; 239: 60–62.
19. Wisner ER, Dickinson PJ, Higgins RJ. Magnetic resonance imaging features of canine intracranial neoplasia. *Vet Radiol Ultrasound* 2011; 52(suppl 1): S52–S61.
20. Robertson I, Thrall DE. Imaging dogs with suspected disc herniation: pros and cons of myelography, computed tomography, and magnetic resonance imaging. *Vet Radiol Ultrasound* 2011; 52(suppl 1): S81–S84.
21. Landis JR, Koch GG. The measurement of observer agreement for categorical data. *Biometrics* 1977; 33: 159–174.
22. Bland JM, Altman DG. Applying the right statistics: analyses of measurement studies. *Ultrasound Obstet Gynecol* 2003; 22: 85–93.

23. Imhof H, Rand T, Trattnig S, et al. Basics of MRI technique and MRI image interpretation [in German]. *Orthopade* 1994; 23: 300–305.
24. Wessmann A, Chandler K, Garosi L. Ischaemic and haemorrhagic stroke in the dog. *Vet J* 2009; 180: 290–303.
25. Garosi L, McConnell JF, Platt SR, et al. Clinical and topographic magnetic resonance characteristics of suspected brain infarctation in 40 dogs. *J Vet Intern Med* 2006; 20: 311–321.
26. Tidwell AS, Robertson ID. Magnetic resonance imaging of normal and abnormal brain perfusion. *Vet Radiol Ultrasound* 2011; 52(suppl 1): S62–S71.
27. Cherubini GB, Platt SR, Howson S, et al. Comparison of magnetic resonance imaging sequences in dogs with multi-focal intracranial disease. *J Small Anim Pract* 2008; 49: 634–640.
28. da Costa RC, Samii VF. Advanced imaging of the spine in small animals. *Vet Clin North Am Small Anim Pract* 2010; 40: 765–790.
29. Cherubini GB, Mantis P, Martinez TA, et al. Utility of magnetic resonance imaging for distinguishing neoplastic from non-neoplastic brain lesions in dogs and cats. *Vet Radiol Ultrasound* 2005; 46: 384–387.
30. Koch MW, Sánchez MD, Long S. Multifocal oligodendroglioma in three dogs. *J Am Anim Hosp Assoc* 2011; 47: e77–e85.
31. Kuriashkin IV, Losonsky JM. Contrast enhancement in magnetic resonance imaging using intravenous contrast media: a review. *Vet Radiol Ultrasound* 2000; 41: 4–7.
32. Joslyn S, Sullivan M, Novellas R, et al. Effect of delayed acquisition times on gadolinium-enhanced magnetic resonance imaging of the presumably normal canine brain. *Vet Radiol Ultrasound* 2011; 52: 611–618.
33. Fike JR, Cann CE, Turowski K, et al. Differentation of neoplastic from non-neoplastic lesions in dog brain using quantitative CT. *Vet Radiol* 1986; 27: 121–128.

34. Gandhi SN, Brown MA, Wong JG, et al. MR contrast agents for liver imaging: what, when, how. *Radiographics* 2006; 26: 1621–1636.

35. Lamb CR, Croson PJ, Cappello R, et al. Magnetic resonance imaging findings in 25 dogs with inflammatory cerebrospinal fluid. *Vet Radiol Ultrasound* 2005; 46: 17–22.

36. Taeymans O, Schwarz T, Duchateau L, et al. Computer tomographic features of the normal canine thyroid gland. *Vet Radiol Ultrasound* 2008; 49: 13–19.

37. Mihara F, Hirakata R, Hasuo K, et al. Gd-DTPA administered MR imaging of intracranial mass lesions: a comparison with CT and precontrast MR. *Radiat Med* 1989; 7: 227–235.

Chapter 4
Low-field MRI and multislice CT for the detection of cerebellar (foramen magnum) herniation in Cavalier King Charles Spaniels

Adapted from: K. Kromhout*, H. van Bree, B.J.G. Broeckx, S. Bhatti, L. Van Ham, I. Gielen Low-field MRI and multislice CT for the detection of cerebellar (foramen magnum) herniation in Cavalier King Charles Spaniels. *Journal of Veterinary Internal Medicine* 2015: 29:238-241.

Summary

Cavalier King Charles Spaniels (CKCS) have a high prevalence of Chiari-like malformation (CM). Herniation of the cerebellum into the foramen magnum is a key diagnostic feature for CM. Midsagittal MR images are the preferred technique for visualizing cerebellar herniation (CH).

The aim of this study was to investigate whether CT can be used to diagnose CH.

CT and MRI images of 15 client-owned CKCS dogs referred for investigation of the brain and cranial cervical spine on MRI and CT were retrospectively analyzed.

Two reviewers analyzed midsagittal T1WSE and T2WSE MR images and midsagittal pre- and postcontrast 2D multiplanar reformatted CT images from each dog for the presence of CH. And, if present, the length (mm, CHL) of the herniation was measured. The results were analyzed statistically.

There was no significant difference between the different observers and techniques for the detection of CH and measurement of CHL. Overall, the CHL had a tendency to be longer (but not significantly so) on the CT images.

Both techniques are useful for detecting CH and measuring CHL. Because CHL does not have a known direct impact on the clinical presentation of CM, CT can be used as a diagnostic tool in a routine clinical practice for CM in CKCS when MRI is not available. We emphasize that MRI is the standard screening technique in CKCS for breeding purposes to detect the presence of CM and SM and, at the current time, CT cannot replace MRI.

Introduction

Cavalier King Charles Spaniels (CKCS) have a high prevalence of Chiari-like malformation (CM). CM is characterized by a disproportion in the volume of the cerebellum and medulla oblongata compared to that of the caudal fossa.[1,2,3,4] These abnormalities are associated with displacement or caudal herniation of part of the cerebellum and brainstem into or through the foramen magnum. [5] Other abnormalities reported in these patients include occipital bone hypoplasia/dysplasia or a shallow caudal cranial fossa[1], kinking of the medulla and malformations of the craniocervical junction[1,2,6], syringomyelia (SM)[7] and ventriculomegaly or hydrocephalus.[3] Indentation and herniation of the caudal cerebellar vermis are most commonly cited as the key diagnostic features for the diagnosis of CM.[3,8] Midsagittal magnetic resonance images (MRI) are mentioned in several articles as the preferred technique for visualizing the caudal fossa and for identifying morphologic changes associated with CM.[1,3,8,9] Diagnostic assessment of the caudal fossa is sometimes difficult when computed tomography (CT) is used because of beam-hardening-artifacts associated with this technique. Studies on the comparison of these imaging modalities for the detection of cerebellar herniation (CH) are absent. The goal of this study was to prospectively evaluate the degree of agreement between low-field MRI and multislice CT for the detection of CH and cerebellar herniation length (CHL) in CKCS.

Materials and Methods

Subjects—This study included 15 client-owned CKCS that were evaluated through the Department of Veterinary Medical Imaging and Small Animal Orthopedics of the Faculty of Veterinary Medicine, Ghent University, between January 2012 and December 2013.
After medical histories were obtained and a complete clinical evaluation including neurologic examination was performed, the dogs underwent (in their clinical work-up) both MRI and CT studies of the brain and cranial cervical spine. Descriptive data were recorded including age, sex, bodyweight and clinical signs. Owner consent was obtained prior to the examinations.

MRI protocol—Imaging was performed using a 0.2 Tesla MRI unit (Airis Mate, Hitachi, Japan). The dogs were anesthetized and positioned in dorsal recumbency with their head in extended position, placed in a multiple array knee coil (paired saddle coil) used in human medicine. Protocols included precontrast sagittal T1-weighted spin echo (T1WSE) imaging (repetition time, 400 to 800 milliseconds; echo time, 17 milliseconds) and T2-weighted spin echo (T2WSE) imaging in sagittal planes (repetition time, 3.000 to 6.000 milliseconds; echo time, 120 milliseconds). Four-millimeter-thick contiguous slices were chosen (image matrix, 512 x 512). Mean examination time was 60 minutes per dog.

CT protocol—Imaging was performed using a 4-slice helical CT device (Lightspeed Qx/i, General Electric Medical Systems, Milwaukee, WI). The dogs were anesthetized and positioned in dorsal recumbency with their head in extended position. Images in 1.25-mm-thick contiguous slices (120 kVp, 140 mAs, image matrix 512 x 512) were obtained, before and immediately after administration of 2ml/kg intravenous iodinated contrast medium (Ultravist 300; N.N. Shering S.A.). The raw data were reconstructed in soft tissue algorithm. Mean examination time was 10 minutes per dog.

Imaging analysis—Prior to analysis, MR and CT images were loaded into an open source imaging software (OsiriX Medical Imaging Software). The imaging studies were provided separate, randomized and the patient information was removed. The images were independently evaluated by two experienced radiologists (IG and HvB). All CT images were reviewed in a brain window (window width, 80 HU to 150 HU; window level, 40 HU to 75 HU). Adjustments of the window width and level were made by the radiologists to allow better visualization. On midsagittal

T1WSE and T2WSE MR images and midsagittal pre- and postcontrast 2D multiplanar reformatted CT images, the presence of a cerebellar herniation was noted and the CHL was measured (mm). The CHL was defined as the position of the tip of the cerebellar vermis relative to the foramen magnum as previously described (Fig. 1)[2,8].

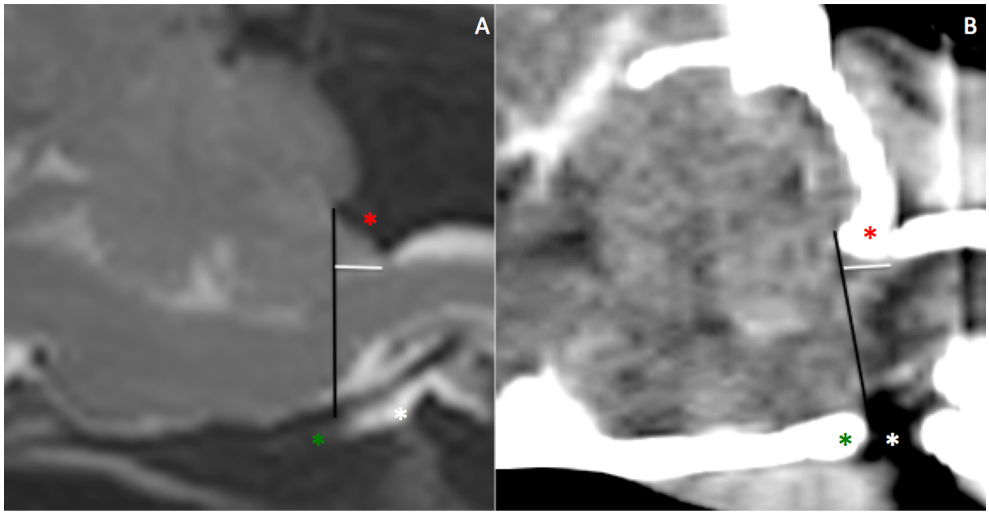

Fig. 1: Midsagittal T2WSE image (A) and postcontrast CT image (B) (soft tissue window) of the brain of the same dog. The supraoccipital bone (red asterisk), basioccipital bone (green asterisk) and occipitoatlantoaxial joint is visible (white asterisk). The foramen magnum limit is set (black line) from the rostrodorsal aspect of the supraoccipital bone to the most caudal aspect of the basioccipital bone. The cerebellar herniation length (mm, white line) is measured caudal from the foramen magnum.

Statistical analysis—Statistical analyses were performed with an open source software package R[10]. Bland-Altman analyses were performed to evaluate the interobserver agreement. Wilcoxon signed-ranked test was used to analyze differences between the observers and modalities. In order to investigate the true effects of the imaging modality instead of the effect of the observer, the mean was used. The Bonferroni correction was applied for multiple comparisons. Data are presented as mean and $P < 0.05$ was considered significant.

Results

Animals—Fifteen CKCS (6 males and 9 females; median age, 66 months [range: 8 to 144 months]) were included in this study. Clinical signs detected or reported by owners at the initial evaluation varied, the most common of which were neck pain, phantom scratching, behavioral change (such as sudden fearfulness, unwillingness to play, agression, etc.), head tilt, ataxia and paresis or paralysis.

Subjective assessment of the presence of CH—There was 100% agreement between the observers concerning the presence of CH on MRI sequences and CT, which determined the evidence of CH in all dogs in the study.

Interobserver agreement—Wilcoxon signed-ranked test showed that there was no significant difference for measuring CHL on T1WSE (P=0.71) and a significant difference for measuring CHL on T2WSE MR images (P=0.04) and pre- (P=0.05) and postcontrast (P=0.01) CT images between the observers. Bland-Altman plots (Fig. 2) showed there was a large variation between measurements of CHL on CT images, before and after contrast medium administration, between the observers.

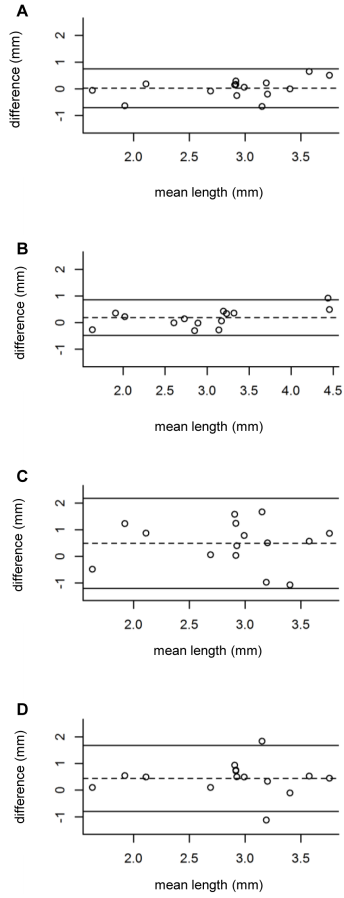

Fig. 2: Bland Altman plot indicating agreement between the observers for the CHL on the different techniques. A) T1WSE MR images, B) T2WSE MR images, C) pre-contrast CT images, D) post-contrast CT images. The x-axis corresponds to the mean value for both observers, whereas the y-axis corresponds to the difference between the 2 observers. The mean of the differences (dashed line) and 95% limits of agreement (upper and lower lines) are indicated.

Intermethod agreement—Wilcoxon signed-ranked test followed by the Bonferroni correction for multiple comparisons (Fig. 3) showed there was no significant difference between the various imaging techniques for measuring CHL: T1WSE and T2WSE MR images (P=1), CT images before and after contrast medium injection (P=0.29), T1WSE MR images and pre- (P=1) and postcontrast (P=0.38) CT images and T2WSE MR images and pre- (P=1) and postcontrast (P=1) CT images.

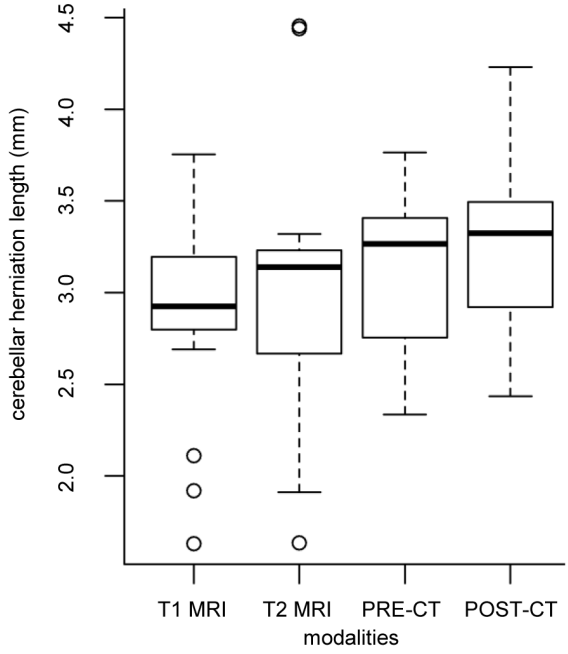

Fig. 3: Box-and-whisker plot, indicating median (horizontal bar), 25th and 75th percentiles (box), and range of CHL (mm) in CKCS on both sequences on MR images and pre- and postcontrast CT images. Overall, the median length and the range of the length of the CH was higher and longer on the CT images.

Discussion

Results of this study indicate that low-field MR and multislice CT imaging can provide comparable information regarding the presence of CH. Computed tomography and MRI are both imaging modalities to visualize the brain and to detect a variety of intracranial lesions in humans and animals. Each method has specific advantages and disadvantages to observe certain brain regions as the patient's general condition, the availability of the equipment and economic considerations determine the choice of either method. More specific compared to MRI studies, CT examinations take less time, hence require shorter anesthesia and therefore are more suitable for unstable patients. The purchase of computed tomography is less expensive and devices are more widely available compared to MRI.[11]

For morphometric studies of the caudal fossa and associated abnormalities related to CM, T1WSE and T2WSE midsagittal MR images are used in both human and veterinary studies. [1] Sagittal images provide a clear delineation of the boundaries of intracranial structures that are orientated in a rostrocaudal direction e.g. the corpus callosum, brainstem and cerebellar vermis.[9] Both sequences provide a good contrast between brain parenchyma and cerebrospinal fluid. T1WSE images reveal better the gross external anatomy and structure of the cerebellum and bony components, as T2WSE sequences provide a better view of the internal anatomy of the cerebellum and pathological conditions.[12]

In our study no significant difference was detected for measuring or detecting CH between both sequences. Computed tomography scans of the caudal fossa are not routinely performed to evaluate the cerebellum because of the presence of several artifacts, foremost partial volume effect and beam hardening, which are reported to influence the evaluation. These artifacts are most prominent at the caudal fossa because of the thick petrous temporal bone and are more pronounced in older CT devices. Multislice CT devices use filters to

perform beam hardening correction to reduce artifacts and provide better temporal and contrast resolution.[13] Also, opting for thin slices, increases the in-plane resolution and decreases the partial volume effects.[14] The use of different reconstruction variables optimizes the image quality of specific brain regions such as the caudoventral cerebellar margin.[14] The ability to reconstruct thick slices from thin slices reduces skull-base-related artifacts.[15] A bone algorithm was not used in this study to reconstruct CT images and to measure the CH. Although the use of a bone reconstruction algorithm would enhance the boundary between the cerebellum and the surrounding bone, it would also increase noise, making the boundary between the cerebellum and the other soft tissues more difficult to delineate.

Statistical analysis performed in this study confirmed that there was no significant difference in MRI and CT for the measurement of the CHL, but overall, the length of the cerebellar herniation was longer on CT (Fig. 4).

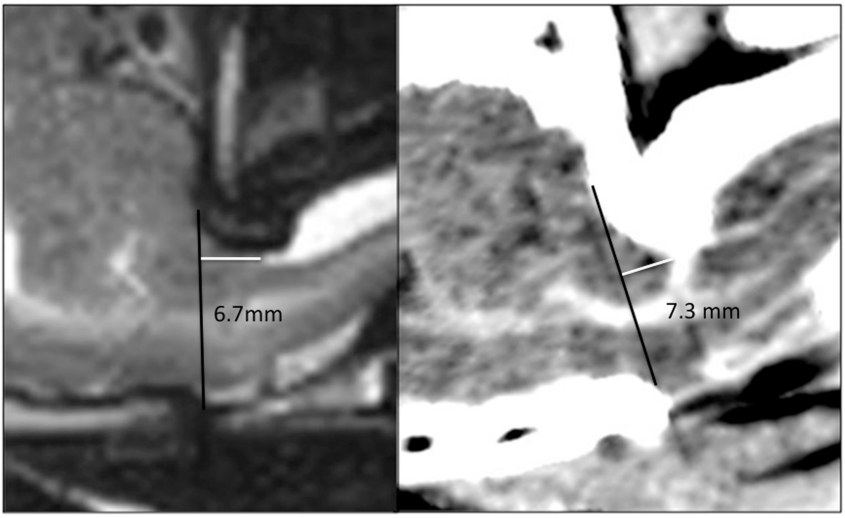

Fig. 4: Midsagittal T2WSE image (A) and postcontrast CT image (B) (soft tissue window) at the level of the cerebellum of the same dog. The cerebellar herniation length is longer on the CT image.

Because the measurements of the CHL were made on images of live dogs, and no autopsy could be performed, the actual CHL cannot be verified. The differences in length on the images, between both the techniques, can be explained by the different technical properties. MRI provides greater soft tissue detail which might allow for a better delineation of the cerebellum. Also the use of a variable window level and width used by the observers can have a effect on the accuracy of the CT measurements [16] compared with those on the MR images. The effect of different voxel size and spatial resolution between CT and MR can also explain the discrepancy in the measurements.

Furthermore on MR images the dorsal atlanto-occipital membrane is visible in the extended head position, at the dorsocaudally border of the cerebellum[17] (Fig. 5).

Fig. 5) Midsagittal T2WSE image at the level of the cerebellum. A hypointense soft tissue structure (atlanto-occipital membrane) (white arrow) is visible dorsal to the spine, between the dorsal edge of the foramen magnum and the cranial border of the arch of the atlas (white asterisk).

This limits the extent of the CH and can be used as the end border of the CH on these images. On CT images structures, such as this ligament in this region are not consistently visualized due to lesser soft tissue detail and the presence of artifacts as mentioned before. This can decrease the visibility of the caudal border of the herniation and be a cause for the increase of CHL on CT images compared with MR images.

The degree of cerebellar herniation is significantly worse in dogs with a flexed compared to an extended head position.[17] Keeping this in mind, because the dogs in our study were positioned with their head in an extended position, measurements both on our MR and CT images can already be an underestimate of the herniation length in the more natural flexed position.

Previous studies have not found an association between the degree of cerebellar herniation and either clinical signs or SM in CKCS with CM.[2,4,7,8] The difference in CHL between MR and CT images and the less natural head position does therefore not have an impact on the clinical signs and SM. Herniation of the cerebellar vermis into the foramen magnum[8] is next to indention of the cerebellum by the occipital bone[3], a diagnostic feature for the diagnosis of CM. The occurrence of CM on its own is not enough to exclude CKCS from breeding programs[5] but the presence of SM is a crucial factor in this decision.

Syringomyelia is characterized by the development of fluid-filled cavities within the spinal cord[7] and has been associated with neurological signs such as thoracic and pelvic limb ataxia and neuropathic pain in CKCS. [2,18,19] The size (diameter) and asymmetry of the syrinx[18] is an important predictor of pain.

Further studies have to be performed to investigate if SM can be equally visible on CT and MR images to determine if CT can be used as an alternative imaging technique for CM/SM in CKCS. From this study, we can draw the following conclusions regarding the clinical relevance of the study findings. Because CH is consistently identified by different observers on CT and on MRI, CT can in certain clinical circumstances be used as a diagnostic tool for CM in CKCS when MRI is not available.

Furthermore the results of this study suggest that CT can be used to confirm or rule out CH in other situations such as when considering a cisternal puncture for cerebral spinal fluid collection or cisternal injection for myelography.[14] We emphasize that, at the current time, CT cannot replace MRI as the standard screening technique for CKCS for breeding purposes for the presence of CM and SM.

References

1. Carrera I., Dennis R., Mellor DJ. et al. Use of magnetic resonance imaging for morphometric analysis of the caudal cranial fossa in Cavalier King Charles Spaniels. *Am J Vet Res* 2009; 70: 340-345.

2. Cerda-Gonzales S., Olby N.J., Mccullough S. et al. Morphology of the caudal fossa in Cavalier King Charles Spaniels. *Vet Radiol Ultrasound* 2009; 50: 37-46.

3. Cross H.R., Cappello R., Rusbridge C. Comparison of cerebral cranium volumes between Cavalier King Charles Spaniels with Chiari-like malformation, small breed dogs and Labradors. *J Small Anim Pract* 2009; 50: 399-405.

4. Driver C.J., Rusbridge C., Cross H. et al. Relationship of brain parenchyma within the caudal cranial fossa and ventricle size to syringomyelia in Cavalier King Charles Spaniels. *J Small Anim Pract* 2010; 51: 382-386.

5. Capello R., Rusbridge C. Report from the Chiari-like malformation and syringomyelia working group round table. *Vet Surg* 2007; 36: 509-512.

6. Marino D.J., Loughin C.A. et al. Morphometric features of the craniocervical junction region in dogs with suspected Chiari-like malformation determined by combined use of magnetic resonance imaging and computed tomography. *Am J Vet Res* 2012; 73: 105-111.

7. Rusbridge C., Macsweeney JE., Davies JV. et al. Syringohydromyelia in Cavalier King Charles Spaniels. *J Am Anim Hosp Assoc* 2000; 36: 34-41.

8. Lu D., Lamb CR., Pfeiffer DU. Et al. Neurological signs and results of magnetic resonance imaging in 40 Cavalier King Charles Spaniels with Chiari type 1-like malformation. *Vet Rec* 2003; 153: 260-263.

9. Benigni L., Lamb CR. Comparison of fluid-attenuated inversion recovery and T2-weighted magnetic resonance images in dogs and cats with suspected brain disease. *Vet Radiol Ultrasound* 2005; 46: 287–292.

10. R Core team (2012). R: A language and environment for statistical computing. R Foundation for Statistical Computing, Vienna, Austria. ISBN 3-900051-07-0, URL http://www.R-project.org/.

11. Gielen I., Kromhout K., Gavin P. et al. Agreement between low-field MRI and CT for the detection of suspected intracranial lesions in dogs and cats. *J Am Vet Med Assoc* 2013; 243: 367-375.

12. Parizel P.M., van den Hauwe L., De Belder F. et al. Magnetic Resonance Imaging of the brain. In: Reimer P., Parizel P.M., Meaney J.F.M. et al. editors. Clinical MR Imaging. 3rd ed. Berlin: Springer; 2010. p. 107-195.

13. Schwarz T., Saunders J., editors. Veterinary Computed Tomography. 1st edition, West-Sussex: John Wiley & Sons Ltd., 2011.

14. Zarelli M., Schwarz T., Puggioni A. et al. An Optimized protocol for multislice computed tomography of the canine brain. *Vet Radiol Ultrasound* 2014; 55: 387-392.

15. Porat-Mosenco Y., Schwarz T., Kass P.H. Thick-section reformatting of thinly collimated computed tomography for reduction of skull-base-related artifacts in dogs and horses. *Vet Radiol Ultrasound* 2004; 45: 131-135.

16. Auriemma E., Voorhout G., Barthez P.Y. Determination of optimal window width and level for measurement of the canine pituitary gland height on computed tomographic images using a phantom. *Vet Radiol Ultrasound* 2007; 48: 113-117.

17. Upchurch J.J., McGonnell I.M., Driver C.J. et al. Influence of head positioning on the assessment of Chiari-like malformation in Cavalier King Charles spaniels. *Vet Rec* 2011;169: 277-282.

18. Rusbridge C., Carruthers H. Dube M.P. et al. Syringomyelia in Cavalier King Charles Spaniels: The relationship between syrinx dimensions and pain. *J Small Anim Pract* 2007; 48: 432-436.

19. Rusbridge C. & Jeffery N.D. Pathophysiology and treatment of neuropathic pain associated with syringomyelia. *Vet J* 2008; 175: 164-172.

Chapter 5
Low-field MRI and multislice CT for the detection of cervical syringomyelia in dogs

Adapted from: K. Kromhout *, H. van Bree , B. J. G. Broeckx, S. Bhatti, S. De Decker, I. Polis, I. Gielen. Low-field MRI and multislice CT for the detection of cervical syringomyelia in dogs. *Journal of Veterinary Internal Medicine* 2015;29:1354-1359.

Summary

Syringomyelia (SM) is defined as the presence of fluid-containing cavities within the parenchyma of the spinal cord. Sagittal MR images have been described as the preferred technique for visualizing SM in dogs and humans.

The aim of this study is to investigate whether CT can be used to diagnose SM.

CT and MR images of 32 client-owned dogs referred for investigation of the cervical spine on MRI and CT were analyzed retrospectively.

Two reviewers analyzed sagittal and transverse T1WSE MR images and CT images from each dog for the presence of SM and, if SM was present, the width (mm, SW) was measured. The results were analyzed statistically.

For the presence of SM there was a moderate interobserver agreement for MR (81%, κ= 0.54) and almost perfect agreement for CT (94%, κ= 0.87). There was a moderate intraobserver intermodality agreement for both observers (observer 1 81%, κ= 0.59; observer 2 81%, κ= 0.57). For measurement of SW the repeatability was the best on the midsagittal T1WSE images (95% repeatability coefficient < 0.52mm) and the reproducibility was the best on midsagittal images in both modalities (95% limits of agreement -0.55-0.45; p= 0.002)

Both techniques can be used to detect SM. Midsagittal MR and CT images are best used for measuring SW. CT can be used as a diagnostic tool for SM when MRI is not available, but CT cannot replace MRI as the standard screening technique for the detection of SM in Cavalier King Charles Spaniel (CKCS) for breeding purposes.

Introduction

Syringomyelia (SM) is a condition characterized by the development of fluid-containing cavities in the spinal cord.[1] The fluid in the cavities resembles cerebrospinal fluid but has a lower protein content.[2,3] SM has been considered as a rare disease in veterinary medicine, but is more and more recognized in animals due to the increased availability of magnetic resonance imaging (MRI) and the high prevalence in certain breeds such as Cavalier King Charles spaniels (CKCS)[4], Griffon Bruxellois[5] and other small or 'toy' breeds[6]. One of the most common causes in dogs is Chiari-like malformation in CKCS.[1,7,8] In this disorder there is a mismatch between the caudal cranial fossa volume and brain parenchyma which leads to cerebellar herniation, medullary kinking, obstruction of the dorsal craniocervical subarachnoid space and alteration of cerebrospinal fluid flow.[7] Other causes of SM in dogs include trauma[9,10], caudal fossa masses[11] and hydrocephalus.[12]

MRI is mentioned in several articles in human and veterinary medicine as the preferred imaging technique for visualizing changes in the spinal cord and to detect SM.[1,13,14,15,16] However plain CT and CT after intrathecal injection of non-ionic contrast media have also been used in human medicine to detect SM.[16] Studies on the comparison of these imaging modalities for the detection of SM are not yet available in veterinary medicine. The goal of this study was therefore to retrospectively evaluate the agreement within and between sagittal and transverse low-field MRI and multislice CT for the detection of SM and measurement of syrinx width (SW) in dogs.

Materials and Methods

Subjects—This retrospective study included client-owned dogs that were evaluated through the Department of Veterinary Medical Imaging and Small Animal Orthopedics of the Faculty of Veterinary Medicine, Ghent University, between January 2012 and August 2014. After medical histories were obtained and a complete clinical evaluation including a general physical and neurologic examination was performed, the dogs underwent (as part of their clinical work-up) both MRI and CT studies of the cervical region. Thirty two dogs were included in the study. Dog breeds were CKCS (n=12), French Bulldog (n=7), Maltese dogs (n=2), Border Collie (n=2), Bordeaux Dog (n=2) and one each of the following: Shi Tzu, Chihuahua, Yorkshire Terrier, English Springer Spaniel, Jack Russell Terrier, Rottweiler and Galgo Espanol. Amongst dogs, 17 were female and 15 were male. The mean age was 63 months (range 6 to 144 months) in the dogs. Clinical signs detected or reported by owners at the initial evaluation varied, the most common of which were neck pain, ataxia and tetraparesis.

MRI protocol—Imaging was performed using a 0.2 Tesla MRI unit (Airis Mate, Hitachi, Japan). The animals were anesthetized and positioned in dorsal recumbency, with the area of interest placed in a human neck/cervical spine coil or a quadrature flexible spine/body coil used in human medicine. Protocols included precontrast sagittal and transverse T1-weighted spin echo (T1WSE) imaging and T2-weighted spin echo (T2WSE) imaging in the same planes. Four-millimeter-thick contiguous slices were chosen (image matrix, 512 x 512).

CT protocol—Imaging was performed using a 4-slice helical CT device (Lightspeed Qx/i, General Electric Medical Systems, Milwaukee, WI). The animals were anesthetized and positioned in dorsal recumbency. Images in 1.25-mm-thick contiguous slices (120 kVp, 140

mAs, image matrix 512 x 512) were obtained, before and immediately after administration of 2 ml/kg (600 mg Iodine/kg body weight) intravenous iodinated contrast medium (Ultravist 300 (300 mg Iodine/ml); N.N. Shering S.A.). The raw data were reconstructed in soft tissue algorithm.

Imaging analysis—Prior to analysis, MR and CT images were loaded into open source imaging software (OsiriX Medical Imaging Software). Images were blinded, randomized and independently evaluated by two experienced observers (KK and IG). All CT images were reviewed in a brain window. Adjustments of the window width and level were made by the radiologists individually to allow better visualization. SM was defined by the presence of an intramedullary fluid filled cavity with uniform signal intensity and density identical to cerebrospinal fluid (T1WSE: hypointense to spinal cord parenchyma; CT: hypodense to spinal cord parenchyma) in the ventricular system. The presence of SM on the MRI and CT images was noted as absent or present.

Morphometric procedure—In case SM was present, the maximal dorsoventral SW (Fig. 1) was measured perpendicular to the longitudinal axis of the spinal cord on the midsagittal images and by measuring the widest dorsoventral diameter of the syrinx on the transverse images at the same level. Different planes in both modalities were used for the measurements: midsagittal and transverse T1WSE MR images and postcontrast transverse and midsagittal 2D multiplanar reformatted CT images.

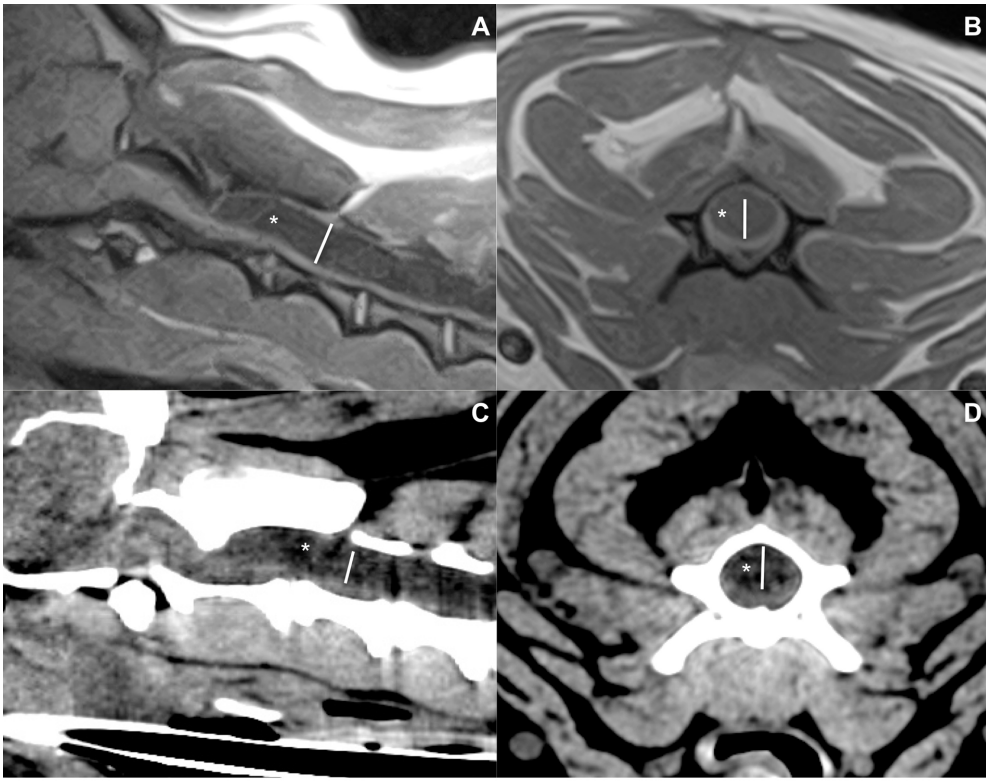

Fig. 1 Midsagittal (A) and transverse (B) T1WSE image and corresponding midsagittal (C) and transverse (D) CT images of the cranial cervical spine of the same dog. A hypointense (A,B) or hypodense (C,D) cavity (white asterisk) is visible within the spinal cord. The SW (white line) is measured perpendicular to the longitudinal axis of the spinal cord on the midsagittal images. On the transverse images the widest diameter (white line) at the same level is measured.

Statistical analysis—Statistical analyses were performed in R[17]. The analysis was subdivided in the assessment of the agreement for a categorical variable (the presence or absence of a syrinx) and a continuous variable (SW).

All dogs (n = 32) were included, to assess the agreement on determining the presence or absence of a syrinx.

For this diagnosis, each observer had access to both the sagittal and transverse plane from the same modality (CT or MR). To determine the repeatability, one observer assessed each patient twice with a two week interval between the assessments, for both CT and MR (= intraobserver intramodality agreement). To determine the reproducibility within a modality (CT or MR), the diagnosis from both observers was compared (interobserver intramodality agreement). To determine the reproducibility between modalities for each individual observer, the diagnosis from each observer was compared for CT and MR (intraobserver intermodality agreement). For each analysis, the overall agreement (dogs with agreement divided by total number of dogs) and a kappa statistic were calculated.[18]

Only dogs where the agreement on the presence of a syrinx was unanimous for both imaging modalities, were used to assess the agreement on the measurement of the SW, This ensures the observed differences are not caused by a different number of dogs or by the in- or exclusion of specific dogs. Hence, all values can be compared directly. To determine the repeatability, each dog was measured three times by one observer. Using these results, the 95% repeatability coefficient was calculated as suggested by Bland and Altman[19] (intraobserver intramodality intraplanar agreement). To determine the reproducibility, the mean difference (a measurement for systematic bias) and the 95% limits of agreement were calculated[19]. A paired Student's t test was performed to determine whether the systematic bias was significantly different from zero. Three different comparisons were made. First, the reproducibility within one plane and modality (= interobserver intramodality intraplanar agreement) for two different observers was assessed. Next, the agreement within one modality between planes for two different observers was assessed (= interobserver intramodality interplanar agreement). Finally, the agreement for two different observers between modalities within a plane (= interobserver intermodality intraplanar agreement) was calculated.

Results

Categorical variable

repeatability and reproducibility (table 1)—There was a perfect intraobserver intramodality agreement for detection of a syrinx on CT and MR images in consecutive viewings. There was a moderate interobserver intramodality agreement for MR and almost perfect agreement for CT on the detecting of a syrinx. There was a moderate intraobserver intermodality agreement for both observers.

Table 1. Agreement between MRI and CT and observers for the detection of a syrinx (total n examined = 32)

	κ	% of agreement
REPEATABILITY intraobserver intramodality		
MRI CT	1 1	100% 100%
REPRODUCIBILITY interobserver intramodality		
MRI CT	0.54 0.87	81% 94%
intraobserver intermodality		
observer 1 observer 2	0.59 0.57	81% 81%

κ, kappa value; levels of agreement: almost perfect (0.8<κ≤1), substantial, (0.6< κ ≤0.8), moderate (0.4<κ≤0.6), fair (0.2<κ≤0.4), slight (0.2<κ≤0).

Continous variable

repeatability— As determined by the 95% repeatability coefficient, 95% of 32 consecutive readings of SW will be within 0.52 mm for the T1WSE midsagittal images, 0.60 mm for the midsagittal CT images, 0.61mm for the T1WSE transverse and 0.62 mm for the transverse CT images.

reproducibility— (table 2)

A) interobserver intramodality intraplanar agreement

A systematic bias significantly different from zero was identified for measuring SW on T1WSE midsagittal, T1WSE transverse images and midsagittal CT images between the observers. There was no significant difference present for measuring SW on transverse CT images between the observers. The reproducibility was highest for midsagittal T1WSE, followed by transverse T1WSE, transverse CT and midsagittal CT.

B) interobserver intramodality interplanar agreement

A bias significantly different from zero was identified for measuring the SW between T1WSE midsagittal and transverse images. No significant difference was identified for measurements between midsagittal and transverse CT images. MR images had the highest reproducibility.

C) interobserver intermodality intraplanar agreement

The bias was significantly different from zero for the measurement of SW between T1WSE midsagittal and midsagittal CT images and no significant difference in between T1WSE transverse and transverse CT images. The midsagittal images over modalities had the highest reproducibility.

Table 2. Reproducibility agreement between MRI and CT for the measurement of SW (total n examined = 17)

	bias	*P*-value	95% LOA (lower-upper limit)	SD
interobserver intramodality intraplanar				
midsagittal T1WSE	-0.09	<0.01	-0.25—0.06	0.08
transverse T1WSE	-0.052	0.029	-0.23—0.13	0.09
transverse CT	-0.041	0.16	-0.27—0.19	0.12
midsagittal CT	-0.063	0.046	-0.30—0.18	0.12
interobserver intramodality interplanar				
midsagittal & transverse T1WSE	-0.043	<0.01	-0.53—0.45	0.25
midsagittal & transverse CT	-0.0043	0.62	-0.52—0.51	0.26
interobserver intermodality intraplanar				
midsagittal T1WSE & CT	-0.049	0.002	-0.55—0.45	0.26
transverse T1WSE & CT	-0.01	0.61	-0.55—0.53	0.28

SD, standard deviation; LOA, limits of agreement

Discussion

Results of this study demonstrate that low-field MR and multislice CT imaging provide comparable information regarding the presence of SM. Analyses of the intraobserver repeatability resulted in the best repeatability for measurement of SW on the midsagittal images (T1WSE > CT) and the least on transverse images (T1WSE > CT). An almost similar result was obtained for the interobserver reproducibility.

Significant bias was identified in some comparisons, This is no issue however as this indicates the systematic differences between modalities/observers or planes. A systematic difference can be easily corrected by subtracting or adding this bias to the results from one technique, to obtain the values for the other technique. A bigger issue is a large standard deviation (and consequently large limits of agreement) as they indicate a non-systematic difference and cannot be corrected for.

For the diagnosis and morphometric studies of SM, MR is the imaging modality of choice both in human and veterinary studies, because of its high contrast resolution and multiplanar capabilities. This was also reflected in the results of this study. Thin section images should be obtained to limit partial volume effects and allowing optimal visualization of small syrinx cavities. In human medicine, most of the investigations concerning SM have been carried out on T1WSE images.[20, 21] Veterinary studies have used T2WSE images[13,22] and T1WSE images[8, 14, 23] to evaluate SM. T1WSE images were used for the measurements in this study. Measurements of the syrinx on T2WSE images may result in an overestimation of the size because the borders of the syrinx are not well demarcated[23] as they can include the hyperintense signal associated with interstitial oedema. This interstitial oedema or pre-syrinx state[20,24] is an accumulation of fluid in the parenchyma prior to syrinx formation. In addition, several artifacts interfere more on T2WSE images compared with T1WSE images. Two such artifacts are the truncation and susceptibility artifact.

Truncation artifact is a common source of high signal intramedullary bands on midsagittal T2WSE images which can be mistaken for a syrinx.[25] Susceptibility artifacts due to metallic foreign bodies, such as ID microchips in veterinary patients, are commonly seen on MR images of the cervical spine. These are more obvious on T2WSE images and cause a distortion of the spinal cord on this level which may influence the detection of SM in the cervical spine.[26] CT is not routinely used to investigate intramedullary changes due to the lesser contrast resolution compared with MRI. Images from plain CT are considered unreliable due to imaging distortions of the surrounding bone (beam artifact).[27] This artifact is more pronounced in past generation CT scanners. Multislice CT scanners, such as the one used in this study, can reduce these artifacts and provide better temporal and contrast resolution. An advantage of CT compared with MRI is the ability to acquire thin slices without loss of detail on the reformatted images and a high signal to noise ratio in contrast to MRI where thinner slices result in a decrease in detail and a decreased signal to noise ratio. In our study a different slice thickness has been used for both modalities (MRI = 4 mm; CT = 1.25 mm) to optimize the visualization of the spinal cord. Optimal CT and MRI imaging parameters, including slice thickness, for the cervical spine have already been established in previous articles.[28,29] We are aware that the small CT slice thickness used during our examinations can be different from the thickness that is used standard in other clinics and can influence the detection of SM in those cases.

Previous articles have stated that CT only allows detection of large intramedullary cavities. Smaller cavities are only seen if they fill with contrast (= CT myelography).[30] CT myelography is able to show swelling and fixation of the spinal cord and localized cerebrospinal fluid flow obstruction.[27] A syrinx is identified by delayed accumulation of water-soluble contrast within the spinal cord in less then 4 hours. In human medicine, 10-50% of syrinxes are not detected using CT myelography.[31] In addition, this technique is invasive and is reported to cause adverse effects such as seizures or neurological deterioration.[32]

Consequently and due to the infrequent use of CT myelography in our clinic, this technique was not used in this study.

When we look at the differences in measurements between the different planes in MR and CT images and between the modalities there is a significant mean difference between the transverse and midsagittal planes in MR and the midsagittal planes between MR and CT. The discrepancy between the SW on midsagittal and transverse MR images can be attributed to the fact that we choose midsagittal images based on the visualization of the spinous process to assure that the measurements were made at the maximum diameter of the spinal canal and cord. This can be off midline (Fig. 2) resulting in a different width compared with the transverse images. Furthermore the large thickness of the slices on MR compared to the size of the cervical spinal cord can also produce off midline images. This might also (partially) explain the differences between the midsagittal MR and CT images. With CT, we can work with reformatted and smaller thickness images where we can create images almost exact in the midline.

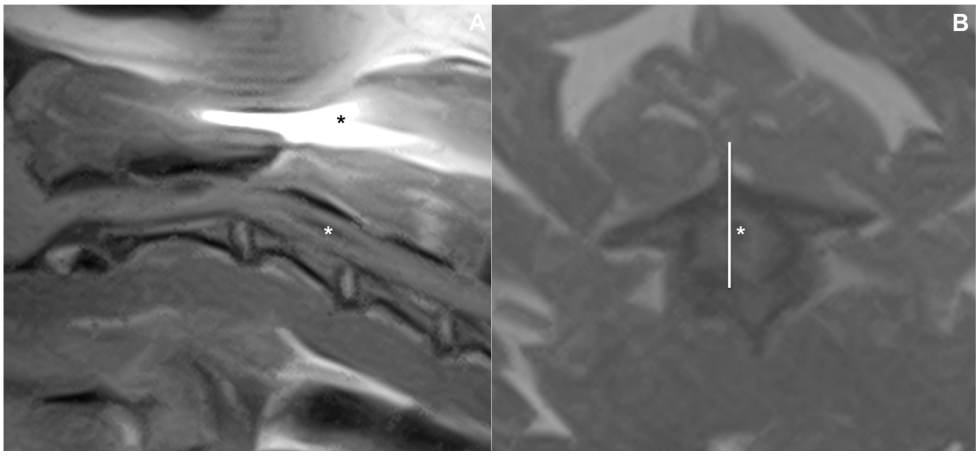

Fig. 2: Midsagittal (A) and transverse (B) T1WSE image of the cranial cervical spine of the same dog. A hypointense cavity (white asterisk) is visible within the spinal cord. A susceptibility artifact (*) is visible due to the present of a microchip. The corresponding slice (white line) of the sagittal image is off midline compared to the transverse image.

The common definition of a syrinx is the presence of a fluid-containing cavity within the spinal cord parenchyma with a diameter ≥ 2 mm at his widest point.[13] This is also the cut-off value that is used in the breeding recommendations of CKCS.[33] The central canal is normally just appreciable on MR images and not visible in normal circumstances on CT images. However, any dilatation of the central canal should be considered abnormal. Hence, the detection of smaller dilatations on both MR and CT is important as progressive central canal dilatation is a precursor of syrinx formation.[1,34] Furthermore results of a previous study suggest that SW progresses with time in CKCS.[34] SW has been shown to be the strongest predictor of pain in CKCS. A syrinx of > 6.4mm wide causes clinical signs in 95% of CKCS[12]. In a study conducted in American Brussels Griffon dogs there was no association found between the size and pain, only between size (>1mm and <2mm) and Chiari malformation signs.[35] Also in human medicine signs of pain are not well correlated with the size of the syrinx. Damage to the dorsal horn of the spinal cord is a key feature in the presence of pain.[36] Further studies have to be conducted in other breeds to see if the size of asyrinx has an effect on symptoms in these dogs. This study did not find an association between the detection of a small dilatation and use of technique (Fig. 3).

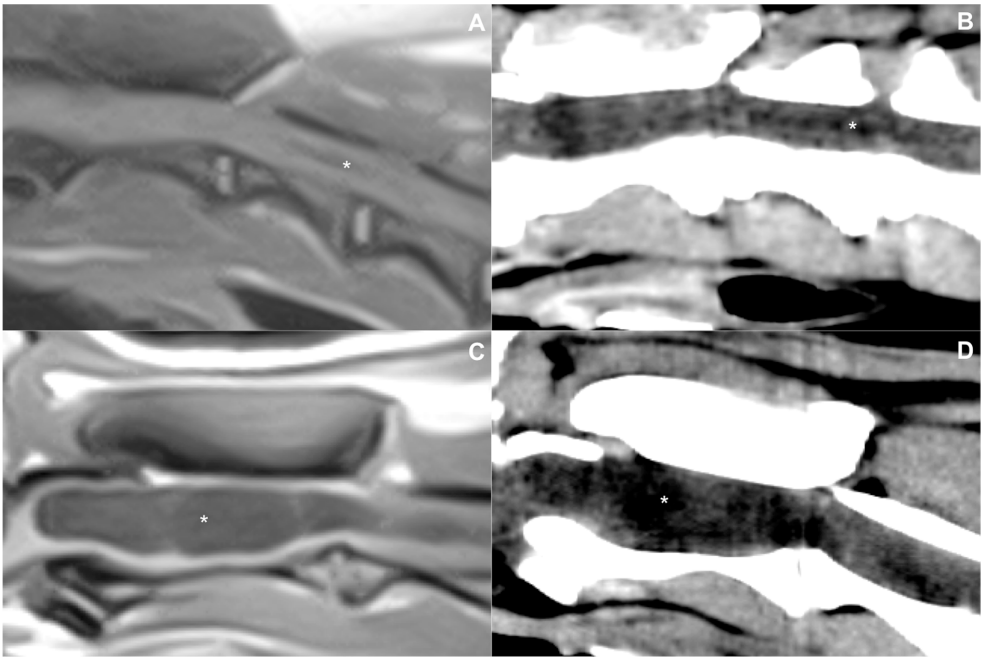

Fig 3. Midsagittal (A) T1WSE and corresponding (B) CT image of the cranial cervical spine of dog 1 and midsagittal (C) T1WSE and corresponding (D) CT image of the cranial cervical spine of dog 2. A, B: a small (<1.5mm, white asterisk) dilatation of the central canal is visible. C, D: a large (>4mm, white asterisk) syrinx is visible.

The difference in detection and measurement can be attributed to the experience of the observer and the presence of several of the artifacts mentioned earlier.

Overall, we conclude that SM is consistently identified by different observers on CT and on MRI. Additionally, the results of this study suggest that when a syrinx is detected the highest agreement is present for measuring SW on both midsagittal MR and CT images. SM and SW have been shown to explain at least some of the clinical signs in dogs. As CT scanners are more readily available in veterinary practices compared with MRI equipment,

CT can be used as a diagnostic tool for SM when MRI is not available. Cerebellar herniation is consistently identified by different observers on CT and on MR images of CKCS.[37] Bearing this in mind, we can conclude, that CT can be used as an alternative imaging technique for Chiari-like malformation/syringomyelia in CKCS when MRI is not available. We emphasize that, at the current time, CT cannot replace MRI as the standard screening technique for the detection of SM in CKCS for breeding purposes, more specific for the detection of the pre-syrinx state.[20,24]

References

1. Rusbridge C., Greitz D., Iskandar B.J. Syringomyelia: Current Concepts in Pathogenesis, Diagnosis, and Treatment. *J Vet Intern Med* 2006; 20: 469-479.

2. Levine D.N. The pathogenesis of syringomyelia associated with lesions at the foramen magnum: a critical review of existing theories and proposal of a new hypothesis. *J. Neurol Sci* 2004; 220: 3-21.

3. Greitz D. Unraveling the riddle of syringomyelia. Neurosurg Rev 2006; 29: 251-263.

4. Cross HR, Cappello R, Rusbridge C .Comparison of cerebral cranium volumes between Cavalier King Charles spaniels with Chiari-like malformation, small breed dogs and Labradors. *J Small Anim Pract* 2009; 50: 399–405.

5. Rusbridge C., Knowler S.P. et al. Chiari-like malformation in the Griffon Bruxellois. *J Small Anim Pract* 2009; 50: 386–393.

6. Dewey C., Berg J. et al. Foramen magnum decompression for treatment of caudal occipital malformation syndrome in dogs. *J Am Vet Med Assoc* 2005; 227: 1270-1275.

7. Driver C.J., Volk H.A., Rusbridge C., Van Ham L.M. An update on the pathogenesis of syringomyelia secondary to Chiari-like malformations in dogs. *Vet J* 2013; 198: 551-559.

8. Parker J.E., Knowler S.P., Rusbridge C. et al. Prevalence of asymptomatic syringomyelia in Cavalier King Charles spaniels. *Vet Rec* 2011; 168: 667.

9. Olby N. The Pathogenesis and Treatment of Acute Spinal Cord Injuries in Dogs. *Vet Clin North Am Small Anim Pract* 2010; 40: 791-807.

10. Feliu-Pascual A.L., Garosi L., Dennis R. et al. Iatrogenic brainstem injury during cerebellomedullary cistern puncture. *Vet Rad Ultrasound* 2008; 49 :467-471.

11. da Costa R.C., Parent J.M., Poma R. et al. Cervical syringohydromyelia secondary to a brainstem tumor in a dog. *J Am Vet Med Assoc* 2004; 225: 1061-1064.

12. Kitagawa M., Ueno H., Watanabe S. et al. Clinical improvement in two dogs with hydrocephalus and syringohydromyelia after ventriculoperitoneal shunting. *Aus Vet J* 2008; 86: 36-42.

13. Rusbridge C., Carruthers H., Dubé M.P. et al. Syringomyelia in Cavalier King Charles spaniel: the relationship between syrinx dimensions and pain. *J Small Anim Pract* 2007; 48: 432-436.

14. Couturier J., Rault D., Cauzinille L. Chiari-like malformation and syringomyelia in normal Cavalier King Charles spaniels: a multiple diagnositic imaging approach. *J Small Anim Practice* 2008; 49: 438-443.

15. Kirberger R.M., Jacobson L.S., Davies J.V. et al. Hydromelia in the dog. *Vet Radiol Ultrasound* 1997; 39: 30-38.

16. Doyon D., Benoudiba F., Iffenecker C. et al. Imaging of syringomyelia. *Neurochirurgie* 1999; 45: 105-114.

17. R Core team (2012). R: A language and environment for statistical computing. R Foundation for Statistical Computing, Vienna, Austria. ISBN 3-900051-07-0, URL http://www.R-project.org/.

18. Landis J.R., Koch G.G. The measurement of observer agreement for categorical data. *Biometrics* 1977; 33: 159–174

19. Bland J.M., Altman D.G. Measuring agreement in method comparison studies. *Stat Methods Med Res* 1999; 8: 135-160.

20. Akiyama Y., Koyanagi I., Yoshifuji I. et al. Interstitial spinal-cord oedema in syringohydromyelia associated with Chiari type 1 malformations. *J Neurol Neurosur Ps* 2008; 79: 1153-1158.

21. Trigylidas T., Baronia B., Vassilyadi M. et al. Posterior fossa dimension and volume estimates in pediatric patients with Chiari i malformations. *Child Nerv Syst* 2008; 24: 329-336.

22. Carruthers H., Rusbridge C., Dube M.P. et al. Association between cervical and intracranial dimensions and syringomyelia in the Cavalier King Charles spaniel. *J Small Anim Pract* 2009; 50: 394-398.

23. Loderstedt S., Benigni L., Chandler K. et al. Distribution of syringomyelia along the entire spinal cord in clinacally affected Cavalier King Charles Spaniels. *Vet J* 2011; 190: 359-363.

24. Fishbein N.J., Dillon W.P., Cobbs C. et al. The "Presyrinx" State: A reversible Myelopathic Condition That May Precede Syringomyelia. *Am J Neuroradiol* 1999; 20: 7-20.

25. Bou-Haider P., Peduto A.J., Karunaratne N. Differential diagnosis of T2 hyperintense spinal cord lesions: Part A. *J Med Imaging Radiat Oncol* 2009; 52: 535-543.

26. Hecht S., Adams W.H., Narak J. et al. Magnetic Resonance Imaging susceptibility artifacts due to metallic foreign bodies. *Vet Radiol Ultrasound* 2011; 52: 409-414.

27. Klekamp J., Samii M. Syringomyelia: Diagnosis and Management, first edn. Springer, Berlin; 2002:195.

28. Drees R., Dennison S.E. et al. Computed tomographic imaging protocol for the canine cervical and lumbar spine. *Vet Radiol Ultrasound* 2009; 50: 74-79.

29. Dennis R. Optimal magnetic resonance imaging of the spine. *Vet Radiol Ultrasound* 2011; 52 Supp.1: S72-S80.

30. Lee B.C.P., Zimmerman R.D., Manning J.J. et al. MR imaging of syringomylia and hydromelia. *Am J Neuroradiol* 1985; 6: 221-228.

31. Brodfelt A.R., Stoodley M.A. Post-traumatic syringomyelia: a review. *J Clin Neurosci* 2003; 10: 401-408.

32. Barone G, Ziemer L.S, Shofer F.S, et al. Risk factors associated with development of seizures after use of iohexol for myelography in dogs: 182 cases (1998), *J Am Vet Med Assoc* 2002; 220: 1499–1502.

33. Capello R., Rusbridge C. Report from the Chiari-like malformation and syringomyelia working group round table. *Vet Surg* 2007; 36: 509-512.

34. Driver C.J., De Risio L., Hamilton S. et al. Changes over time in craniocerebral morphology and syringomylia in cavalier King Charles spaniels with Chiari-like malformation. *BMC Vet Res* 2012; 8: 215.

35. Freeman A.C., Platt S.R. Kent M. et al. Chiari-Like Malformation and Syringomyelia in American Brussels Griffon Dogs. *J Vet Intern Med* 2013; 28: 1551-1559.

36. Todor D.R., Harrison T.M., Millport T.H. Pain and syringomyelia: A review. *Neurosurg Focus* 2008; 8: 1-6.

37. Kromhout K.,van Bree H., Broeckx B. J.G. et al. Low-field MRI and multislice CT for the detection of cerebellar (foramen magnum) herniation in Cavalier King Charles Spaniels. *J Vet Intern Med;* Epub 2014 Nov 19.

General discussion

Imaging modalities – such as MRI and CT – are often used in the diagnostic workup of a veterinary neurology patient. In both human and veterinary medicine MRI is considered the imaging modality of choice for detecting lesions of the brain and spinal cord. This is mainly because of the superior soft tissue contrast of MRI when compared to CT.[1] In addition, pathological changes are better visualized on MRI, because of its analytical sensitivity for soft tissue alterations.[2]

However, in small animal medicine, there is a lack of comparative studies between MRI and CT of the normal or diseased brain and spinal cord. Comparative studies of normal anatomy are limited to anatomical MRI and CT atlases of dogs [3-4], the normal anatomy of skull foramina and cranial nerve emergence in dogs and cats [5-6] and a comparison of MRI and CT for vertebral body and vertebral canal measurements in dogs.[7] Moreover, MRI and CT comparative studies concerning intracranial lesions and spinal cord abnormalities are also scarce. [8-14]

The **first part** of this thesis documents a comparative study of MRI and CT images of the brain of 58 patients (51 dogs and 7 cats) for the detection of intracranial lesions. To our knowledge, no veterinary studies containing a large group of animals and direct comparison of MRI and CT images have been conducted. In studies where histopathology of lesions was present and MRI and/or CT was used, CT imaging proved to be less accurate for detection of an intracranial mass than MRI.[15-17] In humans, direct comparative studies have shown that MRI and CT can be used in a complementary manner – although computed tomography was considered to be less accurate in the detection of intracranial lesions.[18-21] However, these studies are rather dated – they used older generation MRI and CT devices, which can influence the image quality and interpretation. In our study clinical data was not given to the radiologist before evaluation of the images. Image blinding was utilized and dogs without lesions were included in the clinical setup to reduce potential limitations.[22] We found substantial agreement between the two modalities for the initial visualization of the

lesions. One or more intracranial lesions were detected in 38 of 58 patients either by CT or MRI, or both. In 30 of these 38 patients the lesions were seen by both modalities. Still, 7 lesions which were detected on MRI were not visualized on CT. The 1 lesion that was detected on CT but not on MRI is discussed below. This discrepancy may be clinically relevant and suggests that MRI is more reliable for lesion detection than CT. The non-detected lesions on CT in our study were classified by the observers on the MR images as suspected infarctions, oedema or diffuse inflammatory lesions. Because no histopathological information was present these diagnoses could not be verified.

Various theories can be used to explain the discrepancy in detection between both modalities. First of all MRI is more sensitive than CT in detecting increasing amounts of water.[23] As most pathologic processes alter the content, distribution, and ambient environment of hydrogen protons in tissues[24], MRI is an appropriate and sensitive modality for imaging diseases. Also, as mentioned previously, MRI provides excellent soft tissue contrast. The ability of MRI to produce images that are formed by the use of different sequences could explain the higher detection rate. Our study included a FLAIR sequence in addition to T1WSE and T2WSE sequences. FLAIR suppresses the hyperintense signal associated with free fluid, such as cerebrospinal fluid (CSF). This sequence can therefore aid in differentiation of hyperintense pathological lesions (such as brain oedema) and adjacent CSF, which have similar imaging characteristics on the more conventional T2WSE images.[25] When compared to T2WSE, FLAIR also has a higher sensitivity in detecting subtle abnormalities and lesions with multifocal localizations, such as inflammatory diseases.[26] The advantages of FLAIR sequences in brain lesion detection have been studied previously, with a variety of results. In one study FLAIR was compared with T2WSE in dogs and cats with suspected intracranial disease.[25] Overall, very good agreement was found between FLAIR and T2WSE MR images (k= 0.88) for the detection of lesions.

FLAIR sequences were more effective in identifying periventricular or intraventricular lesions and in confirming cystic fluid within lesions. Another study found FLAIR to be the most sensitive sequence for detecting brain lesions and predicting abnormal CSF in dogs with multifocal inflammatory intracranial disease as compared to T2WSE and both pre- and postcontrast T1WSE[27]. Therefore FLAIR should be included in the protocol of imaging of the brain as suggested by Robertson et al..[28] The inclusion of this sequence in our study could partially explain the higher lesion detection on the MRI images. Looking more into detail in which types of lesions were not detected on the CT images, suggests a few other explanations. First of all, detection of infarctions is type- and time-dependent. They can be classified in haemorrhagic or ischemic. Changes associated with ischaemic infarction can be detected by CT as early as 3–6 hours after their onset.[29,30] CT has also proven to be very sensitive in detecting acute and subacute haemorrhage. These can be visualized on CT because of the hyperdense characteristics of haemorrhage compared to normal brain parenchyma[31]. The density gradually decreases to become isodense over days and weeks.[32] Chronic haemorrhage may be invisible on CT.[32] For the detection of ischemic infarcts, MRI is superior to CT due to its excellent soft tissue contrast and its ability to detect subtle lesions.[33] MRI has been reported to be more sensitive than CT for early diagnosis of infarction, with changes seen within 1 hour.[34,35] However, a recent study shows that CT can detect infarctions from less than 12 hours and up to 6 days after onset of clinical signs.[36] The time lapse between the initial appearance of symptoms and the imaging is important and this can explain the absence of these types of lesions on our CT images. Diffuse inflammatory lesions are not well visualized on CT: they can have signal attenuation similar to surrounding tissue and little or no contrast uptake, and so they can be missed on CT. Hence, in these cases, MRI is the modality of choice.

In our study one lesion was detected with CT but not with MRI. This was a contrast-enhanced multifocal lesion that was categorized as encephalitis after cerebrospinal fluid analysis. The exact reason why this lesion was undetectable on both pre- and postcontrast MRI images is unclear. The interval between contrast medium injection and image acquisition (immediately after intravenous injection of contrast) on MRI in our study may have been too short. MRI contrast media function indirectly by altering the local magnetic environment.[37,38] Contrast enhancement of intracranial lesions is a dynamic process. The detection of enhancement is influenced by the time between contrast administration and sequence acquisition.[39,40] In the absence of an intact blood-brain barrier, contrast medium diffuses first into well vascularized lesions and from there into areas of gliosis, necrosis and oedema.[41] Studies in human medicine have concluded that in most instances, lesion detection does not change between initial and delayed MRI images.[42] In our study, only postcontrast transverse T1WSE sequences were acquired. When postcontrast images are acquired in different planes, immediate and delayed contrast images are produced which could have an influence on the detection of lesions.

Once a lesion is detected, further characterization aids in determining the differential diagnosis. Veterinary studies have been conducted to see if it is possible to differentiate neoplastic, inflammatory and vascular brain lesions in dogs primarily on the basis of specific characteristics.[43] These studies tend to show that MRI findings are often non-specific and are shared between major disease categories.[44-47] In our study following variables were evaluated: lesion pattern (solitary or multiple), mass effect, lesion localization, aspect of margins, pre- and postcontrast size of the lesions, and presence and pattern of contrast enhancement. The results of our study indicated various levels of agreement between MRI and CT for these parameters.

° Computed tomography and MRI had a perfect agreement for the presence of a *mass effect*. Mass effect is present when there is a shift of the brain parenchyma or when a compression of the ventricular system is observed.[15] Detecting a mass effect is important, because it indicates that healthy brain structures are being displaced (with potential functional consequences) and this is associated with elevated intracranial pressure.[48] Mass effect can sometimes help to differentiate lesions.[15,45]

° There was almost perfect agreement between both modalities for *contrast enhancement* of the lesions on the images in our study. Results of an MRI study indicated that the administration of contrast medium is not necessary for lesion detection.[49] When a lesion is not detected on precontrast T1WSE, T2WSE or FLAIR images, it is unlikely (1,9%) we would detect a lesion on postcontrast images. The findings of that study are similar to a CT study of the brain in equine patients.[50] However, contrast should be administered in patients with persistent neurological deficits, where an inflammatory or infectious disease is suspected[27,51] and to identify certain intracranial neoplasms (cranial nerves or small lesions with no mass effect).[49] The basic principle of contrast medium uptake by tissues is the same for iodinated and gadolinium-based contrast, which might explain the almost perfect agreement between CT and MRI in detecting the presence of contrast medium enhancement.

° The *pattern of enhancement* differed to a greater extent between the two imaging modalities in our study. This is important, because the degree or pattern of contrast enhancement can assist in the characterization of lesions. It can be used to evaluate tumour type[52,53] and to differentiate neoplastic from non-neoplastic lesions such as inflammation and cerebrovascular disease.[43,44] However, contrast enhancement patterns do not consistently reflect the histologic features of an intracranial lesion.[54]

° Important characteristics which had lesser agreement in our study were *localization* and *dimensions*. Lesions in the temporal and piriform lobes and brainstem were not consistently detected on the CT images. The presence of artefacts in this region can mask the presence of a lesion. The most important ones are beam hardening and partial volume effect[55]. They are most prominent at the level of the caudal fossa, between the thick dens petrous parts of the temporal bone. These artefacts manifest as a broad hypodense streak bordered by a less distinct area of elevated CT numbers.[56] The partial volume artefact can be seen when tissues of different signal intensity become part of the same voxel.[57,58] In canine patients these artefacts can influence the diagnostic assessment of the caudal fossa.[59,60]

° The *lesion dimensions* did not agree well. Overall, the lesion dimensions were larger on CT images than on MRI images. As mentioned before, the presence of artefacts might have influenced this. Partial volume averaging and blooming artefacts can cause blurring and misinterpretation of the lesion margins.[61] Also the better soft tissue detail of MR compared to CT allows better delineation of the lesions. Lesion size can be important when used tot evaluate treatment response in cancer.[62] The more recent multislice (multidetector) CT scanners enable submillimetre thickness image data sets to be acquired for a patient. These very high-resolution image data sets can also be used with advanced three-dimensional (3D) techniques to visualize and quantify anatomy and pathology with unprecedented detail and accuracy.[62]. Contrast medium is routinely used to improve the delineation of lesions and their margins.[63] Our findings suggested that the use of contrast did not lead to improved agreement between CT and MRI images for lesion dimension.

Our study had a few limitations.

First of all we used a low-field (LF) MRI device. Limitations are mainly a result of the low signal-to-noise ratio (SNR). Signal-to-noise ratio is the key factor for image quality, being the ratio of useful signal to unwanted (noise) signal in the image.[64] Because SNR,

contrast and resolution all increase almost linearly with the field strength, LF MRI is generally associated with decreased spatial resolution, leading to less sharp, but still diagnostic images.[65] In human medicine[66-68] there is no significant difference between HF MRI and LF MRI diagnostic capabilities for certain diseases of the brain. Only iron deposits, minimal vascular deformities and minimal inflammatory or neoplastic changes appear to be to harder to identify with a LF system.[67]

Also, slices are usually thicker in LF devices. The decrease in slice thickness allows better spatial resolution and more SNR.[69,70] Thus, thick-slice images are blurry but contain little noise, whereas thin-slice images are sharp but noisy. Thicker slices both in MRI and CT studies can produce artefacts that can reduce image interpretation. Partial volume artefact and beam hardening are the most important (see above). This limitation also applies to our following studies in which a LF device was also used.

Second, because we used a LF MRI with thick slices (4mm) we choose CT slices with equal thickness. This could have contributed to the lower detection of lesions on our images due to the lesser in-plane resolution and the above mentioned artefacts. This is also a disadvantage when creating multiplanar reconstructions (MPR). The quality of the MPR depends on the slice thickness.[71] Slice thickness of 1 mm results in high-quality MPRs, whereas MPRs from 2-mm-thick slices are of poor quality.[72] Creating MPR images with thicker slices and non overlapping sections can cause stair-step artefacts[58] on the sagittal and coronal reconstructed images and limit detection. Stair-step artefacts are virtually eliminated in multiplanar and three-dimensional reformatted images from thin slices and overlap obtained with multislice scanners.[58] All recent LF systems allow high-resolution 3D T1-weighted imaging. With this sequence acquisition of isotropic 1 mm slices is possible. These images have a high resolution, therefor small and/or subtle contrast uptake can be detected.[65] This could have an impact on the detection of smaller lesions in our study.

In human studies - when applying these sequences - the detection rate increases for small lesions in cortical and subcortical areas of the brain [73] and the pituitary gland.[74]

Third a limited number of study subjects (particular cats) were used. This could have an impact on the statistics. In selected analyses (lesion anatomic location and enhancement pattern), sample sizes were also low. In these cases κ values should be interpreted with caution.

Fourth and finally, this was a descriptive study of the agreement between imaging modalities, and because it did not take the final diagnosis into account, no conclusions could be made as to the accuracy of either technique.

The use of cats as study objects, with a different skull conformation and brain volume compared to dogs, should not have an impact on the detection of the lesions. This is because there were also dogs included with a different skull conformation (brachy-, meso- and dolichocephalic types) and accordingly different brain volumes. The results for the detection of an intracranial lesion are similar compared to those observed in humans.[18,19,75]

Given the aforementioned limitations, we can draw the following conclusions. Although there was a substantial degree of agreement for the detection of lesions between both modalities the degree of disagreement is clinically relevant. Once a lesion is detected, however, CT and MRI are concordant for the most diagnostically important imaging characteristics (i.e. mass effect and contrast enhancement). The use of advanced imaging techniques in intracranial lesions is becoming more and more commonplace in veterinary medicine: they play a role in treatment planning and the assessment of therapeutic response, and they will be used more frequently in biopsy-based diagnosis. So, it is essential that the right technique be used in these cases.

CT can be used as an alternative to MRI when not available, but CT should not be used as the diagnostic imaging modality of choice for intracranial lesions when MRI is available. The exception is traumatic events, as stated in other articles, where CT is generally the imaging modality of choice for initial evaluation, because it can be performed rapidly and it accurately detects skull fractures and intracranial hemorrhage.[76]

The **second part** of this thesis examines the agreement between low-field MRI and multislice CT for the detection of specific brain and cervical spine abnormalities.

The ***first study*** in this part focused on the agreement between both modalities for the detection of cerebellar herniations. For this study, we choose Cavalier King Charles Spaniels (CKCS) because they have a high prevalence[77,78] of Chiari-like malformation (CM). Cerebellar herniation, indention and impaction are considered diagnostic characteristics for CM.[79,80] However, a recent article suggested that indention and impaction are unsuitable as a definition for CM because of the high prevalence in normal dogs (asymptomatic, non-CKCS).[81] MRI is cited in several articles as the preferred technique for visualizing the caudal fossa and for identifying morphologic changes associated with CM.[77-80] CT is less favourable because of the presence of artefacts (see above). In human medicine, CT is used complementary to MRI in assessing craniocervical junction abnormalities to determine what structures are causing the compression on the neural tissues.[82,83] CT is also used in morphometric studies to determine total brain volume, total cranial volume and cranial and caudal fossa volumes to explain the origin and neurological signs in dogs with CM.[78,84-86]
In our study, we used sagittal images in both modalities to evaluate the caudal fossa. Intracranial structures (e.g. corpus callosum, brainstem and cerebellar vermis) that are orientated in rostrocaudal direction are best visualized on sagittal images.

Midsagittal MRI images are mentioned in several veterinary articles[28,48,77,87] as the preferred imaging plane for visualization of cerebellar herniations. Sagittal MPR CT images can provide valuable information concerning anatomic locations, such as the tentorium and craniovertebral junction which are subjected to beam hardening artefacts from osseous structures[88]. MPRs are easily performed and should be used routinely in the evaluation of the brain and spine.[89,90]

In our study there was a perfect agreement regarding the presence of CH on midsagittal MRI and midsagittal 2D MPR CT images. This suggests that CT can be used to detect CH and this not only in dogs with CM but also to rule out CH in other situations. Cerebellar or foramen magnum herniation in which caudal parts of the cerebellum are displaced into and through the foramen magnum[91] can be a result of the presence of a large dorsal rostrotentorial mass that is localized very caudally.[92] Also CH is widely thought to be associated with elevated intracranial pressure in dogs and cats.[93,94] In humans, the extent of hind brain herniation is correlated with the severity of elevated intracranial pressure[95], but this did not appear to be the case in a recent study in dogs.[49] When considering a cisternal puncture for cerebrospinal fluid collection or cisternal injection for a myelography, CT can be used as a screening tool. This can avoid potentially fatal complications such as direct brainstem trauma, cerebral and/or cerebellar herniation and central nervous system haemorrhage[96] which can occur in cisternal puncture. The incidence of brain herniation following a CSF collection has been found to be slightly higher in cats than in dogs.[97] CT can then potentially be used as an alternative to other imaging methods, such as ultrasound[98,99] to quickly evaluate the craniovertebral junction. This can be especially valuable when a CT myelography[99,100] is requested.

Statistical analysis performed in our study confirmed that there was no significant difference between MRI and CT for the measurement of the CHL, but overall, the length of CH was considered to be longer on CT.

This was also described in an article in which vertebral body length was overestimated on CT compared to MRI.[7] In addition to the better soft tissue detail on MRI images, this can also be explained by the variable use of window level and window width used by the observers.[101] Another study showed that the most accurate measurement of an object on CT images is obtained by setting the window level at half of the difference of Hounsfield units (HU) between the object and the background.[102]

A higher level will underestimate the size, whereas a lower level will overestimate it. The histopathology, of the lesions was not available in any of our studies, and so exact measurement of lesion sizes was not possible. Fixed windows were not used in our studies. Adjustment of the window width and level were made by the individual radiologist to allow better evaluation. The differences can be therefore explained due to the differences in observers. This limitation is always present in studies that compare various imaging modalities.[103,104] Observers can have different backgrounds, training and experience. However, this situation is routinely encountered in normal clinical settings in the decision making process of cases that undergo advanced diagnostic imaging.
Another possible explanation can be the difference in spatial resolution between CT and MRI. Lower spatial resolution is present in most CT scanners when we use reconstructed images in the sagittal plane, because of the partial volume effect.[98]

When assessing cerebellar herniation length, the position of the patient and the timing of the scan can be important. A previous study[105] revealed that the degree of cerebellar herniation was significantly worse in CKCS with a flexed as opposed to an extended head position. The flexed position, mimics the normal posture of a dog[106]. The cerebellum appears to have more space caudally in dogs with a flexed head position. Furthermore in dogs diagnosed with CM, 30% have atlanto-occipital overlap (AOO) as cause of compression of the caudal aspect of the cerebellum [106]. AOO seems to increase with neck extension[107].

Therefore some authors suggest that when imaging of the craniocervical region is requested both imaging in extension and flexion should be acquired to obtain maximal diagnostic information[108,109] . Also during the cardiac cycle the CHL can vary.[110] Previously in, human medicine, the diagnosis of clinically significant CM was based on the size of cerebellar herniation, with greater than 3-5mm being significant[111]. However, a study showed that size of herniation was not related to clinical signs but to a combination of other factors including decreased cerebellomedullary cistern volume and decreased cerebrospinal fluid around the cerebellar tonsils[112]. Previous veterinary studies have not found an association between the degree of CH/CHL and either clinical signs and SM in CKCS with CM. [78-80,112-114] The difference in CHL between MR and CT images and the less natural head position used in our study should therefore have no impact on the clinical signs in CKCS and syringomyelia (SM). In one study[78] a positive correlation was found between foramen magnum size and cerebellar herniation length. Occipital hypoplasia/ dysplasia and cerebellar herniation can play a role in the development of syringomyelia in CKCS with CM among other factors such as differences in parenchyma[115,116], changes in cerebrospinal fluid flow characteristics[105,116] cerebellar pulsation[92] and abnormal jugular foramina size leading to venous congestion.[117]

We can draw the following conclusions regarding the clinical relevance of our study's findings. Because CH is consistently identified by different observers on CT and MRI, CT can be used as an alternative for MRI in certain clinical circumstances. The clinical impact of the difference in CHL between both modalities must be investigated.

The ***second study*** of this second part of this thesis, was a comparative study conducted to see if there was an agreement between both modalities in detecting syringomyelia, not only in CKCS but also in other breeds of dogs as well. MRI is again mentioned in several articles as the preferred modality to visualize changes in the spinal cord and detect SM. [118-122] Human medicine studies that included CT and MRI imaging have shown that MRI is

more effective for the detection of SM.[123,124] In a comparative study between MRI and CT myelography (CTM) by Deeb et al.[125], CTM gave false negative results in 29% of the patients, whereas MRI was positive in 100% of the cases. CT is not used routinely to investigate intramedullary changes due to the lesser contrast resolution compared to MRI. Furthermore, CT images can be distorted due to the surrounding bone (beam hardening artefact) of the spinal canal.[126] The difference between CT and MRI for the detection of SM was confirmed in our study and reflected in the moderate intramodality agreement.

With regard to the observers themselves, there was a moderate agreement for MRI and perfect agreement for CT. This can be explained by the difference in experience of the observers as mentioned previously. For example, truncation artefacts can be mistaken for a syrinx.[127] Truncation artefact, also known as Gibb's or spectral leakage artefact occurs when time and frequency domains of data are undersampled at locations of sharp tissue interfaces, such as the subarachnoidal space and the spinal cord. The data will then become truncated along the data columns.[128] Alternating lines of hyperintensity and hypointensity on sagittal T2-weighted images may create a longitudinally oriented hyperintense spinal cord signal. This type of artefact, which is especially common in the cervical spine[129], is ignored when it is seen on only one plane and cannot be confirmed in an orthogonal view.

In our study we used T1WSE and T2WSE images to detect SM. The difference between T1WSE and T2WSE sequences for the detection of SM was not included in our study. These sequences are part of a normal imaging protocol of the spine.[130] SM is normally imaged as hypointense compared to CSF on T1WSE and isointense compared to CSF on T2WSE images.[131] Intensity can vary due to the presence of flow.[106] Signal void can appear on T2WSE due to the pulsation of CSF. These occur in spin echo imaging when flowing protons move so quickly through the selected slice that they are not exposed to both the 90° excitation radiofrequency (RF) pulse and the 180° refocusing RF pulse. The protons do not produce a signal, which then appears as a signal void.[127] This can be the case in imaging of SM, which appears as a hypointense signal on the T2WSE images. Furthermore, the fluid

in the cavities of a syrinx closely resembles cerebrospinal fluid but has a significant lower protein content. This can cause differences in intensity on the images.[105,128]
In our study, we used T1WSE images to measure the SW. Measurement of the syrinx on T2WSE images may result in an overestimation of the size because the borders of the syrinx are not well demarcated as they can include the hyperintense signal associated with interstitial oedema.[132]

In our study, there was a significant mean difference for SW between the transverse and midsagittal planes in MRI. This difference can be explained by the fact that we chose midsagittal images based on visualization of the spinous process to assure that the measurements were made at the maximum diameter of the spinal canal and spinal cord[133]. This can be off midline resulting in a different width compared with the transverse images. Using large slice thickness (4mm) on MRI compared to the spinal cord could also be a cause of this discrepancy.

There was also a significant mean difference in the midsagittal images between the 2 modalities used in our study. The difference in slice thickness between MRI (= 4 mm) and CT (= 1.25 mm) can partially explain the difference. When using a small slice thickness on CT, high quality midsagittal MPR images can be created (see above) that are almost exactly in the midline.

Overall the repeatability of measurements of SW was the best on the midsagittal T1WSE images and the reproducibility was the best on midsagittal images of both modalities. When looking at the 95% repeatability coefficient for the midsagittal images, 95% of consecutive readings of SW will be within 0.52mm (T1WSE) and 0.60mm (CT). This suggests that the SW is considered to be wider on CT than on MRI images. The width of a syrinx is considered as a predictor of pain in symptomatic CKCS.

Especially large SW and asymmetric distribution of the syrinx affecting the dorsal horn can be the cause of pain.[134,135] A syrinx of > 6.4 mm wide causes clinical signs in 95% of CKCS.[136] In American Brussels Griffon dogs and humans, signs of pain are not well correlated with the size of the syrinx.[137,138] Another study suggests that CKCS can have clinical signs without the presence of a SM.[132]

Dogs with CM without SM can experience discomfort and pain possibly due to a direct compression of the medulla oblongata.[139, 140] Keeping this in mind, the difference in size between both modalities does not influence the diagnosis. This can only have an effect when considering using CT for screening of CKCS for breeding purposes. A syrinx of 2mm is considered as a cut-off value for identifying a dilatation of the central canal as a syrinx or not.[141]

When combining our last two studies we can conclude, because CH and SM are consistently identified by different observers on CT and MRI, CT can be used as an alternative to MRI for CM/SM in CKCS when MRI is not available. Nevertheless CT cannot replace MRI as the standard screening technique for detecting SM in CKCS for breeding purposes. In these cases not only the presence of a visible SM is important but also the detection of a pre-syrinx state should be considered.[142,143] Pre-syrinx or interstitial oedema is the presence of oedema in the spinal cord parenchyma and is considered a reversible myelopathy that may precede syringomyelia.[141] The detection of small dilatations is also important, as progressive central canal dilatation is a precursor of syrinx formation.[119,144] Our study did not find an association between the detection of small dilatations and use of technique. To our knowledge no articles have been published where the detection limit of SM on CT was mentioned.

The main conclusion of this research work is that when using a CT scanner intracranial lesions and SM can be identified in most cases on the images. Whereas the detection of CH is 100%. Therefore, CT can be used as an valuable alternative to MRI if this modality is not available. This is of great value, because in recent times more and more smaller clinics have a CT machine but not an MRI available. Nevertheless, these results, should be interpreted with caution, because not all lesions are seen on CT, and this is of clinical importance.

Further studies must be conducted to see if the differences in CHL and SW between MRI and CT have a clinical impact. Also other comparison studies between MRI and CT for identification of other abnormalities associated with CM such as medullary kinking and ventriculomegaly/hydrocephalus can be of importance.

References

1. d'Anjou M-A. Principles of computed tomography and magnetic resonance imaging. In: Thrall DE (ed.). Textbook of veterinary diagnostic radiology, 6th ed. St. Louis (MO): Saunders, Elsevier; 2013. p. 50–73.

2. Berquist TH, Ehman RL, King BF, et al. Value of MR imaging in differentiating benign from malignant soft-tissue masses: study of 95 lesions. *Am J Roentgenol* 1990; 155: 1251–1255.

3. Couturier L., Degueurce C., Ruel Y. et al. Anatomical study of cranial nerve emergence and skull foramina in the dog using magnetic resonance imaging and computed tomography.V*et Radiol Ultrasound* 2005; 46: 375-383.

4. Gomes E., Degueurce C., Ruel Y. et al. Anatomic study of cranial nerve emergence and associated skull foramina in cats using CT and MRI. *Vet Radiol Ultrasound* 2009; 50: 398-40

5. Mihaljevik M., Kramer M. & Gomercic H. 2009, CT und MRT atlas: Transversalanatomie des Hundes, Parey, Singhofen, Germany.

6. Assheuer J. & Sager M., 1997, MRI and CT atlas of the dog, Blackwell Wissenshaft, Berlin, Germany.

7. De Decker S., Gielen I.M., Duchateau L. et al. Agreement and repeatability of linear vertebral body and canal measurements using computed tomography (CT) and low field magnetic resonance imaging (MRI). *Vet Surg* 2010; 39: 28-34.

8. Morozumi M., Miyahara K., Sato M. et al. Computed tomography and magnetic resonance findings in two dogs and a cat with intracranial lesions. *J Vet Med Sci* 1997; 59: 807-810.

9. Gonzalo-Orden J.M., Altónaga J.R., Orden M.A. et al. Magnetic resonance, computed tomographic and radiologic findings in a dog with discospondylitis. *Vet Radiol Ultrasound* 2000; 41: 142-144.

10. Auriemma E., Barthez P.Y., van der Vlugt-Meijer R.H. et al. Computed tomography and low-field magnetic resonance imaging of the pituitary gland in dogs with pituitary-dependent hyperadrenocorticism: 11 cases (2001-2003). *J Am Vet Med Assoc* 2009; 235: 409-414.

11. Okada M., Kitagawa M., Nagasawa A. et al. Magnetic resonance imaging and computed tomography findings of vertebral osteosarcoma in a cat. *J Vet Med Sci* 2009; 71: 513-517.

12. De Decker S., Gielen I.M., Duchateau L. et al. Intraobserver, interobserver, and intermethod agreement for results of myelography, computed tomography-myelography, and low-field magnetic resonance imaging in dogs with disk-associated wobbler syndrome. *J Am Vet Med Assoc* 2011; 238: 1601-1608.

13. Cooper J.J., Young B.D., Griffin J.F. 4th et al. Comparison between noncontrast computed tomography and magnetic resonance imaging for detection and characterization of thoracolumbar myelopathy caused by intervertebral disk herniation in dogs. *Vet Radiol Ultrasound* 2014; 55: 182-189.

14. Martin-Vaquero P., da Costa R.C., Drost W.T. Comparison of noncontrast computed tomography and high-field magnetic resonance imaging in the evaluation of Great Danes with cervical spondylomyelopathy. *Vet Radiol Ultrasound* 2014; 55: 496-505.

15. Thomas WB, Wheeler JS, Kramer R, et al. Magnetic resonance imaging features of primary brain tumors in dogs. *Vet Radiol Ultrasound* 1996; 37: 20–27.

16. Gavin PR, Fike JR, Hoopes PJ. Central nervous system tumors. *Semin Vet Med Surg (Small Anim)* 1995; 10: 180– 189.

17. Snyder J.M., Shofer F.S., Van Winkle T.J. et al. Canine intracranial primary neoplasia: 173 Cases (1986–2003). *J Vet Int Med* 2006; 20/ 669–675.

18. Brant-Zawadzki M, Badami JP, Mills CM, et al. Primary intracranial tumor imaging: a comparison of magnetic resonance and CT. *Radiology* 1984;150: 435–440.

19. Bradley WG, Waluch V, Yadley RA, et al. Comparison of CT and MR in 400 patients with suspected disease of the brain and cervical spinal cord. *Radiology* 1984;152: 695–702.

20. Deck M. D., Henschke C., Lee B.C et al. Computed tomography versus magnetic resonance imaging of the brain. A collaborative interinstitutional study. *Clin Imaging* 1989; 13:2-15.

21. Chang KH, Han MC, Kim CW. Magnetic resonance imaging in neurological diseases—comparison with computed tomography. *J Korean Med Sci* 1987;2 :53–63.

22. Whiting P., Rutjes A.W, Dinnes J. et al. Development and validation of methods for assessing the quality of diagnostic accuracy studies. *Health Technol Assess* 2004; 8: 1-234.

23. Imhof H, Rand T, Trattnig S, Kramer J. Basics of MRI technique and MRI image interpretation. *Orthopade* 1994;23:300-305

24. Hecht S., Adams W.H. MRI of brain disease in veterinary patients part 1: Basic Principles and Congenital Brain disorders.*Vet Clin North Am Small Anim Pract* 2010; 40: 21-38.

25. Benigni L., Lamb C.R. Comparison of fluid-attenuated inversion recovery and T2-weighted magnetic resonance images in dogs and cats with suspected brain disease. *Vet Radiol Ultrasound* 2005; 46: 287-292.

26. Cherubini G.B., Platt S.R., Anderson T.J. et al. Characteristics of magnetic resonance images of granulomatous meningoencephalomyelitis in 11 dogs. *Vet Rec* 2006; 159:110–115.

27. Cherubini G.B., Platt S.R., Howson S. et al. Comparison of magnetic resonance imaging sequences in dogs with multi-focal intracranial disease. *J Small Anim Pract* 2008; 49: 634-640.

28. Robertson I. Optimal magnetic resonance imaging of the brain.*Vet Radiol Ultrasound* 2011; 52(1 Suppl 1):S15-22.

29. Wall S.D., Brant-Zawadski M,. Jeffrey R.B. et al. High-frequency CT findings within 24 hours after cerebral infarction. *Am J Roentgenol* 1982; 138: 307-311.

30. McConnell J.F., Garosi L., Platt S.R. Magnetic resonance imaging findings of presumed cerebellar cerebrovascular accident in twelve dogs. *Vet Radiol Ultrasound* 2005; 46: 1-10.

31. Beauchamp N.J. Jr, Barker P.B., Wang P.Y. et al. Imaging of acute cerebral ischaemia. *Radiology* 1999, 212: 307-324.

32. Hoggard N., Wilkinson I.D., Paley M.N. et al. Imaging of haemorrhagic stroke. Clin Radiol 2002; 57, 957–968.

33. Heiland S. Diffusion- and perfusion-weighted MR imaging in acute stroke: principles, methods, and applications. Imaging Decisions MRI 2003; 7, 4–12.

34. Brant-Zawadzki M, Periera B, Weinstein P. MR Imaging of acute experimental ischaemia in cats. *Am J Neuroradiol* 1986; 7: 7-11.

35. Mayer T.E., Schulte-Altedorneburg G., Droste D.W. Serial CT and MRI of ischaemic cerebral infarcts: frequency and clinical impact of haemorrhagic transformation. *Neuroradiology* 2000; 42: 233-239.

36. Paul A.E.H, Lenard Z., Mansfield C.S. Computed tomography diagnosis of eight dogs with brain infarction. *Aust Vet J* 2010: 88; 374-380.

37. Kuriashkin IV, Losonsky JM. Contrast enhancement in magnetic resonance imaging using inravenous contrast media; a review. *Vet Radiol Ultrasound* 2000;41:4-7.

38. Joslyn S, Sullivan M, Novellas R et al. Effect of delayed acquisition times on gadolinium-enhanced magnetic resonance imaging of the presumably normal canine brain. *Vet Radiol Ultrasound* 2011; 52:611-618.

39. Merhof K., Lang J., Dürr S. et al. Use of contrast-enhanced fluid-attenuated inversion recovery sequence to detect brain lesions in dogs and cats. *J Vet Intern Med* 2014; 28:1263-1267.

40. Schorner W., Laniado M., Niendorf H.P. et al. Time-dependent changes in image-contrast in brain-tumors after Gadolinium-DTPA. *Am J Neuroradiol* 1986; 7:1013-1020.

41. Pronin I.N., McManus K.A., Holodny A.I. et al. Quantification of dispersion of Gd-DTPA from the initial area of enhancement into the peritumoral zone of edema in brain tumors. *J Neurooncol* 2009; 94: 399-408.

42. Mathews V.P., Caldemeyer K.S., Ulmer J.L. et al. Effects of contrast dose, delayed imaging, and magnetization transfer saturation on gadolinium-enhanced MR imaging of brain lesions. *J Magn Reson Imaging*, 1997; 7:14-22.

43. Wolff C.A., Holmes S.P., Young B.D. et al. Magnetic resonance imaging for the differentiation of neoplastic, inflammatory, and cerebrovascular brain disease in dogs. *J Vet Intern Med* 2012; 26:589-597.

44. Cherubini G.B., Mantis P,. Martinez T.A. Utility of magnetic resonance imaging for distinguishing neoplastic from non-neoplastic brain lesions in dogs and cats. *Vet Radiol Ultrasound* 2005; 46: 384-387.

45. Cervera V., Mai W., Vite C.H. Comparative magnetic resonance imaging findings between gliomas and presumed cerebrovascular accidents in dogs. *Vet Radiol Ultrasound* 2011; 52: 33-40.

46. Vite C.H., Cross J.R. Correlating magnetic resonance findings with neuropathology and clinical signs in dogs and cats. *Vet Radiol Ultrasound* 2011;52(1 Suppl 1):S23–S31.

47. Young B.D., Fosgate G.T., Holmes S.P. et al. Evaluation of standard magnetic resonance characteristics used to differentiate neoplastic, inflammatory, and vascular brain lesions in dogs. *Vet Radiol Ultrasound* 2014; 55: 399-406.

48. Bittermann S., Lang J., Henke D. et al. Magnetic resonance imaging signs of presumed elevated intracranial pressure in dogs. *Vet J* 2014; 201: 101-108.

49. Ives E.J, Rousset N., Heliczer N. et al.
Exclusion of a brain lesion: is intravenous contrast administration required after normal precontrast magnetic resonance imaging? *J Vet Intern Med* 2014;28:522-528.

50. Lacombe V.A., Sogaro-Robinson C., Reed S.M. Diagnostic utility of computed tomography imaging in equine intracranial conditions. *Equine Vet J* 2010; 42: 393-399.

51. Lamb C.R., Croson P.J., Cappello R. et al. Magnetic resonance imaging findings in 25 dogs with inflammatory cerebrospinal fluid. *Vet Radiol Ultrasound* 2005; 46: 17-22

52. Rodenas S., Pumarola M., Gaitero L. Magnetic resonance imaging findings in 40 dogs with histologically confirmed intracranial tumours. *Vet J* 2011; 187: 85-91.

53. Kraft SL, Gavin PR, DeHaan C. Retrospective review of 50 canine intracranial tumours evaluated by magnetic resonance imaging. *J Vet Intern Med* 1997; 11: 218-225.

54. Singh J.B., Oevermann A., Lang J. Contrast media enhancement of intracranial lesions in magnetic resonance imaging does not reflect histopathologic findings consistently. *Vet Radiol Ultrasound* 2011; 52: 619-626.

55. Möstrum U., Ytterbergh C. Artifacts in computed tomography of the posterior fossa: a comparative phantom study. *J Comput Assist Tomogr* 1986; 10: 560-566.

56. Rozeik C,. Kotterer O., Preiss J. Cranial CT artifacts and gantry angulation. *J Comput Assist Tomogr* 1991; 15: 381-386.

57. Bellon EM, Haacke EM, Coleman PE, Sacco DC, Steiger DA, Gangarosa RE. MR artifacts: a review. *Am J Roentgenol* 1986;147: 1271– 1281.

58. Barrett J.F., Keat N. Artifacts in CT: Recognition and Avoidance. Radiographics 2004; 24:1679-1691.

59. Hathcock J.T., Stickle R.L. Principles and concepts of computed tomography *Vet Clin North Am Small Anim Pract* 1993; 23: 399-415.

60. Morozumi M., Miyahara K., Sato M. Computed tomography and magnetic resonance findings in two dogs and a cat with intracranial lesions. *J Vet Med Sci* 1997: 59; 807-810.

61. Taeymans O, Schwarz T, Duchateau L, et al. Computer tomographic features of the normal canine thyroid gland. *Vet Radiol Ultrasound* 2008;49:13–19.

62. McNitt-Gray M.F., Kim G.H., Zhao B. et al. Determining the Variability of Lesion Size Measurements from CT Patient Data Sets Acquired under “No Change” Conditions *Transl Oncol* 2015; 8: 55–64.

63. Mihara F, Hirakata R, Hasuo K, et al. Gd-DTPA administered MR imaging of intracranial mass lesions: a comparison with CT and precontrast MR. *Radiat Med* 1989;7:227–235.

64. Chavhan G.B. MRI Made Easy (for beginners). 2nd ed 2013. Jaycee Brothers Medical Publishers Ltd., New Delhi, India.

65. Konar M., Lang J. Pros and cons of low-field magnetic resonance imaging in veterinary practice. *Vet Radiol Ultrasound* 2011; 1: S1-S14.

66. Orrison W.W. , Stimac G.K. , Stevens E.A. et al. Comparison of CT, low-field-strength MR imaging, and high-field-strength MR imaging. *Radiology* 1991; 181: 121–127.

67. Merl T., Scholz M. ,Gerhardt O. et al. Results of a prospective multicenter study for evaluation of the diagnostic quality of an open whole-body low-field MRI unit. A comparison with high-field MRI measured by the applicable gold standard. *Eur J Radiol* 1999; 30: 43–53.

68. Blasiak B., Volotovskyy V. , Deng C. et al. A comparison of MR imaging of a mouse model of glioma at 0.2 T and 9.4 T. *J Neurosci Met* 2012; 204: 118-123.

69. Joseph PM. Principles of image formation. In: Atlas SW, ed. *Magnetic resonance imaging of the brain and spine*, 2nd ed. Philadelphia: Lippincott- Raven, 1996:46–63

70. Hendrick RE. Image contrast and noise. In: Stark DD, Bradley WG, eds. *Magnetic resonance imaging*, 3rd ed. St. Louis: Mosby, 1999:43–67

71. Kalender WA. Thin section three-dimensional spiral CT: is isotropic imaging possible? *Radiology* 1995; 197: 578–580.

72. van der Vlugt-Meijer R.H. , Meij B.P., Voorhout G. Thin-slice three-dimensional gradient-echo magnetic resonance imaging of the pituitary gland in healthy dogs *Am J Vet Res* 2006; 67: 1865-1872.

73. Filippi M, Yousry T, Horsfield M, et al. A high-Resolution three- dimensional T1-weighted gradient echo sequence improves the detection of disease activity in multiple sclerosis. *Ann Neurol* 1996; 40:901–907

74. Stadnik T, Stevenaert A, Beckers A, et al. Pituitary microadenomas: diagnosis with two- and three-dimensional MR imaging at 1.5 T before and after injection of gadolinium. *Radiology* 1990; 176:419–428.

75. Taghipour Z., Rezaei S., Dehghani F. Evaluation of diagnostic value of CT scan and MRI in brain tumors and comparison with biopsy. *Iran J Ped Hematol Oncol* 2011; 1:121-125.

76. Le T.H., Gean A.D. Neuroimaging of traumatic brain injury. *Mt Sinai J Med* 2009; 76: 145-162. *J Vet Intern Med* 2014; 28:1165-85.

77. Carrera I., Dennis R., Mellor DJ. et al. Use of magnetic resonance imaging for morphometric analysis of the caudal cranial fossa in Cavalier King Charles Spaniels. *Am J Vet Res* 2009; 70: 340-345.

78. Cerda-Gonzales S., Olby N.J., Mccullough S. et al. Morphology of the caudal fossa in Cavalier King Charles Spaniels. *Vet Radiol Ultrasound* 2009; 50: 37-46.

79. Lu D., Lamb CR., Pfeiffer DU. Et al. Neurological signs and results of magnetic resonance imaging in 40 Cavalier King Charles Spaniels with Chiari type 1-like malformation. *Vet Rec* 2003; 153: 260-263.

80. Cross H.R., Cappello R., Rusbridge C. Comparison of cerebral cranium volumes between Cavalier King Charles Spaniels with Chiari-like malformation, small breed dogs and Labradors. *J Small Anim Pract* 2009; 50: 399-405.

81. Harcourt-Brown T.R., Campbell J., Warren-Smith C. et al. Prevalence of Chiari-like malformations in clinically unaffected dogs. *J Vet Intern Med* 2015; 29: 231-237.

82. Goel A, Bhatjiwale M, Desai K. Basilar invagination: a study based on 190 surgically treated patients. *J Neurosurg* 1998; 88: 962-8.

83. Botelho R.V., Neto E.B., Patriota G.C. et al. Basilar invagination: craniocervical instability treated with cervical traction and occipitocervical fixation. Case report. *J Neurosurg Spine* 2007; 7: 444-449.

84. García-Real I., Kass P.H., Sturges B.K. et al. Morphometric analysis of the cranial cavity and caudal cranial fossa in the dog: a computerized tomographic study. *Vet Radiol Ultrasound* 2004; 45: 38-45.

85. Schmidt M.J., Biel M., Klumpp S. et al. Evaluation of the volumes of cranial cavities in Cavalier King Charles Spaniels with Chiari-like malformation and other brachycephalic dogs as measured via computed tomography. *Am J Vet Res* 2009; 70: 508-512.

86. Marino D.J., Loughin C.A., Dewey C.W. et al. Morphometric features of the craniocervical junction region in dogs with suspected Chiari-like malformation determined by combined use of magnetic resonance imaging and computed tomography. *Am J Vet Res* 2012; 73:105-111.

87. Walmsley G.L., Herrtage M.E., Dennis R. et al. The relationship between clinical signs and brain herniation associated with rostrotentorial mass lesions in the dog. *Vet J* 2006; 172: 258-64.

88. Zacharia T.T., Nguyen D.T.D. Subtle pathology detection with multidetector row coronal and sagittal CT reformations in acute head trauma. *Emery Radiol* 2010; 17: 97-102.

89. Drees R., Dennison S.E., Keuler N.S. et al. Computed tomographic imaging protocol for the canine cervical and lumbar spine. *Vet Radiol Ultrasound* 2009; 50: 74-79.

90. Zarelli M., Schwarz T., Puggioni A. et al.An optimized protocol for multislice computed tomography of the canine brain. *Vet Radiol Ultrasound* 2014; 55: 387-392.

91. Kornegay J.N., Oliver J.E. Jr., Gorgacz E.J. et al. Clinicopathologic features of brain herniation in animals. *J Am Vet Med Assoc* 1983; 182: 1111–1116.

92. Walmsley G.L., Herrtage M.E., Dennis R. et al. The relationship between clinical signs and brain herniation associated with rostrotentorial mass lesions in the dog. *Vet J* 2006;172:258-264.

93. R.S. Bagley Pathophysiologic sequelae of intracranial disease. *Vet Clin North Am Small Anim Pract* 1996; 26: 711–733.

94. Okada M., Kitagawa M., Ito D. et al. MRI of secondary cervical syringomyelia in four cats. *J Vet Med Sci* 2009; 71: 1069–1073.

95. Thompson D.N., Harkness W., Jones B.M. et al. Aetiology of herniation of the hindbrain in craniosynostosis. An investigation incorporating intracranial pressure monitoring and magnetic resonance imaging. *Pediatr Neurosurg* 1997; 26: 288–295.

96. Wamsley, H. & Alleman A.R. Chapter 3: Clinical pathology. In: BSAVA Manual of Canine and Feline Neurology, 3rd ed. (S. R. Platt and N. J. Olby, eds). Gloucester: British Small Animal Veterinary Association. 2004 p. 35–53.

97. Etienne A.L., Audigié F., Peeters D. et al. Ultrasonographic percutaneous anatomy of the atlanto-occipital region and indirect ultrasound-guided cisternal puncture in the dog and the cat. *Anat Histol Embryol* 2015; 44: 92-98.

98. Schmidt M.J., Wigger A., Jawinski S. et al. Ultrasonographic appearance of the craniocervical junction in normal brachycephalic dogs and dogs with caudal occipital (Chiari-like) malformation. *Vet Radiol Ultrasound* 2008; 49: 472-476.

99. da Costa R.C., Echandi R.L., Beauchamp D. Computed tomography myelographic findings in dogs with cervical spondylomyelopathy. *Vet Radiol Ultrasound* 2012; 53: 64-70.

100. Dennison S.E., Drees R., Rylander H. et al. Evaluation of different computed tomography techniques and myelography for the diagnosis of acute canine myelopathy. *Vet Radiol Ultrasound* 2010; 51: 254-8.

101. Auriemma E., Voorhout G., Barthez P.Y. Determination of optimal window width and level for measurement of the canine pituitary gland height on computed tomographic images using a phantom. *Vet Radiol Ultrasound* 2007; 48:113-117.

102. Baxter B.S., Sorenson J.A. Factors affecting the measurement of size and CT number in computed tomography. *Invest Radiol* 1981; 16: 337-341.

103. Martin-Vaquero P., da Costa R.C., Drost W.T. Comparison of noncontrast computed tomography and high-field magnetic resonance imaging in the evaluation of Great Danes with cervical spondylomyelopathy. *Vet Radiol Ultrasound* 2014; 55: 496-505.

104. Leclerc M.K., d'Anjou M.A., Blond L. Interobserver agreement and diagnostic accuracy of brain magnetic resonance imaging in dogs. *J Am Vet Med Assoc* 2013; 242: 1688-1695.

105. Upchurch J.J. , McGonnell I.M. , Driver C.J. et al. Influence of head positioning on the assessment of Chiari-like malformation in Cavalier King Charles spaniels *Vet Rec* 2011; 169: 277.

106. Cerda-Gonzalez S. Olby N.J., Broadstone R. et al. Characteristics of cerebrospinal fluid flow in Cavalier King Charles Spaniels analyzed using phase velocity cine magnetic resonance imaging. *Vet Radiol Ultrasound* 2009; 50: 467-476.

107. Loughin C.A., Marino D.J. Atlantooccipital Overlap and Other Craniocervical Junction Abnormalities in Dogs. *Vet Clin North Am Small Anim Pract* 2015 Nov 26 [Epub ahead of print]

108. Cerda-Gonzalez S., Dewey C.W. Scrivani P.V. et al. Imaging features of atlanto-occipital overlapping in dogs. *Vet Radiol Ultrasound* 2009; 50: 264-268.

109. Cerda-Gonzalez S., J., Griffith E.H. Dorsal compressive atlantoaxial bands and the craniocervical junction syndrome: association with clinical signs and syringomyelia in mature cavalier King Charles spaniels. *J Vet Intern Med* 2015; 29: 887-892.

110. Driver C.J., Watts V., Bunck A.C. et al. Assessment of cerebellar pulsation in dogs with and
without Chiari-like malformation and syringomyelia using cardiac-gated cine magnetic resonance imaging. *Vet J* 2013; 198: 88-91.

111. Milhorat T.H., Chou M.W., Trinidad E.M. etaL. Chiari I malformation redefined: clinical and radiographic findings for 364 symptomatic patients. Neurosurgery. 1999;44:1005-1017.

112. Levine D.N. The pathogenesis of syringomyelia associated with lesions at the foramen magnum: a critical review of existing theories and proposal of a new hypothesis. *J Neurol Sci* 2004;220:3-21.

113. Driver C.J., Volk H.A., Rusbridge C., Van Ham L.M. An update on the pathogenesis of syringomyelia secondary to Chiari-like malformations in dogs. *Vet J* 2013;198:551-559.

114. Parker J.E., Knowler S.P., Rusbridge C. et al. Prevalence of asymptomatic syringomyelia in Cavalier King Charles spaniels. *Vet Rec* 2011;168:667.

115. Shaw T.A., McGonnell I.M., Driver C.J.Caudal cranial fossa partitioning in Cavalier King Charles spaniels. *Vet Rec* 2013; 172:341?

116. Driver C.J., Rusbridge C., Cross H.R. Relationship of brain parenchyma within the caudal cranial fossa and ventricle size to syringomyelia in cavalier King Charles spaniels. *J Small Anim Pract* 2010; 51: 382-386.

117. March P.A., Abramson C.J., Smith M. CSF flow abnormalities in caudal occipital malformation syndrome. *J Vet Intern Med* 2005; 19:414.

118. Schmidt M.J., Ondreka N., Sauerbrey M. Volume reduction of the jugular foramina in Cavalier King Charles Spaniels with syringomyelia. *BMC Vet Res* 2012; 8:158.

119. Rusbridge C., Greitz D., Iskandar B.J. Syringomyelia: Current Concepts in Pathogenesis, Diagnosis, and Treatment. J Vet Intern Med 2006;20:469-479.

120. Rusbridge C., Carruthers H., Dubé M.P. et al. Syringomyelia in Cavalier King Charles spaniel: the relationship between syrinx dimensions and pain. J Small Anim Pract 2007;48:432-436.

121. Couturier J., Rault D., Cauzinille L. Chiari-like malformation and syringomyelia in normal Cavalier King Charles spaniels: a multiple diagnositic imaging approach. J Small Anim Practice 2008; 49:438-443.

122. Kirberger R.M., Jacobson L.S., Davies J.V. et al. Hydromelia in the dog. Vet Radiol Ultrasound 1997;39:30-38.

123. González G.I., Escudero M.J.C., Blanco A.M. et al. Syringomyelia: diagnostic value of magnetic resonance and computed tomography in 5 cases. *Rev Clin Esp* 1991;188:138-141.

124. Tashiro K., Fukazawa T., Moriwaka F. et al. Syringomyelic syndrome: clinical features in 31 cases confirmed by CT myelography or magnetic resonance imaging. *J Neurol* 1987;235:26-30.

125. Deeb Z.L., Daffner R.H., Rothfus W.E. et al. Syringomyelia: myelography, computed tomography, and magnetic resonance imaging. *J Comput Tomogr* 1988;12:1-8.

126. Klekamp J., Samii M. Syringomyelia: Diagnosis and Management, firts edn. Springer, Berlin; 2002: 195.

127. Bou-Haider P., Peduto A.J., Karunaratne N. Differential diagnosis of T2 hyperintense spinal cord lesions: Part A. J Med Imaging Radiat Oncol 2009;52:535-543.

128. Aibinu A.M., Salami M.J., Shafie A.A. et al. MRI reconstruction using discrete Fourier trans- form: a tutorial. *Int J Comp Sci* 2008; 42:179–185

129. Hakky M., Pandey S., Kwak E. et al.

Application of basic physics principles to clinical neuroradiology: differentiating artifacts from true pathology on MRI. AJR Am J Roentgenol. 2013;201:369-77.

130. Dennis R. Optimal magnetic resonance imaging of the spine. *Vet Radiol Ultrasound* 2011; 52(1 Suppl 1):S72-80.

131. Enzmann DR (1991) Imaging of syringomyelia. In: Batzdorf U (ed) Syringomyelia. Williams and Wilkins, Baltimore.

132. Loderstedt S., Benigni L., Chandler K. Distribution of syringomyelia along the entire spinal cord in clinically affected Cavalier King Charles Spaniels. *Vet J* 2011;190:359-363.

133. Hecht S., Huerta M.M. , Reedand B.R. et al. Magnetic Resonance Imaging (MRI) Spinal Cord and Canal Measurements in Normal Dogs *Anat Histol Embryol* 2014; 43: 36–41.

134. Rusbridge C., Carruthers H., Dubé M.P. et al. Syringomyelia in Cavalier King Charles spaniel: the relationship between syrinx dimensions and pain. *J Small Anim Pract* 2007;48:432-436.

135. Hu H.Z, Rusbridge C., Constantino-Casas F et al. Histopathological investigation of syringomyelia in the Cavalier King Charles spaniel. *J Comp Pathol* 2012;146: 192-201.

136. Kitagawa M., Ueno H., Watanabe S. et al. Clinical improvement in two dogs with hydrocephalus and syringohydromyelia after ventriculoperitoneal shunting. *Aus Vet J* 2008;86:36-42.

137. Freeman A.C., Platt S.R. Kent M. et al. Chiari-Like Malformation and Syringomyelia in American Brussels Griffon Dogs. *J Vet Intern Med* 2014;28:1551-1559.

138. Todor D.R., Harrison T.M., Millport T.H. Pain and syringomyelia: A review. *Neurosurg Focus* 2008;8:1-6.

139. C. Rusbridge, N.D. Jeffery Pathophysiology and treatment of neuropathic pain associated with syringomyelia *Vet J* 2006; 175: 164–172.

140. F.R. Taylor, M.V. Larkins Headache and Chiari i malformation: clinical presentation, diagnosis, and controversies in management. *Current Pain and Headache Reports* 2002; 6:331–337.

141. Capello R., Rusbridge C. Report from the Chiari-like malformation and syringomyelia working group round table. *Vet Surg* 2007;36:509-512.

142. Fishbein N.J., Dillon W.P., Cobbs C. et al. The “Presyrinx” State: A reversible Myelopathic Condition That May Precede Syringomyelia. *Am J Neuroradio*l 1999;20:7-20.

143. Akiyama Y., Koyanagi I., Yoshifuji I. et al. Interstitial spinal-cord oedema in syringohydromyelia associated with Chiari type 1 malformations. *J Neurol Neurosur Ps* 2008;79:1153-1158.

144. Driver C.J., De Risio L., Hamilton S. et al. Changes over time in craniocerebral morphology and syringomylia in cavalier King Charles spaniels with Chiari-like malformation. *BMC Vet Res* 2012;8:215.

Summary

Magnetic resonance imaging (MRI) and computed tomography (CT) are both advanced cross- sectional imaging techniques that can be used in the diagnostic workup of a veterinary neurology patient. MRI is generally considered as the imaging modality of choice in imaging of the brain and the spinal cord because of the better soft tissue contrast than CT. MRI provides both anatomical and physiological information in multiple planes. CT is mostly used to visualize bone lesions and is used complimentary to MRI in a lot of cases. It is important to be aware of the possibilities and limitations of both techniques. The *general aim* of this thesis is to evaluate if CT can be used as an alternative to MRI in visualizing lesions of the brain and cervical spinal cord.

The **first chapter** provides an insight in the key differences between MRI and CT. Also an overview of the published literature regarding the use of both modalities in imaging of lesions of the brain and the spinal cord is given.

The scientific aims of this work are presented in the **second chapter**. The *first aim* of this research project was to see if there was an agreement between low-field MRI and CT in the detection of suspected intracranial lesions in dogs and cats. The *second aim* was to determine if there was an agreement between low-field MRI and multislice CT for the detection of specific brain and cervical spine abnormalities. Can CT be used as an alternative to MRI for the detection of cerebellar (foramen magnum) herniation in Cavalier King Charles Spaniels and cervical syringomyelia in dogs?

In the **third chapter** CT and MRI images of 51 dogs and 7 cats were reviewed by 2 experienced radiologists. During this prospective study, dogs and cats with a suspected intracranial lesion, who underwent MRI of the brain as part of their diagnostic workup, were also subjected to a CT exam. A low-field MRI and single-slice CT scanner were used. This was conducted during a predetermined interval in a 2-year-period.

The MRI and CT studies were blinded and the presence or absence of an intracranial lesion was noted. When present, the pattern, localization, aspect of the margins, pre- and postcontrast size and the presence and pattern of enhancement were evaluated. Agreement between both modalities for the detection of intracranial lesions and their characteristics were calculated statistically. There was a substantial agreement (79%, $\kappa = 0.72$) between both modalities for the presence of a intracranial lesion. In 30 out of 38 patients, intracranial lesions were detected both on CT and MRI images. Lesions that were undetectable on CT were defined as suspected infarctions, oedema or diffuse inflammatory lesions. This discrepancy may be clinically relevant and suggest that MRI is more reliable for detecting lesions than CT. Once a lesion is detected, CT and MRI may be considered concordant for the most diagnostically important imaging characteristics (perfect agreement ($\kappa = 1$) for the presence of mass effect and contrast medium enhancement). Analysis of lesion dimensions indicated that CT and MRI findings did not agree well. Overall lesion dimensions were larger on CT than on MRI images. The limits of agreement for all measurements revealed that the range of the differences between CT and MRI images was close to or larger than 2 cm. The lesion dimensions may direct treatment, and the poor agreement between CT and MRI may thus be clinically relevant. Poor agreement was also present for the lesion margins ($\kappa = 0.37$) and pattern of contrast enhancement. Substantial to almost perfect agreement was found for lesion localization, except for lesions located in the temporal lobe ($\kappa = 0.53$) and the brainstem ($\kappa = 0.38$). All lesions seen in the pyriform lobe on MRI were not identified on CT. This highly variable agreement between both modalities for the localization of lesions could again influence diagnosis. In view of the clinical importance of intracranial disease, the degree of disagreement between CT and MRI for detection of intracranial lesions should be regarded as clinically relevant, even though κ values indicated substantial agreement. Once a lesion is detected on CT, MRI may be considered concordant for the most diagnostically important imaging characteristics (i.e. mass effect and contrast agent enhancement).

Overall we can conclude that MRI remains the modality of choice for intracranial lesions but CT can be used as a valuable alternative when MRI is not available.

In the **fourth chapter** the objective was to investigate whether there was an agreement between low-field MRI and multislice CT for the detection of cerebellar (foramen magnum) herniation in Cavalier King Charles Spaniels (CKCS). For this retrospective study, CKCS were chosen because of their high prevalence of Chiari-like malformation. Indention and herniation of the cerebellum are key diagnostic features for the diagnosis of Chiari-like malformation. Included in the study were 15 CKCS, who underwent both MRI and CT studies of the brain and cranial cervical spine in their diagnostic workup. A low-field MRI and multislice CT scanner were used for the imaging. The MRI and CT studies were blinded. On midsagittal TW1SE and TW2SE images and midsagittal pre- and postcontrast 2D multiplanar reformatted CT images the presence of cerebellar herniation (CH) was noted. If present, cerebellar herniation length (CHL, mm) was measured. Agreement between both modalities for the detection of CH and the interobserver and intermethod agreement for CHL were calculated statistically. There was perfect agreement between both observers for the presence of CH. There was no significant difference in MRI and CT for the measurement of CHL. Overall the length of CH was greater on CT. We can conclude that, because no known association has been found in other studies between CHL and clinical signs in CKCS, CT can be used as an alternative to MRI when not available. Also CT can be used to confirm or rule out CH in other situations such as when considering a cisternal puncture for cerebral spinal fluid collection or cisternal injection for myelography. But when considering CT for the screening of CKCS for breeding purposes, MRI is still the standard technique because of the ability to evaluate the spinal cord itself.

The objective of the **fifth chapter** was to investigate whether there was an agreement between low-field MRI and multislice CT for the detection of cervical syringomyelia in dogs. This retrospective study included 32 dogs who underwent (as part of their diagnostic workup) both MRI and CT studies of the cervical region. A low-field MRI and multislice CT scanner were used for the imaging. Images were blinded and two experienced radiologists noted the presence of syringomyelia (SM) during evaluation of the images. When present, the maximal dorsoventral syrinx width (SW) was measured on transverse and midsagittal T1WSE MR images and pre- and postcontrast CT images. Statistical analyses were divided in two parts: the agreement for a presence or absence of SM and agreement on the SW between both observers and modalities. For the presence of SM there was a moderate interobserver agreement for MR (81%, $\kappa = 0.54$) and an almost perfect agreement for CT (94%, $\kappa = 0.87$). There was a moderate intraobserver intermodality agreement for both observers (observer 1: 81% $\kappa = 0.59$; observer 2: 81% $\kappa = 0.57$). The images of patients who had SM on both modalities (17 out of 35) were included in the second part of the study. For measurement of SW repeatability was the best on the midsagittal T1WSE images and reproducibility was the best on midsagittal images in both modalities. Overall we can conclude that SM can be consistenly identified by different observers on CT and on MRI. When a syrinx is identified the SW is best measured on midsagittal images. CT can be used as an diagnostic tool and alternative to MRI when this technique is not readily available.

The **sixth** and **last chapter** includes the general discussion and conclusions. When using CT, intracranial lesions and SM can be identified on the images in most cases. Whereas the detection of CH is 100% on the images. Although MRI remains the modality of choice in visualizing lesions of the brain and the cervical spine, CT can be used as an alternative to MRI. This is of great value because in recent times, more and more smaller clinics have a CT machine and not a MRI available.

These results, however, should be interpreted with caution because not all lesions are seen on CT and this is of clinical importance. Further studies have to be conducted to see if the difference in CHL and SW between MRI and CT have a clinical impact. Also other comparison studies between MRI and CT for identification of other abnormalities associated with CM such as medullary kinking and ventriculomegaly/hydrocephalus can be of importance.

Samenvatting

Magnetische resonantie (MR) en computer tomografie (CT) zijn beeldvormingstechnieken die beide kunnen gebruikt worden in de diagnostiek van dieren met neurologische klachten. Omwille van het betere weke delen contrast wordt MR (in tegenstelling tot CT) algemeen aanzien als de techniek bij uitstek om hersenen en ruggenmerg in beeld te brengen. Met MR kan men informatie verkrijgen over de anatomie en fysiologie van een letsel en dit in verschillende anatomische vlakken (transversaal, dorsaal en sagittaal). CT wordt vooral gebruikt om botstructuren in beeld te brengen. In de meeste gevallen is deze techniek een aanvulling op MR. Het is belangrijk om op de hoogte te zijn van de mogelijkheden en beperkingen van beide beeldvormingstechnieken. *Doelstelling* van dit doctoraat is nagaan of CT een volwaardig alternatief is voor MR voor het visualiseren van letsels in de hersenen en het cervicaal ruggenmerg.

Het **eerste hoofdstuk** geeft een overzicht van de belangrijkste verschillen tussen MR en CT. Er wordt tevens een overzicht gegeven van de bestaande literatuur over het gebruik van beide technieken om letsels van hersenen en ruggenmerg in beeld te brengen.

De wetenschappelijke doelstellingen van dit doctoraat worden geformuleerd in het **tweede hoofdstuk**. De *eerste doelstelling* was nagaan of er een overeenkomst was tussen laagveld MR en single-slice CT voor het detecteren van intracraniële letsels bij honden en katten. De *tweede doelstelling* was onderzoeken of er een overeenkomst was tussen laagveld MR en multislice CT voor het opsporen van specifieke afwijkingen t.h.v. de hersenen en het cervicaal ruggenmerg; meer bepaald: kan CT gebruikt worden als alternatief voor het diagnosticeren van een cerebellaire (foramen magnum) hernia bij Cavalier King Charles Spaniels en cervicale syringomyelie bij honden.

Het **derde hoofdstuk** licht een prospectieve studie toe die naging of er een overeenkomst was tussen laagveld MR en single-slice CT voor het detecteren van intracraniële letsels bij honden en katten. Eenenvijftig honden en 7 katten die verdacht werden van een intracraniaal letsel en hiervoor een MR onderzoek ondergingen, werden ook onder de CT-scanner gelegd. Hiervoor werd een laagveld MR-toestel en single-slice CT-toestel gebruikt. Deze onderzoeken werden gepland in een vooraf bepaalde periode over een tijdsspanne van 2 jaar. De MR- en CT-studies werden geanonimiseerd en de aanwezigheid van een intracraniaal letsel werd onderzocht. Bij de aanwezigheid van een letsel werden tevens verschillende karakteristieken beoordeeld: massa-effect, patroon (enkelvoudig of meervoudig), lokalisatie (lobus of regio), aspect van de randen van het letsel (gedefinieerd of niet), pre- en postcontrast afmetingen, contrastcaptatie en het patroon van contrastopname (homogeen, heterogeen, rand). De overeenkomst tussen beide technieken werd statistisch bekeken. Er was een voldoende tot goede overeenkomst (79%, $\kappa = 0.72$) tussen MR en CT voor het detecteren van een intracraniaal letsel. Bij 30 van de 58 patiënten werd het letsel zowel op de MR als op de CT-beelden geïdentificeerd. Letsels die niet gezien waren op CT-beelden maar wel op MR-beelden werden door de radiologen beschreven als een infarct, oedeem of een diffuus inflammatoir letsel. Het niet detecteren van deze letsels op CT is relevant en hieruit kan men besluiten dat MR beter is voor het detecteren van hersenletsels. Wanneer een letsel aanwezig is, is er een goede overeenkomst tussen CT en MR voor de meeste kenmerken (perfecte overeenkomst ($\kappa = 1$) voor aanwezigheid massa-effect en contrastcaptatie). Wat betreft de afmetingen van een letsel is er geen goede overeenkomst tussen beide technieken. De dimensies van de letsels waren bij de meeste gevallen groter op de CT-beelden. Wanneer men keek naar de grenzen van overeenkomst van alle metingen (95% betrouwbaarheidsinterval), was het verschil in dimensies dicht bij of groter dan 2 cm tussen beide technieken. Het verschil tussen beide technieken voor metingen heeft een invloed op de uiteindelijke behandeling van een patiënt en is dus klinisch relevant.

De overeenkomst was matig (κ = 0.37) wat betreft de randen van het letsel en de mate van contrastcaptatie. De overeenkomst wat de lokalisatie van het letsel betreft, was voldoende tot bijna perfect, met uitzondering van letsels in de lobus temporalis (κ = 0.53) en hersenstam (κ = 0.38). Letsels in de lobus piriformis werden niet gedetecteerd op de CT-beelden. De hoge variabele overeenkomst tussen MR en CT voor de lokalisatie van een letsel heeft invloed op de diagnose. Na deze grondige studie kunnen we concluderen dat MR de techniek bij uitstek is om intracraniële letsels te diagnosticeren. CT is een waardevol alternatief voor MR als deze niet beschikbaar is.

In het **vierde hoofdstuk** staat een analyse van de overeenkomst tussen laagveld MR en multislice CT voor het diagnosticeren van een cerebellaire hernia in Cavalier King Charles Spaniels (CKCS) centraal. Voor deze retrospectieve studie werd gekozen voor CKCS omdat deze honden een hoge prevalentie hebben voor Chiari-like malformatie. Indentatie en herniatie van het cerebellum zijn belangrijke diagnostische kenmerken van Chiari-like malformatie. Vijftien CKCS, die een MR- en CT-onderzoek van de hersenen en cervicaal ruggenmerg ondergingen tijdens hun diagnostische work-up, werden geïncludeerd in de studie. Hiervoor werd een laagveld MR en multislice CT-toestel gebruikt. De MR- en CT-studies werden geanonimiseerd en geëvalueerd door 2 ervaren veterinaire radiologen. Op de midsagittale T1WSE en T2WSE MR-beelden en pre- en postcontrast 2D multiplanaire gereformatteerde CT-beelden werd de aanwezigheid van een cerebellaire hernia (CH) genoteerd. Wanneer een CH aanwezig was, werd de lengte gemeten (CHL, mm). De overeenkomst tussen beide technieken voor het detecteren van een CH werd statistisch berekend. Er was een perfecte overeenkomst tussen MR en CT voor het diagnosticeren van een CH. Er was geen significant verschil tussen MR en CT voor de lengte van de CH. In het algemeen was de lengte van de hernia op CT groter. Uit deze studie kunnen we concluderen dat, aangezien er geen eerdere associatie werd gevonden tussen CHL en klinische klachten bij CKCS, CT gebruikt kan worden als een alternatief voor MR.

Ook kan CT gebruikt worden om een CH uit te sluiten in andere situaties, bv. voorafgaand aan een cervicale punctie van cerebrospinaal vocht of een cisternale injectie van contrast bij een myelografie. Bij een screening van CKCS voor fokdoeleinden blijft MR echter de diagnostische techniek bij uitstek aangezien een beoordeling van het ruggenmerg dan eveneens mogelijk is.

Het **vijfde hoofdstuk** maakt duidelijk of er een overeenkomst was tussen laagveld MR en CT voor het diagnosticeren van een cervicale syrinx. Deze retrospectieve studie includeerde 32 honden die als onderdeel van hun diagnostische work-up een MR- en CT-onderzoek van het cervicaal ruggenmerg ondergingen. De MR- en CT-studies werden geanonimiseerd en geëvalueerd op de aanwezigheid van syringomyelie (SM) door 2 ervaren veterinaire radiologen. Bij aanwezigheid van SM werd de maximale dorsoventrale diameter (syrinx width, SW) gemeten op de transversale en midsagittale T1WSE MR-beelden en pre- en postcontrast CT-beelden. De statistische analyse werd in 2 delen opgesplitst: 1) de overeenkomst voor het detecteren van SM en 2) de overeenkomst tussen de SW tussen beide beoordelaars en tussen beide technieken. Er was een redelijke overeenkomst (81%, κ = 0.54) tussen de beoordelaars voor het opsporen van een SM op de MR beelden en een bijna perfecte overeenkomst (94%, κ = 0.87) voor de CT beelden. Tussen beide technieken is er een redelijke overeenkomst (observer 1: 81% κ = 0.59; observer 2: 81% κ = 0.57) bij de verschillende radiologen. Zeventien van de 32 honden waarbij een SM werd gediagnosticeerd op zowel de MR- als de CT-beelden werden opgenomen in het tweede deel. Voor de metingen van de SW was de herhaalbaarheid het best op de midsagittale T1WSE beelden. Bij beide technieken was de reproduceerbaarheid het best op de midsagittale beelden. Uit deze studie kunnen we concluderen dat SM consequent door de 2 beoordelaars werd geïdentificeerd op de MR- en de CT- beelden.

Wanneer een syrinx aanwezig is, kan de dorsoventrale diameter het best gemeten worden op de midsagittale beelden. Ook voor het beoordelen van een syrinx is CT een alternatief voor MR wanneer deze niet beschikbaar is.

De algemene discussie en conclusies van dit doctoraat zijn vervat in het **zesde en tevens laatste hoofdstuk**. In de meeste gevallen zijn intracraniële letsels, een cerebellaire hernia en syringomyelie d.m.v. CT opspoorbaar. MR blijft de techniek bij uitstek om letsels op te sporen in de hersenen en het ruggenmerg, maar CT kan gebruikt worden als alternatief. Dit is van groot belang omdat kleinere dierenklinieken vandaag de dag veelal enkel een CT- en geen MR-toestel in hun bezit hebben. Om na te gaan of verschillen tussen MR en CT wat betreft de lengte van een CH en breedte van de syrinx een klinische impact kunnen hebben, zijn bijkomende studies een conditio sine qua non.

Curriculum vitae

Kaatje Kromhout werd geboren op 6 februari 1974 te Reet.

Na het behalen van het diploma van gegradueerde in de verpleegkunde besloot ze om in de voetsporen te treden van haar papa, dokter-verloskundige. Toch bleek de liefde voor dieren groter waardoor ze haar studies geneeskunde inruilde voor diergeneeskunde. In 2008 studeerde ze als dierenarts af aan de Universiteit Gent.

Aansluitend volgde een jaar internship medische beeldvorming (CT-MRI) aan de vakgroep Medische Beeldvorming van de Huisdieren en Orthopedie van de Kleine Huisdieren. Tot op heden is zij als wetenschappelijk medewerker aan deze vakgroep verbonden. Hier staat zij in voor de dagelijkse onderzoeken en protocollering. Daarnaast werkte zij aan haar doctoraatstudie.

Kaatje Kromhout is auteur of mede-auteur van 16 wetenschappelijke publicaties in nationale en internationale tijdschriften. Zij nam eveneens actief deel aan meerdere nationale en internationale congressen.

Bibliography

Publications

Kromhout K. , van Bree H., Broeckx B.J., Bhatti S., De Decker S., Polis I., Gielen I. Low-field MRI and multislice CT for the detection of cervical syringomyelia in dogs. *Journal of Veterinary Internal Medicine* 2015;29:1354-1359.

De Rycke L.M., Gielen I.M., Dingemanse W., Kromhout K., van Bree H. Computed Tomographic and Low-Field Magnetic Resonance Arthrography: A Comparison of Techniques For Observing Intra-articular Structures of the Normal Canine Shoulder. *Veterinary Surgery* 2015;44:704-712.

Kromhout K., van Bree H., Broeckx B.J., Bhatti S., Van Ham L., Polis I., Gielen I. Low-field MRI and multislice CT for the detection of cerebellar (foramen magnum) herniation in Cavalier King Charles Spaniels. *Journal of Veterinary Internal Medicine* 2015;29:238-241.

Doom M., de Rooster H., van Bergen T., Gielen I., Kromhout K., Simoens P., Cornillie P. Morphology of the Canine Omentum Part 1: The Omental Bursa and its Compartments Materialized and Explored by a Novel Technique. *Anatomica Histologica Embryologia* Epub 2014.

Doom M., de Rooster H., van Bergen T., Gielen I., Kromhout K., Simoens P., Cornillie P. Morphology of the Canine Omentum Part 2: The Omental Bursa and its Compartments Materialized and Explored by a Novel Technique. *Anatomia Histologica Embryologia* Epub 2014.

Hauspie S., Vanderperren K., Gielen I., Pardon B., Kromhout K., Martens M., Saunders J. Magnetic Resonance Imaging of the dorsal proximal synovial plica of the equine metacarpo-/metatarsophalangeal joint. *Anatomica Histologica Embryologia*. Epub 2014.

De Rycke* L.M., Kromhout* K., van Bree H.J., Bosmans T., Gielen I.M. Computed Tomography Atlas of the Normal Cranial Canine Abdominal Vasculature Enhanced by Dial-phase Angiography. *Anatatomia Histologia Embryologia* 2014;43:413-422.

Cornelis I., Bosmans T., Doom M., Binst D., Van der Vekens E., Kromhout K., Cornillie P., Van Ham L. Unilateral shunt formation with thoracic aortic dissection in a Whippet. *Journal of Small Animal Practice* 2014; 55:337-339.

de Bakker E., Gielen I., Kromhout K., van Bree H., Van Ryssen B. Magnetic resonance imaging of primary and concomitant flexor enthesopathy in the canine elbow. *Veterinary Radiology and Ultrasound* 2013;55:337-339.

Kromhout* K., Gielen*I., Gavin P., Van Ham L., Polis I., van Bree H. Agreement of low-field MRI and CT for the detection of suspected intracranial lesions in dogs and cats. *Journal of the American Veterinary Medical Association* 2013;243:367-375.

Cornelis I., De Decker S., Gielen I., Gadeyne C., Chiers K., Vandenabeele S., Kromhout K., Van Ham L. Idiopathic sterile inflammation of epidural fat and epaxial muscles causing paraplegia in a mixed-breed dog. *Journal of the American Veterinary Medical Association* 2013;242:1405-1409.

Kromhout K., Wouters A., Gielen I. Computertomografie voor de detectie van longnodulen bij de hond. *Vlaams Diergeneeskundig Tijdschrift* 2013;82:91-96.

Kromhout K., Gielen I., De Cock H.E.V., Van Dyck K., van Bree H. Magnetic resonance and computed tomography imaging of a carotid body tumor in a dog.
Acta Veterinaria Scandinavica 2012;54:24.

De Decker S., Gielen I., Duchateau L., Corzo N., van Bree H., Kromhout K., Bosmans T., Van Ham L. Intraobserver, interobserver and intermethod agreement of myelography, postmyelographic computed tomography, and low-field magnetic resonance imaging in dogs with disk associated wobbler syndrome (cervical spondylomyelopathy). *Journal of the American Veterinary Medical Association* 2011 238;12:1601-1608.

Kromhout K.,Van der Heyden S., Cornelis I., Bosmans T., van Bree H., Gielen I. Canine nasal adenocarcinoma with atypical intracranial extension : computed tomography and magnetic resonance findings. *European Journal of Companion Animal Practice* 2011 21; 2:151-154.

Kromhout K., Gielen I., Van Caelenberg A., Van Ham L., van Bree H.
The use of magnetic resonance imaging in the detection of intracranial lesions in three cats. Magnetische resonantie bij de detectie van intracraniale letsels bij drie katten.
Vlaams Diergeneeskundig Tijdschrift 2009 78, 2:121-128.

Scientific presentation

Kromhout K., Gielen I. CT vs. MRI in brain lesions, when is CT the modality of choice. *Proceedings of the 3rd International CT-Users Meeting*, 30th november - 1st december 2013 Ghent, Belgium, 68-70.

Gielen I., Kromhout K. CT in small animal brain diseases. *Proceedings of the 3rd International CT-Users Meeting*, 30th november - 1st december 2013 Ghent, Belgium, 54-55.

Kromhout K., Bhatti S., Van Ham L., Van Bree H., Gielen I. Comparison of MRI and CT for the detection of cerebellar (foramen magnum) herniation in Cavalier King Charles Spaniels. *Proceedings of the 3rd International CT-Users Meeting*, 30th november - 1st december 2013 Ghent, Belgium, 20. (Poster presentation/first prize winner)

Kromhout K.,Van Soens I., Bosseler I., Bhatti S., Gielen I.Computed tomography characteristics of a spinal epidural hemangiosarcoma in a young dog. *Proceedings of the 3rd International CT-Users Meeting*, 30th november - 1st december 2013 Ghent, Belgium, 14. (Poster presentation)

Cornelis I., Van Ham L., Kromhout K., Goethals K., Gielen I., Bhatti S.
Sole prednisolone therapy in canine meningoencephalitis of unknown origin: 45 cases (2006-2012)
Proceedings of the 26th Symposium of European Society of Veterinary Neurology and European college of Veterinary Neurology: Neuro-emergency and critical care, 26th-28th september 2013 Paris, France, 91.

Mauler D., De Rooster H., Kromhout K., Guzman A.R., Gielen I.
Horner's syndrome associated with a frontal sinusitis in a dog.
Proceedings of the 26th Symposium of European Society of Veterinary Neurology and European college of Veterinary Neurology: Neuro-emergency and critical care, 26th-28th september 2013 Paris, France, 97.

Gielen I., Kromhout K., Dingemanse W., Van Bree H.Update on diagnostic imaging in elbow disease. *Proceedings of the 27th annual meeting of the International Elbow Working Group*, 11th april 2012, Birmingham, United Kingdom, 13-14.

De Rycke L., Gielen I., Dingemanse W., Kromhout K., Van Bree H. Magnetic resonance arthrography (MRA) and CT arthrography (CTA) of the normal canine shoulder;
Proceedings of the 6th European Veterinary MRI User Meeting, 11th-12th may 2012, Merelbeke, Belgium, 86-88.

Doom M., De Rooster H., Gielen I., Kromhout K., Simoens P., Cornillie P.Exploring an enigmatic organ: surgery-oriented anatomy of the canine omentum majus. *Proceedings XXIXth Congress of European Association of Veterinary Anatomists*, 25th-28th july 2012, Stara Zagreb, Bulgaria (poster presentation).

Gielen I., Kromhout K., van Bree H. Lumbosacral disease (LS): an update on diagnostic imaging techniques. *Proceedings of the 20th Annual Scientific Meeting of the European College of Veterinary Surgery*, 7th-9th july 2011, Ghent University, Belgium, 137-139.

Kromhout K., Gielen I., Van Ham L., van Bree H. CT and MRI findings of cervical stenosis caused by malformation of the articular facets and meningeal fibrosis of C2-C3 in two young large breed dogs. *Proceedings of the 16th European Veterinary Diagnostic Imaging Annual Conference*, 1st-3rd september 2010, London, United Kingdom, 83. (poster presentation)

De Decker S., Gielen I., Duchateau L., Corzo N., van Bree H., Kromhout K., Bosmans T., Van Ham L. Agreement of myelography, postmyelographic computed tomography (CTM) and low-field magnetic resonance imaging (MRI) in dogs with disk associated cervical spondylomyelopathy: a randomized, blinded study. *Proceedings of the 23rd Annual Symposium of the European Society of Veterinary Neurology and European college of Veterinary Neurology,* 16th-18th september 2010, Cambridge, United Kingdom, 53.

K. Kromhout, P. Gavin, L.Van Ham, H. van Bree, I. Gielen. A comparison of CT and MRI for the detection of intracranial lesions in dogs and cats. *Proceedings of the 15th Conference of the International Veterinary Radiology Association*, 26th-31th july 2009, Buzios, Brazil, 198.

Dankwoord

Mijn lieve mama en papa waren mensen die enorm veel belang hechtten aan waarden en normen. Ten tijde van '*Cheers'* dacht ik altijd dat ze het over waard Sam Malone en tooghanger Norm Peterson hadden. In het meervoud dan. Mijn fout.

Waarden en normen. Zoals dankbaarheid. Niet alleen dankbaar zijn, maar dankbaarheid tonen. Sommige realisaties zijn zoveel groter dan datgene wat ik ooit voor ogen had. Net dankzij de steun van mensen rondom mij. Dichtbij en veraf.

Tijdens mijn studies zweerde ik dat het effectief realiseren van een doctoraat pure magie was, maar jullie maakten van mij de goochelaar die ik nu ben. Niet letterlijk uiteraard en al maar goed ook of mijn patiënten zouden geen Cavalier King Charles Spaniels, maar konijnen en duiven geweest zijn, op medische beeldvorming uit mijn hoed getoverd of mouw geschud.

Aan mijn promotor, Dr. Ingrid Gielen, dank u. U haalde mij aan boord van de CT-MRI-unit waardoor ik heel veel fijne mensen heb leren kennen.

Professor Dr. Luc Van Ham, Dr. Sofie Bhatti, jullie steun en expertise maakten van mij een nog betere veterinaire radioloog. Eentje met een grote liefde voor neurologie. Een vanzelfsprekendheid daar ik wel eens last durf te hebben van zenuwen. Ook graag nog een woord van oprechte dank aan jullie beiden voor het nalezen wanneer de deadline met rasse schreden naderde. Als wereldreiziger kreeg *last minute* plots een heel andere betekenis.

Dank aan mijn examencommissie, vooreerst Professor Dr. Kurt Houf, voorzitter. Sta mij toe te zeggen dat er naar mijn mening een deel in uw familienaam ontbreekt: "ijzer". Niet omdat u een man van staal zou zijn, maar omwille van het geluk dat u brengt. Uw talent om alles in goede banen te leiden, maken mee dat ik bovendien trots kan en mag zijn op het resultaat.

Professor Dr. Henri van Bree, u bezorgde mij mee de kans deel uit te maken van een team gemotiveerde dierenartsen. Daar ben ik u zeer dankbaar voor. Tevens bezorgde u mij zeer vaak een glimlach. Kennis is macht, maar humor des te meer. Bij deze: ik weet dat u niet van Bree, maar van Wetteren bent. *You don't fool me*.

Professor Dr. Jimmy Saunders, woorden schieten te kort en met een krop in de keel (en inktprop in de pen) een blijk van enorme appreciatie om niet alleen zoals Professor Dr. Houf alles in goede banen te leiden, maar mij ook warm te maken om mijn professioneel terrein te verruimen en te motiveren het beste uit mezelf te halen. Er bestaat geen twijfel dat u een uitstekende nieuwe vakgroepvoorzitter zal zijn. Succes!

Dr. Steven De Decker, *mahalo*. Bezorgde ik je bij het lezen van mijn artikelen fronsende wenkbrauwen? Ik wist dat je kritische blik vanuit het Verenigd Koninkrijk nooit veraf was wat mij sterkte in mijn overtuiging om er meer dan helemaal voor te gaan. Wanneer ik me (terecht) op de vingers getikt voelde, dacht ik aan diezelfde vingers die mijn mails naar jou over Kaua'i, O'ahu en Big Island typten.

Dr. Bart Broeckx, dé enige echte statisticus. Al kan hier sprake zijn van bias. Bart, jouw genetisch onderzoek naar heupdysplasie fascineert me en… stelt me tevens gerust voor wanneer het moment daar is dat ook ik een nieuwe heup nodig heb. Dank ook voor het uitbreiden van mijn woordenschat. Onze gesprekken in het Aantwaarps zen een hiel pak raiker na we't oek kunne hemme over Bland Altman (bruur van de Robert) en boxplots (plots oep een boeksmatch), t-testen (ge wet wol, Earl Grey van Lipton). Ik klink dankze aa gelek nen eachte Aantwaarpse statisticus.

Ook hartelijk dank aan Dr. Frank De Waele.

Dr. Massimo Baroni, grazie.

Collegae van medische beeldvorming, wat zou ik zijn zonder jullie?

Walter, Annemie, Casper en Billie, bedankt.

Aquilino Villamonte Chevalier, ik waardeer je enorm als medegrondlegger van het Flemlish. Weet dat schoonheid niet alleen in jouw naam schuilt, maar vooral in jou als persoon. Weet ook dat Panama niet ver weg is. Met de Aeromodeller van de Belgische beeldhouwer Henri Van Herwegen ben ik er ongetwijfeld zo. Kan niet anders. Zijn pseudoniem – Panamarenko – is onlosmakelijk verbonden met je land van herkomst. Maar stel je voor dat ik kom aankloppen en Sofie zegt dat je verhuisd bent naar de Death Star. Ik acht het niet onmogelijk. *May the force be with you!*

Eva, hoe zou ik jou ooit kunnen vergeten te bedanken. Altijd druk bezig op scintigrafie. Je loopt zo vaak heen en weer dat ik je stiekem Scinty Lauper noem. *Girls just want to have fun!* En je lijkt perfect op je plek te zitten daar. Je houdt je o.a. bezig met joodbehandelingen bij katten met schildklierproblemen. Ik ga dus niet alleen voor die nieuwe heup terechtkunnen bij Bart, maar ook bij jou wanneer er iets misloopt in het atoomcentrum in Mol en ik zonder joodpillen zit. Je weet, ik verhuis naar Turnhout, het hart van de Kempen.

With the uttermost respect, many thanks to four incredible veterinarian ladies who burst with talent. Not in the least because they fluently speak one of the most difficult languages on planet earth: French.

Laure, how I love your hustle and your raucous laughter. I can hear your exuberance and energy when I'm at home while you're staying in France for a weekend or holiday. Remind me – safety first – I will provide you with some ear plugs for those cute little monkeys in Africa.

Caroline Fina and Woody. What a duo! Time and again you both amaze me when you board an airplane and travel to Cannes together. I've always thought you were heir to the oil company of the same name. Let me tell you a secret: I sincerely hope that when oil prices go through the roof, you will be there for me like you were now in the clinic.

Olivia (I'm tempted to say I can hear your footsteps that mark the way you walk, but they are overshadowed by Laure's exuberance) and Blandine (why does the CT always overheat in your presence?), thank you to the both of you for helping me.

Met minder woorden een even grote portie dank aan Els, Katrien, Elke, Emmelie & Fritske, Inez, Stijn H. en Kim. Kim, ik bewonder hoe je al die hengsten de baas kunt, zowel die op het werk als die ene bij je thuis. Spijtig dat ik geen deel meer uitmaak van je 15 minuten powernap. Nog dit: dankzij jou zal Zalando nooit failliet gaan.

Verder wil ik ook de collega's van orthopedie mijn dank betuigen.

Prof. Dr. Bernadette Van Ryssen (soms zo verstrooid als het zout op mijn frieten), Yves, Stijn , Eva, Melania en oud-collega's Lynn, Astrid, Hannah, Seppe en Kathelijn.

Evelien, ook al is de fysieke gelijkenis volgens mij afwezig, je bent voor mij zoals een praatpaal langs de snelweg. Een ingebouwde veiligheid voor automobilisten die panikeren bij een sputterende motor, een zekerheid bij een platte band, de stem aan de andere kant van de lijn die zegt dat alles in orde komt. Je bent de Max. Alleen heb je Godzijdank niet zo'n grijze snuit, blaf je niet zo hard en heb je niet evenveel last van flatulentie. Bedankt voor de wandelingen in jullie aangenaam gezelschap.

Geert, jij in het bijzonder bedankt om ons Fonske niet alleen terug alle kracht te geven, gevolgd door een goed herstel, maar tevens voor zijn internationale carrière. Hij is er zich welbewust van, maar van sterallures geen sprake. Netjes met de pootjes op de grond.

Dit doctoraat heeft me meer dan eens slapeloze nachten bezorgd. Ik heb vaak op het punt gestaan één van mijn dierbare collega's anesthesie te bellen om 3 uur 's ochtends. Eén keer heb ik het gedaan, maar ik kreeg die zangeres aan de lijn, Anastasia.

Bossie, je bent niet alleen een gedienstige, sportieve anesthesist, maar meer nog – na je uren – een Amerikaans rockzanger, gitarist en liedsjesschrijver, *'cause tramps like us, baby we were born to run*. Oh, dat is *the boss* zeker… Tim, eeuwige dank voor je hulp en je kent de weg naar mijn luisterend oor.

Virginie, de kilometers die je aflegt op je loopband zijn een inspiratie geweest voor mij. De lange afstand (met verwachte en onverwachte hindernissen) gaf me een gevoel dat we hetzelfde pad bewandelden – of beter liepen – richting eindmeet. Ik kan me inbeelden dat jouw conditie erop vooruit gegaan is, maar ik merk weinig tot geen verschil. Naast mijn dank heb je mijn steun bij het verdere verloop van je doctoraat. *You go girl!*

Alix, ook jij bedankt, want ik weet dat achter elke man een sterke vrouw staat. Lang dacht ik dat dat bij Kenny Barbie was. Niet dus.

Diego, mijn Spaanse God, gracias!

Ilaria, thanks for being there for me and Fonske. I will keep on calling you Hilaria when you crack me up while having crazy conversations. Come to think of it… Just imagine your last name would be 'Clinton'. You might be the first woman to become president of the United States of America. God Bless!

Andere anesthesisten die nog aanwezig of afwezig zijn: Anna B. (be careful with those piercings near the MRI), Annika (succes met je residency chirurgie), Caroline, Inge en Tim W. out of sight but not out of mind.

Ook het team van neurologie stond altijd voor me klaar met de nodige prikkels.

Kenny Privé wil ik bedanken voor bijstand in moeilijke PhD- en Facebookmomenten. Je vindt zelfs mijn meest waardeloze posts leuk. Ik dacht “Hopelijk meende hij het wanneer hij zei dat hij zeer enthousiast was over mijn doctoraat.” Maar die twijfel was snel weg want ach “Die uitspraak niet menen? Dat Kenny niet maken”.

Ine, wanneer jij op me afkomt, weet ik dat er een spervuur van vragen zal volgen. Dan waren mondelinge examens een lachertje. Je houdt me scherp en wakkert bij mij de wens aan om steeds bij te leren en kennis te delen. Ik kijk naar je op, gewoon al door je imposante lengte. Dank voor alle hulp en steun. Ik kijk uit naar wat de toekomst voor ons brengt qua samenwerking.

Emilie jij moet de neuroloog zijn met de grootste fanbasis onder de eigenaars van de patiënten. Daaruit begrijp ik dat mijn lang dankwoord aan jou meer op zijn plaats is op je Facebookprofiel. Igorke, het is altijd uitkijken wanneer je door de gangen scheurt. Oppassen voor die Gentse ‘superflitspaal’!.

Valentine dankzij jou heb ik veel extra dubbelstudies kunnen doen, ook al waren ze niet echt nodig.

Kimberley, bij het bedanken meteen ook een vraag: waar heb jij toch dat voorkruipen met je patiënten geleerd? Aan de kassa van Proxy Delhaize in Lasne-Chapelle-Saint-Lambert? Ik denk dat niemand beter doet. Klasse!

Marnix, bedankt voor je technische hulp, het babbelen over renoveren en vooral het oneindig herstellen van de positioneringskussentjes van CT en MRI. Misschien toch eens tijd voor nieuwe.

Marleen, Claudine en Sandra. Jullie verrichten heel wat werk achter de schermen. Bedankt daarvoor.

Thanks aan alle andere collega-dierenartsen kleine huisdieren, residents, interns en studenten. Teveel om op te noemen. De sfeer en de werking van de klinieken zouden niet zo aangenaam zijn zonder jullie hulp.

Johan en Iris, wat zijn we een geolied team. 's Avonds werd heel wat van mijn tijd opgeslorpt door patiënten van Orion, vaak tot diep in de nacht. Soms dacht ik dat het allemaal wat teveel werd maar dan keek ik naar de sterrenhemel en wist ik dat altijd alles goed komt. Nu de rust terug is mag je het aantal patienten per dag gerust verdubbelen. Bedankt dat ik mijn steentje aan jullie geweldige kliniek mag bijdragen.

Familie, vrienden en vriendinnen die ik hier niet allemaal bij naam gaan noemen, jullie weten zelf wel wie ik bedoel. Bedankt om er voor mij te zijn, in goede en slechte tijden.

Elise toch een speciale dank voor jou. Samen ergens begonnen aan de studie diergeneeskunde, samen dezelfde hindernissen overwonnen, samen afgestudeerd. Ik ging ooit eens op babybezoek komen… ondertussen is die schattige baby al bijna 4. *Shame on me!*

John Silberstein, thank you very much for being the native speaker I was looking for. I hope to meet you, Pam en Speck in person very soon. We are saving up for a plane ticket to Philly!

Denise, Bettina en Flor, een paar jaar geleden waren jullie daar plots. Om niet meer uit mijn en ons leven te verdwijnen. Het is telkens gezellig bij jullie wekelijks bezoek, al is het niet zo goed voor onze gezondheid. Door de drukte van het doctoraat heb ik heel wat afspraken gemist. En mijn berekeningen leren mij dat ik 38 ‘pateekes’ achter sta. Die schade moet dringend ingehaald worden, maar misschien niet in 1 keer.

Marie-Louiske, mama van Ann en toch ook van mij. Al die jaren heb je jouw thuis mijn thuis gemaakt. Ik kan er altijd terecht. Bedankt om mijn woordenschat te verruimen met Turnawts: mastentoppen, meurig, zeksmojer,…

Moemoe en vava van Ann. Wat mis ik jullie en jullie lekker eten.

S. Tante Mit, S. nonkel Hubert en S. tante Yvonne, ook jullie zijn na al die jaren mijn familie. Bedankt voor de regelmatige updates over beleggingen, rentevoeten en interesten. De lotto hoef ik niet meer te winnen want jullie zijn voor mij de jackpot.

Aan alle poezen in mijn leven, Wortel, Molly, Jefke en last but not least, Fons. Wat zou ik zijn zonder jullie. Buiten het krabben, vechten, blazen en grommen, hou ik van jullie en jullie geluidjes. Het spinnen kalmeert mij. Fonske sponske ik ben blij dat je er nog bent!

Ann, ik ben zo blij dat jij in mijn leven bent gekomen. Jouw liefde, zelfde humor als ik, geduld en ongeduld zijn voor mij onmisbaar. Bedankt dat je er altijd voor mij bent. Ik kijk uit naar iedere dag met jou! Ik kijk uit naar ons huis, dat al bloed, zweet en tranen heeft gekost, maar fantastisch zal zijn als het af is. Al weet ik niet of het groot genoeg is om al onze rommel in kwijt te kunnen, …
Ann, we stick together like a sticker and glue.

Mama, papa, jullie zijn er beiden niet meer maar ik weet dat jullie trots zijn. Bedankt voor de jaren, al waren ze veel te kort, die we samen hebben doorgebracht. Papa, je moest je geen zorgen maken, ik ben echt wel goed terechtgekomen. En mama, ja je mag nu eindelijk zeggen dat je dochter doctor is.

Kaatje

"Dream as if you'll live forever. Live as if you'll die today."
James Dean

"Life is about balance. The good and the bad. The highs and the lows. The pina and the colada."

Ellen Degeneres